Julia Raunicher, BSc

Latex blends – influence of the blending ratio on the mechanical properties

MASTER'S THESIS

to achieve the university degree of

Diplom-Ingenieurin

Master's degree programme: Technical Chemistry

submitted to

Graz University of Technology

Supervisor

Assoc. Prof. DI Dr. Gregor Trimmel

Institute for Chemistry and Technology of Materials
Graz University of Technology

Graz, January 2018

AFFIDAVIT

I declare that I have authored this thesis independently, that I have not used other than the declared sources/resources, and that I have explicitly indicated all material which has been quoted either literally or by content from the sources used. The text document uploaded to TUGRAZonline is identical to the present master's thesis.

05.01.2018
Date

Raichl Julia
Signature

ACKNOWLEDGEMENTS

This thesis could not have been realized without a great deal of guidance as well as mental and practical support. I would like to thank all those people who provided me with everything I needed during the time I was working on this project.

First and foremost I want to thank my supervisor Gregor Trimmel of the Institute for Chemistry and Technology of Materials (ICTM) at the University of Technology Graz for giving me the opportunity to work on this interesting topic. The door to his office was always open whenever I needed advise. He consistently allowed this thesis to be my own work, but guided me into the right direction when it was necessary.

Furthermore, I want to express my gratitude to the Polymer Competence Centre Leoben GmbH (PCCL) for the financial support. The research work of this master thesis was performed within the COMET-project "*Rubber-metal and rubber-thermoplast interfaces in elastomer technology*" (project-no.: VI-1.03) at the Polymer Competence Center Leoben GmbH within the framework of the COMET-program of the Federal Ministry for Transport, Innovation and Technology and the Federal Ministry of Science, Research and Economy with contributions by the University of Technology Graz (ICTM) and Semperit Technische Produkte GmbH. The PCCL is founded by the Austrian Government and the State Governments of Styria, Upper Austria and Lower Austria.

Special thanks go to Sandra Schlögl from PCCL, who provided me with helpful advice and always had an open ear for my questions. Furthermore, I want to thank Peter Pölt and Sanja Šimić from the Austrian Centre for Electron Microscopy and Nanoanalysis for their support with the ESEM-EDX measurements.

I am also very grateful to all the people of the ICTM, especially to the people from my working group, for the good collaboration and the fun we had in the last months. Special thanks go to Lucas Mixich for his mental support during our numberless coffee breaks.

Finally, I want to thank all my friends and my family for their continuous encouragement throughout my years of study and for supporting me spiritually during the work on this thesis and my life in general.

ABSTRACT

In medical practice, gloves constitute an essential feature for the protection of patients and medical personnel from infectious organisms. Nowadays, most of the examination gloves are made from natural rubber (NR) latex. NR-latex provides excellent physical properties, but it contains proteins, which can cause allergic reactions to some people. Therefore, acrylonitrile-butadiene rubber (NBR) latex gloves are used as an alternative for allergic people, though they are not that comfortable to wear. This leads to the desire to find a material with the same or even improved properties as NR-latex, which could be achieved by the blending technology. This work is focused on the investigation of different latex blends concerning the influence of the blend ratio on the mechanical properties. Isoprene rubber (IR) latex and NBR-latex were blended with chloroprene rubber (CR) latex. For the purpose of comparison, NR-latex was blended with CR-latex. The thin-film latex blends were prepared in the blending ratios 100:0, 75:25, 50:50, 25:75 and 0:100 (w:w, based on the dry rubber content) using the dipping method. Differential scanning calorimetry (DSC) measurements showed, that the produced latex blends represent immiscible systems. The morphology was investigated by environmental scanning electron microscopy coupled with energy dispersive X-ray spectroscopy (ESEM-EDX). Different sample preparations were performed, whereat the surface as well as the fracture areas were analysed. All pre-vulcanized samples show a very homogeneous distribution of the vulcanization agents and no phase separation could be observed with this method. The mechanical properties were determined by tensile tests. The tensile strength of all pre-vulcanized latex blends decreases with increasing amounts of CR-latex. The pre-vulcanized NR/CR-latex blends show the highest tensile strength, followed by the NBR/CR-latex blends and the IR/CR-latex blends. On the other hand, the ultimate elongation is improved with increasing amounts of CR-latex. The pre-vulcanized IR/CR-latex blends exhibit the highest ultimate elongation, whereas the NBR/CR-latex blends have the lowest. Additionally, the influence of the drying conditions as well as the effect of different vulcanization agents on the mechanical properties of chosen latex blends were investigated.

ZUSAMMENFASSUNG

Latexhandschuhe schützen sowohl Patienten als auch das medizinische Personal vor ansteckenden Organismen und sind daher unentbehrlich in der Medizin. Untersuchungshandschuhe bestehen üblicherweise aus Naturlatex (NR), welcher exzellente physikalische Eigenschaften aufweist. Diese beinhalten jedoch Proteine, die bei manchen Menschen allergische Reaktionen hervorrufen können. Alternativ verwenden allergische Personen daher Handschuhe aus Acrylnitril-Butadien-Latex (NBR), die allerdings keinen hohen Tragekomfort besitzen. Mithilfe der Blendtechnologie soll deshalb ein Material gefunden werden, welches dieselben oder sogar bessere Eigenschaften aufweist wie NR-Latex. Diese Arbeit beschäftigt sich mit der Untersuchung unterschiedlicher Latexblends hinsichtlich des Einflusses des Mischungsverhältnisses auf die mechanischen Eigenschaften. Dafür wurden Isopren- (IR) und NBR-Latex mit Chloropren-Latex (CR) verblendet. Zum Vergleich wurde auch NR-Latex mit CR-Latex gemischt. Die Blends wurden mittels Tauchverfahren in den Verhältnissen 100:0, 75:25, 50:50, 25:75 und 0:100 (w:w, basierend auf den Trockengehalt) hergestellt. Durch dynamische Differentialkalorimetrie (DSC) wurde gezeigt, dass es sich bei allen hergestellten Blends um unmischbare Systeme handelt. Außerdem wurde die Morphologie mithilfe eines Rasterelektronenmikroskops gekoppelt mit energiedispersiven Röntgenspektroskopie (ESEM-EDX) untersucht. Es wurden unterschiedliche Probenvorbereitungen durchgeführt, wobei sowohl die Oberflächen als auch die Bruchflächen analysiert wurden. Alle vorvulkanisierten Proben zeigen eine homogene Verteilung der Vulkanisationsadditive, wobei keine Phasenseparation festgestellt wurde. Die mechanischen Eigenschaften wurden mithilfe von Zugversuchen bestimmt. Dabei wurde gezeigt, dass die Zugfestigkeit aller vorvulkanisierten Blends mit zunehmenden Gehalt an CR-Latex abnimmt. Die vorvulkanisierten NR/CR-Latexblends zeigen die höchste Zugfestigkeit, gefolgt von den NBR/CR-Latexblends und den IR/CR-Latexblends. Im Gegensatz dazu nimmt die maximale Dehnung mit zunehmenden Gehalt an CR-Latex zu. Die vorvulkanisierten IR/CR-Latexblends weisen die höchste maximale Dehnung auf, während NBR/CR-Latexblends die geringste maximale Dehnung haben. Zusätzlich wurde an ausgewählten Proben der Einfluss der Trocknungsbedingungen und der Effekt von unterschiedlichen Vulkanisierungsmittel auf die mechanischen Eigenschaften untersucht.

ABBREVIATIONS

NR	natural rubber
IR	isoprene rubber
NBR	nitrile rubber
CR	chloroprene rubber
drc	dry rubber content
UCST	upper critical solution temperature
LCST	lower critical solution temperature
DSC	Differential scanning calorimetry

CONTENTS

1 INTRODUCTION 1

2 THEORETICAL BACKGROUND 3

2.1 Polymer Blends 3

2.1.1 Types of polymer blends 3

2.2 Latex 6

2.2.1 Natural rubber latex (NR) 6

2.2.2 Synthetic rubber latex 7

2.2.2.1 Isoprene rubber latex (IR) 8

2.2.2.2 Nitrile rubber latex (NBR) 10

2.2.2.3 Chloroprene rubber latex (CR) 12

2.2.3 Compounding additives 14

2.2.3.1 Vulcanization agents 14

2.2.3.2 Vulcanization activators 15

2.2.3.3 Vulcanization accelerators 15

2.2.3.4 Other ingredients 15

2.3 Latex manufacturing processes 16

2.3.1 Dipping method 16

2.3.2 Foaming process 18

2.3.3 Casting process 18

2.3.4 Other methods 19

3 AIM OF THE THESIS 20

4 EXPERIMENTAL 21

4.1 Materials and equipment 21

4.2 Preparation of the latex blends 22

4.2.1 Preparation of NR/CR-latex blends 22
4.2.2 Preparation of IR/CR-latex blends 23
4.2.3 Preparation of NBR/CR-latex blends 24
4.3 Characterization methods 24
4.3.1 Tensile test 24
4.3.2 Environmental scanning electron microscopy – energy dispersive X-ray spectroscopy (ESEM-EDX) 26
4.3.3 Differential Scanning Calorimetry (DSC) 27
5 RESULTS 28
5.1 Preparation of the thin-film latex blends 28
5.2 Thickness of the different thin-film latex blends 28
5.3 Miscibility of the different latex blends 31
5.4 Morphology of the different latex blends 37
5.5 EDX-Mapping of the pre-vulcanized IR/CR-latex blends 44
5.6 Mechanical properties of the different latex blends 46
5.6.1 Stress-strain behaviour of the latex blends without pre-vulcanization 46
5.6.2 Stress-strain behaviour of the pre-vulcanized latex blends 48
5.6.3 Comparison of the results obtained from the two different shouldered bars (50 mm and 75 mm) 51
5.6.4 Influence of the drying temperature 54
5.6.5 Stress-strain behaviour of pre-vulcanized IR/CR-latex blends using PM30 and ZnO as vulcanizing agent 55
6 SUMMARY AND OUTLOOK 57
7 REFERENCES 60
8 LIST OF FIGURES 63
9 LIST OF TABLES 69
10 APPENDIX 71

10.1 DSC diagrams 71

10.1.1 DSC diagrams of the NR/CR-latex blends without pre-vulcanization 71

10.1.2 DSC diagrams of the IR/CR-latex blends without pre-vulcanization 74

10.1.3 DSC diagrams of the NBR/CR-latex blends without pre-vulcanization .. 77

10.1.4 DSC diagrams of the pre-vulcanized NR/CR-latex blends 80

10.1.5 DSC diagrams of the pre-vulcanized NBR/CR-latex blends 83

10.2 ESEM results 86

10.2.1 ESEM pictures of the NR/CR-latex blends with and without pre-vulcanization 86

10.2.2 ESEM pictures of the IR/CR-latex blends with and without pre-vulcanization 88

10.2.3 ESEM pictures of the NBR/CR-latex blends 92

1 INTRODUCTION

Latex has long been known to indigenous people as a material to craft useful objects for their daily lives. The milky juice collected from the "weeping tree" (*Caao-Chu*) is an aqueous dispersion of rubber – or, more precisely – of poly(*cis*-1,4-isoprene). In 1495 Christopher Columbus observed residents of Haiti playing with an elastic ball. A quarter of century later, Fernando Cortez brought knowledge of this elastic material to Europe. More than 200 years later, in 1765, the first moulded articles were produced by Macquer and Hérrissant. With the discovery of the hot vulcanization in 1839 by Charles Goodyear many new applications were possible. Only six years later, R. W. Thomson patented the first air-filled tires, leading to a sharply increasing demand of rubber. During the First World War, when Germany was isolated form natural rubber supply, large-scale production of synthetic rubber was carried out by Bayer [1-2].

The global consumption of natural and synthetic rubber increases almost continuously, as it is shown in Figure 1 [3]. They are mainly used for tires, followed by automotive and nonautomotive mechanical goods, footwear as well as wire covering. However, it must be considered that the quantity of directly processed latex is quite small compared to the amount of processed solid rubber [1].

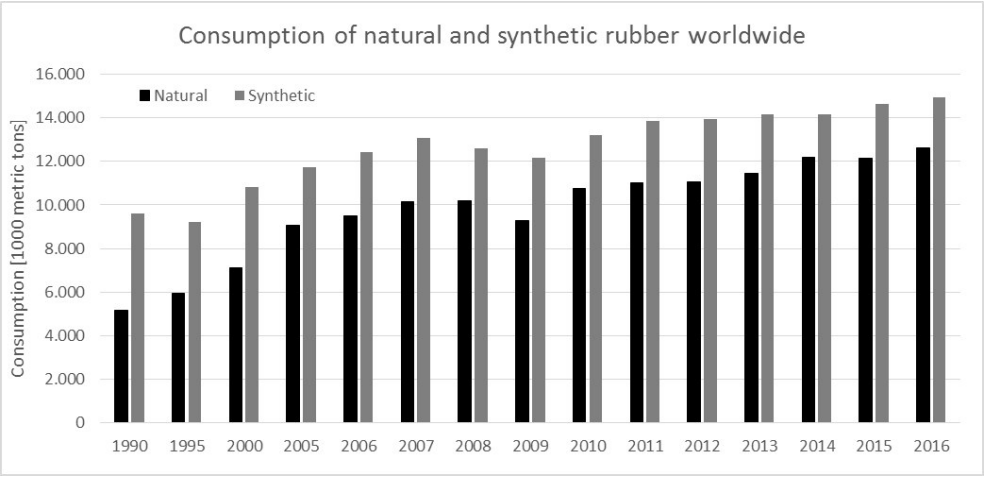

Figure 1: Consumption of natural and synthetic rubber worldwide [3].

Compared to the synthetic rubber latex, natural rubber latex has many advantages like for example excellent mechanical properties. Thus, natural rubber latex is attractive for numerous applications like surgeon and examination gloves, condoms, balloons etc. [4].

Natural rubber latex is mainly produced in Southeast Asia. Depending on the country, different manufacturing processes are used, leading to variable standardized quality rubbers like for example Standard Malaysian Rubber (SMR) or Standard Indonesian rubber (SIR). However, the prices may rise if the wage level in the countries producing NR-latex increases. Furthermore, natural rubber latex contains proteins which can cause allergic reactions in some cases. These facts as well as the increasing complexity of products lead to the desire to find improved and cheaper materials. This can be achieved by blend technology, which includes the combination of two existing materials to obtain enhanced and especially adapted properties [1,5].

The first generation of blends was engineered in the 1950s by special polymerization techniques like copolymerization, block or graft polymerization. Beside the improved impact performance, also some undesired properties like poor surface properties where introduced. In the 1960s further blend developments became available with engineering polymers like polycarbonate as basic resins. This second-generation blends showed an improved heat resistance as well as higher continuous use temperatures [5].

Nowadays, the main blending technique is the melt blending carried out in kneaders or compounding extruders [5,6,7]. Less attention has been paid to latex blends, which are produced by mixing the two polymers in their dispersed form. Many successful blending attempts have been carried out by mixing a latex having a low glass transition temperature (soft latex) with a latex having a high glass transition temperature (hard latex) [8,9,10]. Furthermore, NR/(X)SBR as well as NR/NBR blends prepared from latex system have been investigated [11,12,13]. Several researches upon latex blends for coatings and for the modification of concrete and cement mortar have been carried out [14-15].

However, blending in the latex stage can be advantageous especially when the latex blend is directly used for further production like for the manufacture of dipped goods. One example is the fabrication of surgical gloves. Nowadays, most of the surgical gloves are made of natural rubber latex. Because of the possible allergic reaction also synthetic examination gloves made from nitrile rubber latex are available [4,11]. However, synthetic latex gloves exhibit a lower wear comfort which might be improved by the blend technology. This study deals with the investigation of different latex blends concerning the influence of the blend ratio on the mechanical properties.

2 THEORETICAL BACKGROUND

2.1 Polymer Blends

Polymer blends are combinations of two polymers with different properties to obtain better and cheaper products for specific applications. The fact that already existing polymers can be used and thus the cost intensive developing of new polymeric materials can be avoided makes the blend technology quite interesting for industry. Polymer blends are for example used in automotive industry, for electronic and electrical applications, in appliance sector and for packaging applications [5,17].

2.1.1 Types of polymer blends

Based on the miscibility of the two polymers three different types of blends can be distinguished:

- completely miscible
- partially miscible
- fully immiscible

whereat an almost fluid transition is possible.

The thermodynamic relationship is given by the Gibb's free energy of mixing:

$$\Delta G_{mix} = \Delta H_{mix} - T\Delta S_{mix} \quad (1)$$

with ΔG_{mix} … free energy of mixing [J]
ΔH_{mix} … enthalpy of mixing [J]
T … temperature [K]
ΔS_{mix} … entropy of mixing [JK^{-1}].

Complete miscibility is only obtained, if the free energy of mixing ΔG_{mix} is either zero or negative.

$$\Delta G_{mix} < 0 \quad (2)$$

Furthermore, since ΔG_{mix} can vary with the composition a homogeneous blend of the two components 1 and 2 is only produced if

$$\left(\frac{\partial^2 \Delta G_{mix}}{\partial \phi^2}\right) > 0 \tag{3}$$

with Φ… volume fraction of component 2 [5,17-18].

Figure 2 shows possible ΔG_{mix} curves for three different binary mixtures. The curve OBP fulfils both conditions for all mix ratios resulting in a completely miscible and homogenous binary system. Contrary the curve OAP shows an immiscible heterogeneous system, which is thermodynamic instable due to the positive free energy of mixing ΔG_{mix}. The curve OCP represents the most common case: the compositions OD and PE satisfy both conditions producing a thermodynamic stable, miscible homogenous system. However, the compositions DCE only fulfil the first condition resulting in an immiscible state with two phases [17,18,19].

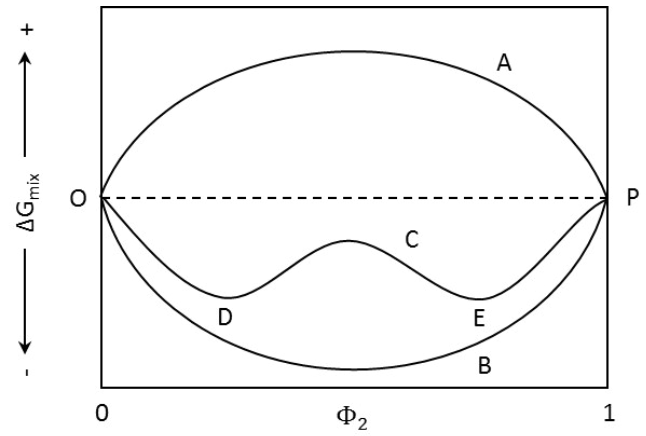

Figure 2: Possible free energy of mixing ΔG_{mix} curves for binary mixtures (based on [17]).

The entropy ΔS_{mix} is direct proportional to the number of different possible combinations and configurations of the molecules. Due to the fact that the segmental movement is limited because of the large molecule weight of polymers, ΔS_{mix} is very small for polymer blends and therefore usually negligible.

The enthalpy ΔH_{mix} results from the interaction energy between the two components which arises due to several interaction forces like dispersion forces, dipole-dipole interaction, hydrogen bonding, etc. A negative enthalpy leads to a completely or partially miscible polymer blend [5,17,20].

A single-phase system is only obtained in case of complete mutual solubility of the two components. Partial solubility results in a two-phase system producing very finely dispersed polymer blends where the interfacial energy is very low. However, most of the polymer mixtures provide an immiscible system since ΔH_{mix} is positive and the molecular weights of both components are large yielding a very small ΔS_{mix}. To prevent phase separation the interaction (dipole-dipole interaction, charge transfer complex formation, hydrogen bonding, etc.) between the different chemical substituents of the two components must be possible. Therefore, the interaction energy between the two components must be increased to improve the miscibility [5].

Furthermore, the miscibility is influenced by the temperature and pressure. Figure 3 shows the phase diagram for polymer blends as a function of temperature. It can be seen that two polymers which are immiscible at low temperature can become miscible by increasing the temperature. The temperature at which the polymers become miscible is called the upper critical solution temperature (UCST). The UCST depends on the composition: it is higher in the middle and lower at both ends. By further increasing of the temperature the polymers become immiscible again and phase separation occurs. This is called the lower critical solution temperature (LCST). Also the LCST changes with the composition [17,20].

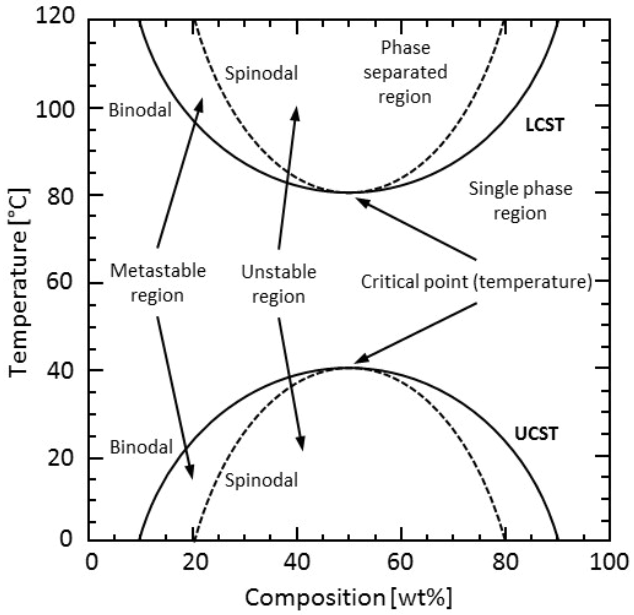

Figure 3: Phase diagram for polymer blends showing the upper critical solution temperature (UCST) and the lower critical solution temperature (LCST) (based on [20]).

To prevent phase separation, compatibilizers can be used. By adding a compatibilizers to the mixture the interfacial tension is reduced while the interfacial adhesion is increased. Furthermore the production of a finer dispersion during mixing is possible and the morphology during processing is stabilized. The most common types are AB block copolymers for a polymer blend consisting of components A and B. The AB block copolymers lead to covalent bonds across the interface, whereat the interfacial tension is decreased. For commercial polymer blends 5-15 wt% of compatibilizers are added [5].

2.2 Latex

Latex is defined as a stable dispersion of rubber particles with a particle size between 0.15 and 3 µm, which are distributed colloidal in an aqueous medium (Figure 4) [21]. Basically two different types of latexes can be distinguished: natural rubber latex and synthetic rubber latex.

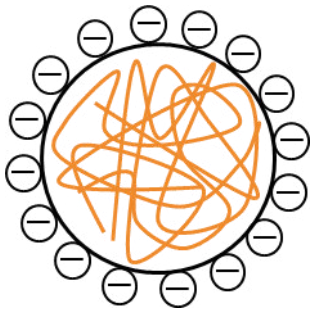

Figure 4: Latex particle.

2.2.1 Natural rubber latex (NR)

Natural rubber latex can be collected from different plants, especially from the *Hevea brasiliensis* trees, which provide more than 99% of the natural rubber. Although the original habitat of these trees is the Amazon rain forest, most of the plantations are located in Southeast Asia. By tapping the bark of the trees a milky fluid is obtained, which is an aqueous dispersion containing approximately 30 % poly(*cis*-1,4-isoprene), 1-2 % proteins, 2 % resins, 1 % fatty acids, 1 % carbohydrates and around 0.5 % of inorganic salts. The rubber particles are stabilized by protein anions, which can be attacked by bacteria when exposed to air leading to a putrid and rancid coagulated latex. To protect the proteins against bacteria, ammonia is added immediately after collecting it from the

tree. The extracted latex is then concentrated by centrifugation (most common), creaming or evaporation to 60 wt% in order to lower the transportation costs [1,4].

Natural rubber goods have a great structural stability with high elasticity resulting in high tensile and tear strength. Furthermore, natural rubber products exhibit very good cold flexibility and dynamic properties as well as excellent barrier protection against the transmission of viruses. However, their ageing, ozone and oil resistance is poor, which can be improved by the addition of stabilizers [1,16,22].

Due to the excellent physical properties, which are unreached by synthetic rubber latex, natural rubber latex provides numerous applications like surgeon and examination gloves, condoms, balloons, thread for clothing, moulded goods, catheters, baby soothers, etc [4].

However, the main problem with NR-latex products are the proteins stabilizing the rubber particles, which can cause allergic reactions. This affects a small percentage of the population, showing skin irritations as a major symptom. In very severe allergy types contact with the protein provokes an anaphylactic shock. To reduce the protein content different technologies like chemical or enzymatic deproteinization, chlorination and polymer coating have been investigated, although the threshold level for sensitization is still unknown. Nevertheless, some natural rubber latex products have been replaced by synthetic rubber products even though the barrier protection is worse [4,16].

2.2.2 Synthetic rubber latex

Synthetic rubber latexes are almost always produced by emulsion polymerisation, whereat the degree of cross-linking and branching can be varied, depending on the type of latex. For instance, the cross-linking is increased for reinforced latexes while it is held back for foam latexes.

Three different types of synthetic rubber latexes can be distinguished: latexes without reactive groups, latexes with reactive groups and latexes with groups capable of self-cross-linking. Latexes without reactive groups are dienes with conjugated double bonds, which can be cross-linked by vulcanization like for example isoprene rubber (IR), acrylonitrile butadiene rubber (NBR), butadiene rubber (BR), styrene butadiene rubber (SBR) and butyl rubber (IIR). Latexes with reactive groups like chloroprene rubber (CR)

are cross-linked by adding a second component like metal-oxides. Latexes with groups that are able to react with one another at elevated temperatures contain for example N-methylol groups [1,19].

An essential difference between synthetic and natural rubber latex is that all synthetic rubber latexes contain tensides as stabilizers. This influences the compounding resulting in very different processing techniques.

2.2.2.1 Isoprene rubber latex (IR)

Polyisoprene [poly(*cis*-1,4-isoprene)] was discovered in 1909 by the German chemist Fritz Hoffmann and represented the first usable synthetic rubber. In 1954 it was first produced via a Ziegler-Natta polymerization by Goodrich Gulf company and 1955 via an anionic polymerization by Firestone company [1,23].

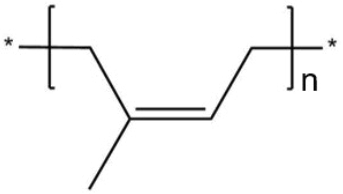

Figure 5: Chemical structure of poly(*cis*-1,4-isoprene).

Contrary to natural rubber latex, where the poly(*cis*-1,4-isoprene) content is 99.9%, isoprene rubber latex contains at the most 98%, depending on the catalyst. Since there are different possible addition directions, also poly(*trans*-1,4-isoprene), poly(1,2-isoprene) and poly(3,4-isoprene) can be formed (Figure 6).

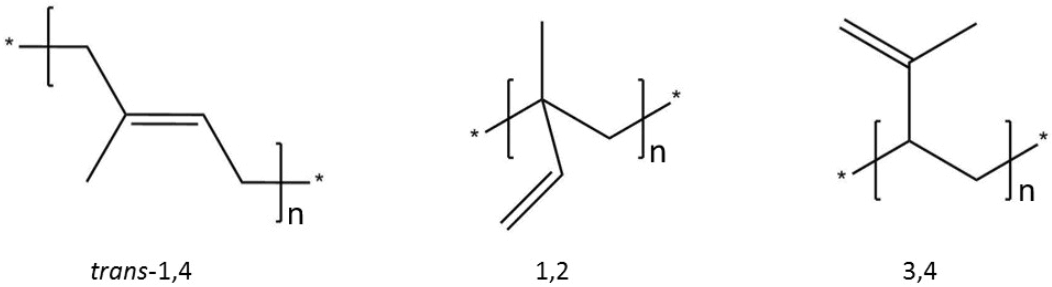

Figure 6: Chemical structure of poly(*trans*-1,4-isoprene), poly(1,2-isoprene) and poly(3,4-isoprene).

The anionic polymerization of isoprene is carried out in presence of Li-alkyl catalysts like n-Butyl-Li in low boiling aliphatic solvents. Even though the Li-alkyl catalysts are less sensitive towards impurities than the Ti-catalysts used for the Ziegler-Natta polymerization, polyisoprene is rarely made by anionic polymerization because the *cis*-content is at most 92%.

High-*cis*-polyisoprene is generally produced by Ziegler-Natta polymerisation of isoprene catalysed by titanium tetrachloride ($TiCl_4$) together with alkylaluminium (AlR_3) in a 1:1 ratio. The reaction is carried out at low temperature in aliphatic solvents like dry pentane or hexane. Also ethers and amines can be added to reduce the formations of oligomers and gels [1,21-22,24].

However, both polymerization techniques provide polyisoprene dissolved in organic solvents, which can be subsequently coagulated and dried to obtain the solid rubber. For the conversion to latex, a post-emulsification is necessary. Therefor the dissolved rubber is mixed with an aqueous soap solution leading to a highly diluted emulsion. The organic solvent is then removed resulting in a concentrated isoprene rubber latex [24].

Even though the molecular differences between natural rubber latex and isoprene rubber latex may seem small, their properties differ significantly. The presence of non-rubber components like proteins in the natural rubber latex have a high impact on the tack, green strength and tensile properties. Moreover, the *cis*-content has a great influence on the properties, as it can be seen in the stress-strain diagram of the pure and un-vulcanized NR and IR rubbers (Figure 7).

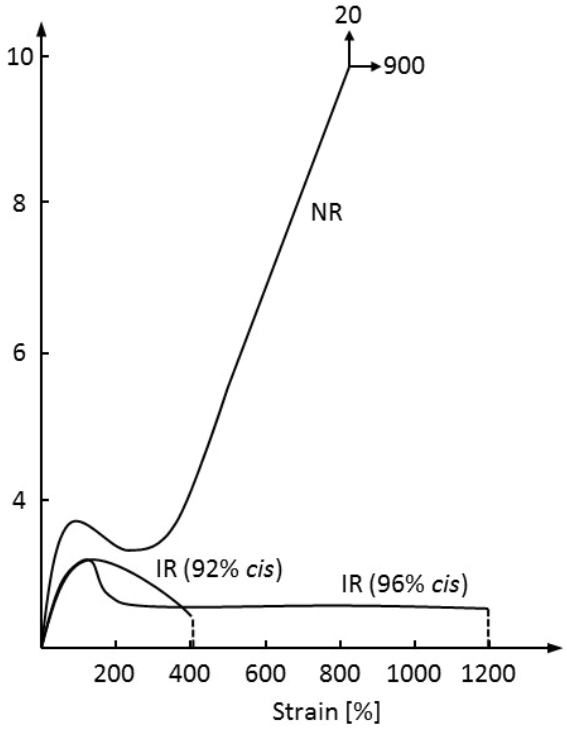

Figure 7: Tensile strength of the pure and un-vulcanized NR and IR;
strain speed: 10 cm/min; temperature: 25°C (based on [22]).

The tensile strength of the un-vulcanized and the vulcanized isoprene rubbers are considerably lower than those of natural rubber. Furthermore, the tear strength and the abrasion resistance are inferior [22,24-25].

Generally, polyisoprene rubber latex made by Ziegler-Natta polymerization can be used for the same applications as NR-latex. IR-latex produced by anionic polymerization can replace natural rubber latex only in some cases [25].

2.2.2.2 Nitrile rubber latex (NBR)

Acrylonitrile-butadiene rubber [poly(acrylonitrile-*co*-1,3-butadiene)] – short nitrile rubber – was first synthesized 1930 at IG Farbenindustrie in Leverkusen.

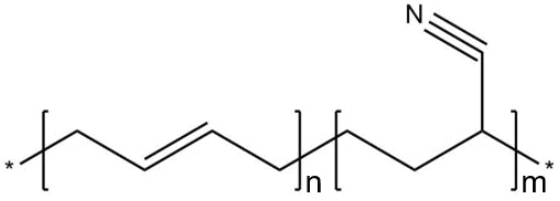

Figure 8: Chemical structure of poly(acrylonitrile-*co*-1,3-butadiene).

NBR rubber latex is produced by copolymerization of acrylonitrile and butadiene in aqueous emulsion at relatively low temperature (0-30 °C) with an operating pressure between 2 and 7 bar. By means of emulsifiers like alkali salts, unsaturated (C_{12}-C_{18}) fatty acids or rosin acids the two different monomers are emulsified in water. The polymerization is then started using an initiator, which mostly consists of redox systems, i.e. mixtures of organic peroxides or persulfate with reducing agents like sodium dithionite. As co-catalysts often metal salts like iron sulphate are used. The polymerization is terminated at 70-80 % conversion by a shortstopper, which can be for example a reducing agent that is soluble in water as well as in organic media. Afterwards the latex is distilled to remove the residual monomers. Sterically hindered phenols or diphenylamines are added as a stabilizer to protect the latex from oxidation. Then the latex can be coagulated by adding electrolytes like NaCl at 80 °C, dried and pressed [1].

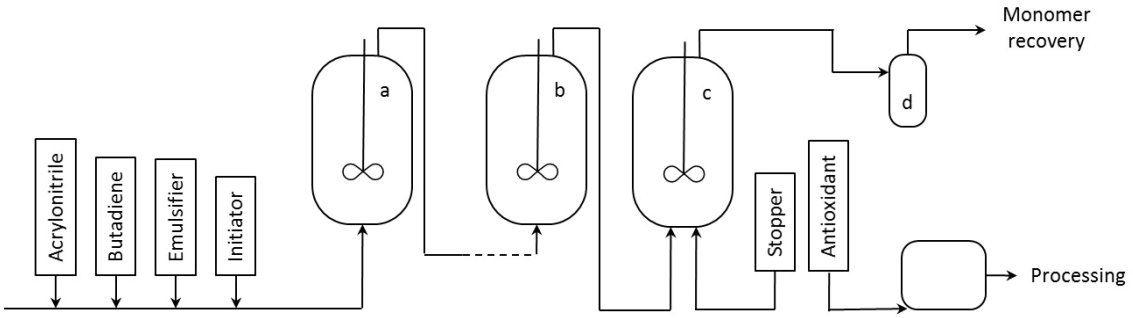

Figure 9: Schematic production of NBR (based on [1]).
a) Stirred tank 1; b) Stirred tank *n*; c) Shortstopping vessel; d) Degassing

The acrylonitrile content has a great influence on the final properties and is determined by the monomer ratio. Nitrile rubbers with an acrylonitrile content between 15-53 wt% are commercially available.

Nitrile rubber has a very good resistance to swelling against oil, fats and fuel, whereat the resistance increases with increasing acrylonitrile content. The nitrile groups lead to gearings of the chain molecules and therefor additional attraction because of the polarity. Non-polar or low polar media cannot insist between the chain molecules because they cannot overcome these polar forces. Indeed, polar solvents like esters and ketones strongly swell nitrile rubbers. The resistance to swelling in polar media decreases with increasing acrylonitrile content. Because of the polarity of the nitrile group, NBR rubbers hardly become electrostatically charged, whereat the risk of sparking is minimized,

making the material perfect for fuel tank tubes. Furthermore, the elasticity, the low temperature flexibility and the gas permeability decrease, whereas the tensile strength, compression set as well as the hardness increase with increasing acrylonitrile content. Therefor it is necessary to adjust the acrylonitrile content for certain applications to achieve the best possible compromise between all properties [1,19].

Nitrile rubber is used for applications, which require not only good mechanical properties but also good fuel, oil, hot air and abrasion resistance. It is applied for O-rings, valves, seals and bellows as well as for tank and hydraulic hosing, brake linings and printing rollers. Furthermore, nitrile rubber latex represents the most important alternative for examination gloves out of synthetic latex [1,4,21].

2.2.2.3 Chloroprene rubber latex (CR)

Polychloroprene [poly(2-chloro-1,3-butadiene)], also known as neoprene, was first produced by Du Pont in 1932.

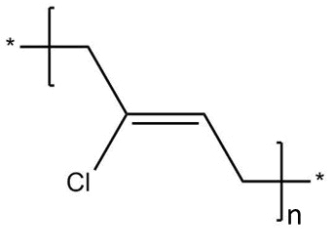

Figure 10: Chemical structure of poly(*trans*-1,4-chloroprene).

Polychloroprene is produced by radical polymerization of chloroprene at temperatures between 10 and 45 °C in aqueous emulsion. The polymerization is carried out at pH 9-13. As an emulsifier mainly alkali salts of disproportionated rosin acids are used. Furthermore, sodium sulfonates are needed. The polymerization is terminated at 70 % conversion by the addition of shortstopper. Acetic acid is used to adjust the pH of the latex to 5.5 to 7.0. The sulfonic acids stay in form of their salts in the latex maintaining the stability at room temperature. Afterwards the latex can be freeze coagulated at -15 °C, washed, dried and crushed [1,22].

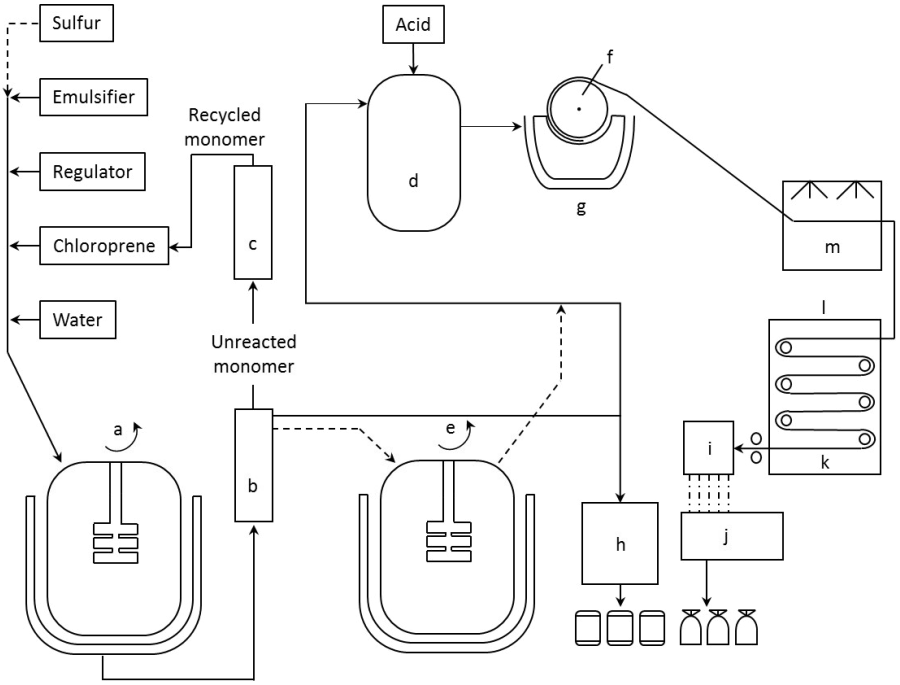

Figure 11: Schematic production of polychloroprene (based on [1]).
a) Polymerization reactor; b) Stripper; c) Purification; d) Neutralization; e) Peptization; f) Rotating cooling drum; g) Coagulation by freezing; h) Latex concentration; i) Chopping machine; j) Dursting machine; k) Roping machine; l) Dryer; m) Washing

During polymerization the chloroprene monomers are incorporated into the polymer chain, whereat different structures can be formed depending on the temperature (Figure 12). The formation of the dominating *trans*-1,4-structure occurs at low temperatures (30 °C) by the head-to-head, tail-to-tail or head-to-tail bonding of the individual chloroprene moieties, which gives the material it's strength. At higher temperature the formation of the *cis*-1,4-, 1,2- and 3,4- structures is increased.

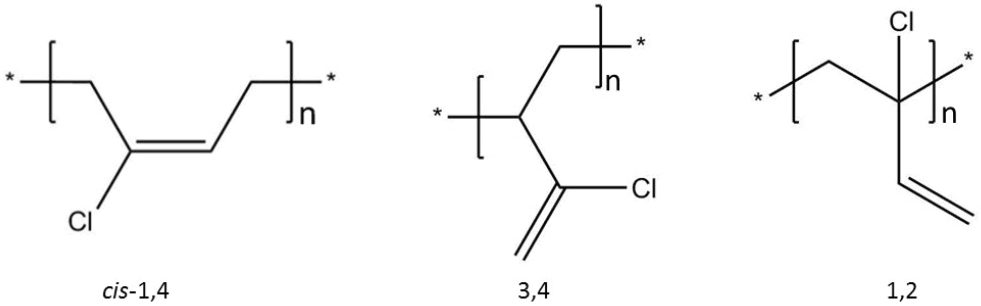

Figure 12: Incorporation of chloroprene monomers into the polymer chain.

The vulcanization of the CR latex with metal oxides occurs via the 1,2-structures by elimination of HCl. The elimination of the Cl-atome opposite the 1,2-vinyl group is easy since it is bonded to a tertiary C-atom and in an allylic position to the double bond. Thus, a certain amount of 1,2-structure is necessary, even though it can also promote ageing [1].

Due to the electronegative Cl-atom the reactivity of the double bond is low resulting in a good weather, ozone and ageing resistance as well as low flammability. Furthermore it has a moderate resistance towards oil, fuels and other chemicals [1,19].

Chloroprene rubber latex is mainly used for dipped articles like meteorological balloons and rubber gloves, as well as for impregnating, coating and lining woven tissues. In addition moulded foams for chair upholstery and mattresses are made of CR-latex. Further applications are binding agents, elastic concrete and improvement of bitumen [1].

2.2.3 Compounding additives

Since latex is a colloidal dispersion in an aqueous medium, all additives must be in form of dispersions or emulsions in order to be miscible and to avoid the disruption of the colloidal balance. For the preparation of dispersions the powder is grinded in the presence of water, a dispersing agent and a suspending agent. Also a pH modifier and a wetting agent for the reduction of the surface tension can be used. An emulsion is made by the reduction of oil drops to microscopic size in a water-miscible medium [1,4].

The addition of vulcanization agents, activators and accelerators influences the rate and state of cure. With the right combination of those additives the desired physical properties of the latex product can be optimized [4].

2.2.3.1 Vulcanization agents

During vulcanization the molecular chains are connected to each other. This happens mostly at elevated temperatures with the help of cross-linkers. Colloidal sulphur is the most commonly used vulcanization agent for all latices containing a diene group. The sulphur dosage depends on the desired cure rate and the amount of other additives used and is generally between 0.3-2.5 phr. For optimum heat resistance also sulphur donors like TMTD (Tetramethylthiuramdisulfide) in combination with thiourea and a metal

oxide are used. In chloroprene rubber latex, however, the chains are crosslinked by the addition of 4.0-5.0 phr zinc oxide forming zinc chloride. Besides, the age resistance of CR is improved by zinc oxide because it acts as a scavenger for the liberated chlorine. Also carboxylated rubbers need metal oxides as a cross-linker. Moreover, natural rubber latex can be vulcanized by organic peroxides and hydroperoxides leading to a higher translucency of the product [4,25,26,27].

2.2.3.2 Vulcanization activators

Since the curing with the sulphur alone would take days, the addition of an activator is necessary. Therefore 0.5-2.5 phr zinc oxide can be used, whereat the cure time is reduced to hours [4,25].

2.2.3.3 Vulcanization accelerators

By the addition of a vulcanization accelerator the cure time is reduced to minutes. There are several accelerators available, but for latex products mostly dithiocarbamates, thiazoles, thiurams or xanthates are used. For chloroprene rubber latex special accelerators such as 1,3-Diphenylguanidin (DPG) or Thiocarbanilide are preferred [1,4,26].

2.2.3.4 Other ingredients

Antioxidants are used in order to protect the latex against attacks of oxygen. However, if the latex is compounded in the presence of a metal dithiocarbamates, it is only necessary to use antioxidants if the article is intended to serve at severe conditions (e.g. for washing with strong detergent) or the product is very thin. The most widely applied antioxidants are sterically hindered mono-, di- and polynuclear phenols because of their minimal discoloration and staining. A better protection performance is achieved by amines like benzimidazoles or arylamines, but their application is limited to areas where discoloration and staining are of no consequence, for example as adhesives for paper [1,4,26].

In comparison to solid rubbers, inorganic fillers like whiting, china clay or slate flour do not have the typical reinforcement effect on latex products. They are only added to obtain cheaper products and to influence the compound flow behaviour. Upon stretching of the latex film, poorly dispersed fillers can be observed which can lead to pinholes and therefor

defects of the product. However, latex articles, which will not be stretched, can be highly filled. Besides, organic fillers like resins can be added to improve the tackiness of an adhesive [4,26].

For the coloration of the latex products inorganic and organic pigments are used. For example, carbon black is mainly used as black pigment. For organic pigments the migration tendency must be considered to ensure constant coloration [1].

Depending on the latex manufacturing process and the application, there are several other additives like wetting agents, foaming agents, antifoams, viscosity modifiers, surface-active agents, fire retardants and corrosion inhibitors [1,4,25-27].

2.3 Latex manufacturing processes

The manufacture of the latex to a certain product is much easier than the processing of the solid rubber. Once the latex is mixed with the required additives, the shaping and coagulation can be performed by different methods like dipping, foaming, casting, etc. [19].

2.3.1 Dipping method

The largest application of latex are dipped products like household gloves, surgical gloves, industrial gloves, balloons, feeding bottle teats, contraceptives, etc. Most of them are processed by coagulant dipping. Therefore, the cleaned and heated formers, which are usually made of porcelain but can also be glass, plastic wood etc. are first dipped into a coagulant solution bath for a certain dwell time. There are several coagulants like calcium chloride or cyclohexyl ammonium acetate, whereat calcium nitrate is the most common one. The coagulant solution can also include a parting agent like calcium carbonate, which prevents the solid latex from adhering to the former. Upon drying, a uniform coating of the coagulant is accomplished on the formers, which is completely incompatible with the latex. Then the formers are dipped into the latex bath, whereat the coagulant is re-dissolved. This leads to a high concentration of the salt in the vicinity of the former resulting in a destabilization of the latex, which then forms a layer on the former (Figure 13). Optionally, the latex may be pre-vulcanized, whereat the curing is partially developed before dipping.

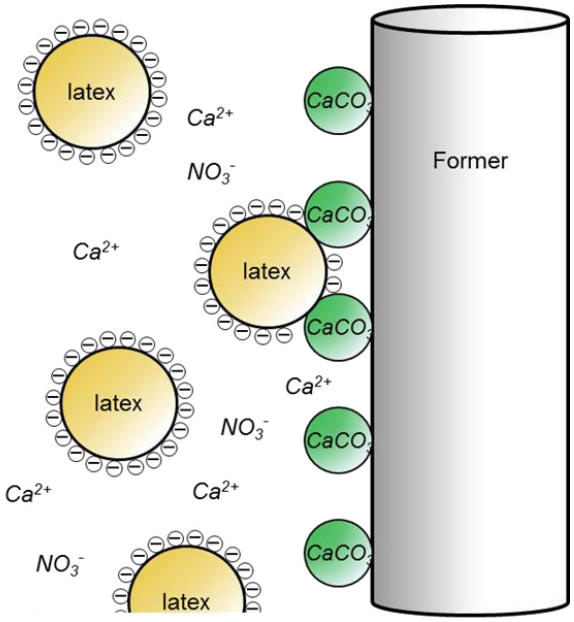

Figure 13: Coagulant dipping mechanism (based on [24]).

After a certain dwell time the former is removed and the deposited latex builds up some wet-gel strength. The formers are then immersed into hot water for the leaching process, whereat all water-soluble agents like residual coagulant and stabilizers are removed. Afterwards the former is put in an oven when the leached latex is dried and vulcanized. After removing the former from the oven, the processing can vary significantly. Since there is some residual tack, the latex can be powdered or chlorinated, which can be performed before stripping from the former (on-line) or as a post-treatment.

The final thickness of the produced latex is an important characteristic and is essentially influenced by the dwell time in the latex bath, the concentration of the latex and the number of dipping processes (single- or multi-dipping). Thin-walled products like membranes or condoms are produced without any coagulants (straight-dipping). In this process the latex is deposited on the former only because of the viscosity and the tendency to wet the former.

Very thick deposits can be obtained by heat-sensitized dipping, where a heat-sensitized compound is added to the latex. In general, aluminium formers are used, which are first heated and then dipped into the cooled latex. Thus, the heat-sensitizer is activated leading to a coagulation of the latex on the former. The final thickness depends on the temperature and heat capacity of the former as well as the heat sensitivity of the latex compound [4,16,19,24,26].

2.3.2 Foaming process

Mattresses and pillows can be produced by the foaming process. Two different methods can be distinguished: the Dunlop and the Talalay process, whereat also combinations of these two are possible.

In the Dunlop process the latex is mechanically frothed by the introduction of air or other gases. The foaming tendency depends on the pH and can be increased by adding foam promoters like potassium oleate. The foamed latex is then gelled in the suitable mould. As a gelling agent often sodium silicofluoride is used. The vulcanization is carried out by steam under atmospheric pressure. The vulcanized latex foam is then stripped of the mould, trimmed and washed.

In the Talalay process the foaming of the latex is achieved by applying a vacuum on the closed mould or / and by catalytically decomposition of hydrogen peroxide. Subsequently lowering of the temperature leads to freezing of the latex. Afterwards carbon dioxide is introduced, whereat the latex is gelled.

However, many latex foam products are replaced by polyurethane foam because of the cheaper and simpler processing. Nevertheless, high quality latex mattresses, pillows and carpet backings are still produced [4,19,26].

2.3.3 Casting process

Latex toys and bulbs are produced by the casting process, where the latex is gelled in the inside of a mould cavity. Several different modes of moulds are possible like slush and rotational moulding. For the slush moulding the latex is poured into the mould. After the desired thickness is achieved, the residual latex is removed leaving the latex film on the inside of the mould. For the rotational moulding a just sufficient amount of latex is filled into the moulds, which is then rotated over several axes simultaneously for an even spreading. Irrespective which mode is used, the mould can be opened after drying of the latex and the product can be extracted [4,19,26].

2.3.4 Other methods

In addition to the listed manufacturing processes there are more ways to produce latex goods like for example extrusion, by which latex threads can be obtained. Paper coatings, carpet backing as well as textile treatments can be manufactured by latex spreading. Adhesives can be engineered using resins or modifiers [4,26].

3 AIM OF THE THESIS

The aim of this thesis is to investigate a latex blend, which can be used as a material for synthetic examination gloves. It should possess better or the same mechanical properties with additional wear comfort as the gloves made out of natural rubber latex. Moreover, a proper setup of analytical tools for the characterization of the latex blends should be determined.

Two different latex blends were taken into account:

- isoprene rubber latex (IR) blended with chloroprene rubber latex (CR)
- nitrile rubber latex (NBR) blended with chloroprene rubber latex (CR).

For the purpose of comparison, also natural rubber latex (NR) was blended with chloroprene rubber latex (CR). To investigate the influence of the blend ratio on the mechanical properties, samples with the ratios 100:0, 75:25, 50:50, 25:75 and 0:100 (w:w, based on the dry rubber content) were produced. To get a general idea about the miscibility of the different latexes, samples without pre-vulcanization were studied first. Based on this preliminary study, the influence of pre-vulcanization using a vulcanizing agent was tested.

All latex blends were investigated by tensile tests focused on the tensile strength, ultimate elongation and the stress at 100 % elongation. Moreover, the samples were examined with an environmental scanning electron microscope coupled with energy dispersive X-ray spectroscopy (ESEM-EDX). Further characterization was carried out using a differential scanning calorimeter (DSC).

4 EXPERIMENTAL

4.1 Materials and equipment

Table 1: List of used chemicals.

Chemical	Source	Purity
Natural rubber latex (60 drc)	Semperit Technische Produkte GmbH	Technical
Isoprene rubber latex (60 drc)	Semperit Technische Produkte GmbH	Technical
Nitrile rubber latex (40 drc)	Kumho	Technical
Chloroprene rubber latex (Lipren T, 60 drc)	Synthomer	Technical
Coagulation solution	Semperit Technische Produkte GmbH	Technical
Potassium hydroxide	Roth	≥ 85 %
PM30 dispersion	Semperit Technische Produkte GmbH	Technical
ZnO dispersion	Semperit Technische Produkte GmbH	Technical
Starch (Maizena®)	Unilever Austria	-

Table 2: List of used devices.

Device	Producer
Micrometer screw	Mitutoyo
Oven kelvitron®t	Heraeus
Tensile tester (AGS-X – 5 kN)	Shimadzu
Environmental scanning electron microscope (Quanta 200) coupled with energy dispersive X-ray spectroscopy (EDAX)	FEI, Genesis
Environmental scanning electron microscope (Quanta 600) coupled with energy dispersive X-ray spectroscopy (EDAX)	FEI, Genesis
Differential scanning calorimeter	Mettler Toledo [1)]

1) Measured by Semperit Technische Produkte GmbH.

4.2 Preparation of the latex blends

All latex blends were prepared by the coagulant dipping method (Figure 14). Therefore, porcelain formers were thoroughly cleaned with distilled water and acetone and heated up to 100-120 °C (depending on the type of latex) in the oven. In the first step the formers were dipped for 30 seconds into the coagulation solution containing calcium chloride as coagulant and calcium carbonate as a release agent. After drying in the oven, the formers were immersed into the latex bath for 20 seconds, which was cooled with water, and dried again. The drying conditions as well as the preparation of the latex bath are described in the chapters 4.2.1 – 4.2.3. The samples were then stripped of and powdered with starch.

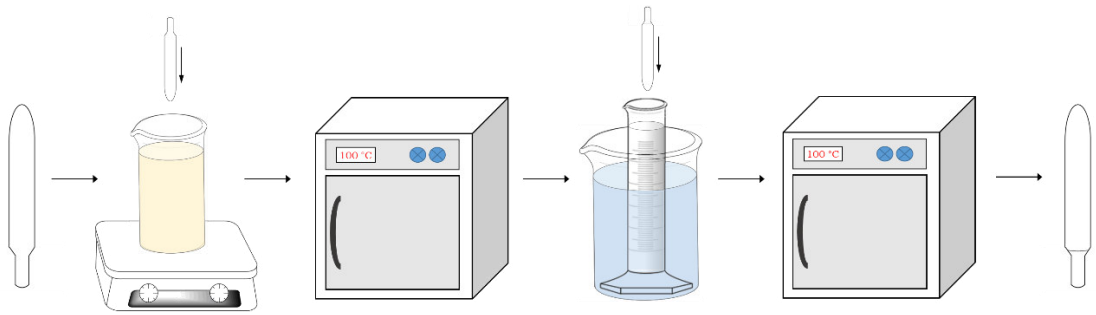

Figure 14: Coagulant dipping method.

4.2.1 Preparation of NR/CR-latex blends

For the preparation of the NR/CR-latex blends, natural rubber latex and chloroprene rubber latex were mixed for around 2 minutes at room temperature with the following blending ratios (w:w; based on the dry rubber content):

Table 3: Blend ratios for NR/CR-latex blends.

NR/CR-latex blends
100 % NR / 0 % CR
75 % NR / 25 % CR
50 % NR / 50 % CR
75 % NR / 25 % CR
0 % NR / 100 % CR

The mixture was diluted to a dry rubber content of 40% using distilled water and 2 wt% of KOH (10 wt%). The solution was then gently stirred at room temperature for around 10 minutes before dipping.

In case of pre-vulcanization, also 3.5 phr PM30 were added and the mixture was stirred at 50 °C for 3 hours.

After dipping, the formers were dried in the oven at 120 °C for 20 minutes.

4.2.2 Preparation of IR/CR-latex blends

The preparation of the IR/CR-latex blends was similar to that of the NR/CR, except the drying conditions. Blends with the following ratios were produced (w:w; based on dry rubber content):

Table 4: Blend ratios for IR/CR-latex blends.

IR/CR-latex blends
100 % IR / 0 % CR
75 % IR / 25 % CR
50 % IR / 50 % CR
75 % IR / 25 % CR
0 % IR / 100 % CR

The IR/CR-latex blends with the blending ratio 100:0, 75:25 and 50:50 were dried at 100 °C for 15 minutes. The blends with the ratio 25:75 and 0:100 were dried at the same temperature for 17 minutes.

Furthermore, one IR/CR-latex blend with the ratio 50:50 was prepared, which contains PM30 together with ZnO as vulcanization agents. Therefore, ZnO (1.75 phr) was used to pre-vulcanize the CR-latex, whereat the IR-latex was pre-vulcanized with PM30 (1.75 phr). After pre-vulcanization, the two latexes were mixed together and stirred for around 2 minutes.

To investigate the influence of the drying temperature, blends with the ratio 75:25, 50:50 and 25:75 containing 3.5 phr PM30 were dried at 110 °C for 30 minutes. These IR/CR-latex blends were not pre-vulcanized and are indicated with an additional [110°C] after the blend name in this thesis.

4.2.3 Preparation of NBR/CR-latex blends

For the production of NBR/CR-latex blends, nitrile rubber latex was mixed with chloroprene rubber latex for around 2 minutes at room temperature with the following blending ratios (w:w, based on the dry rubber content):

Table 5: Blend ratios for NBR/CR-latex blends.

NBR/CR-latex blends
100 % NBR / 0 % CR
75 % NBR / 25 % CR
50 % NBR / 50 % CR
75 % NBR / 25 % CR
0 % NBR / 100 % CR

The pH-value of the mixture was adjusted by adding KOH (1 wt%). Then the solution was gently stirred for around 10 minutes before dipping.

For pre-vulcanized samples 3.5 phr of ZnO were added and the mixture was stirred at 50 °C for 3 hours.

After dipping, the NBR/CR-latex blends were dried in the oven at 120 °C for 20 minutes.

4.3 Characterization methods

4.3.1 Tensile test

To investigate the mechanical properties of the blends, shouldered bars were stamped out and extended by the tensile tester. Two different shouldered bars were used: one with a

clamping length of 50 mm (1), which is usually for thermoplastics, and one with a clamping length of 75 mm (2), which is generally for elastomers (Figure 15). Since the geometry of the shoulder differs, the results obtained by the two different shouldered bars cannot be entirely compared with each other.

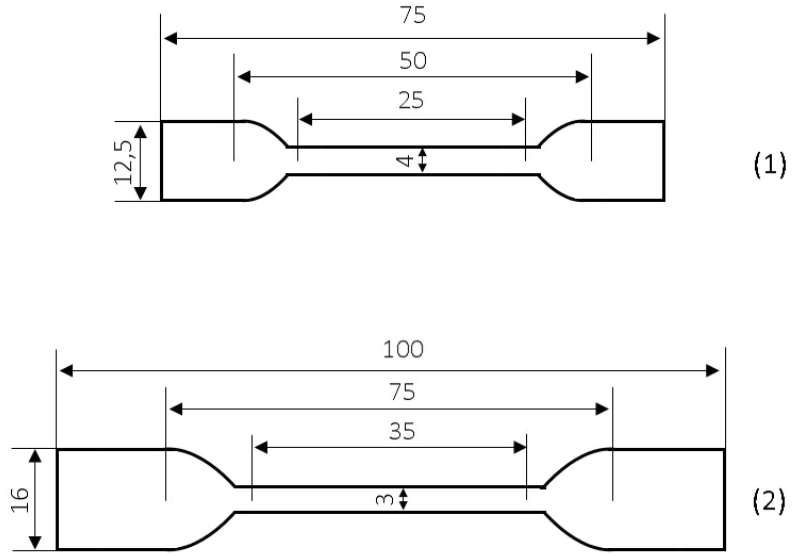

Figure 15: Geometry of the shouldered bars.

The parameters for the tensile test are described in Table 6.

Table 6: Parameters for the tensile tests.

Parameters for tensile tests	
Testing speed [mm / min]	500
Gauge length [mm]	50 or 75
Width [mm}	4 or 3
Sensitivity [%]	10
Level / %FS [%]	0.02

4.3.2 Environmental scanning electron microscopy – energy dispersive X-ray spectroscopy (ESEM-EDX)

For the investigation of the morphology, experiments with an environmental scanning electron microscope coupled with an energy dispersive X-ray spectrometer were carried out. The imaging was performed in the low vacuum mode, while high voltage was applied. Simultaneously the image of the secondary electrons (SE) and the backscattered electrons (BSE) were observed. The experiments were done with the parameters described in Table 7.

Table 7: Parameters for the ESEM-EDX experiments.

Parameters for ESEM-EDX	
Magnification	200 – 3000
Detector	LFD / SSD
Pressure [Pa]	40
Gas	H_2O

The surface of the blends without starch was analysed using the ESEM Quanta 600. Because of a defect of the microscope, all other experiments were carried out with the ESEM Quanta 200.

For further investigations, thicker samples were prepared. Therefore, the coagulant was applied evenly in a hot metallic form and dried in the oven. Then the latex mixture was pipetted onto the form, dried, frozen with nitrogen and broken. The fracture area was then characterized. To compare the results of the thicker samples with the conventionally prepared blends, some blends obtained by the dipping method were also broken after being frozen in nitrogen and the fracture area was analysed.

In addition EDX-Mapping of the fracture area of IR/CR-latex blends were carried out using 4 frames and a dwell time of 1000 sec.

4.3.3 Differential Scanning Calorimetry (DSC)

DSC measurements were performed by Semperit Technische Produkte GmbH to investigate the miscibility of the different latexes. The parameters are described in Table 8.

Table 8: Parameters for the DSC measurements.

Parameters for DSC	
Temperature range [°C]	-120 – 300
Rate of heating [K/min]	15
N_2 gas flow[ml/min]	50

5 RESULTS

5.1 Preparation of the thin-film latex blends

All latex blends were prepared by the coagulant dipping method, whereby thin-films were obtained. Samples with and without pre-vulcanization were produced. Generally, all latex blends show a smooth surface.

However, the NR/CR- and IR/CR-latex blends without pre-vulcanization with the blending ratio 100:0 and 75:25 showed flowmarks before drying, which almost disappeared after vulcanization. When the samples were pre-vulcanized, no flowmarks were formed.

During the pre-vulcanization of 100 % CR-latex with PM30 small grains were formed, which lead to an uneven surface. Moreover, a thick film on the surface of the solution was developed during the pre-vulcanization. When CR-latex was pre-vulcanized with ZnO, no formation of grains or a thick film was observed.

5.2 Thickness of the different thin-film latex blends

The thickness of the resulting thin-films was determined with a micrometre screw. The results constitute an average of at least 6 samples, whereat each sample was measured 5 times at different spots. In Table 9 the thickness for the samples without pre-vulcanization are shown.

Table 9: Thickness of the latex blends without pre-vulcanization.

Sample	**Thickness [mm]**
100 % NR	0.283 ± 0.045
75 % NR / 25 % CR	0.309 ± 0.021
50 % NR / 50 % CR	0.272 ± 0.026
25 % NR / 75 % CR	0.207 ± 0.026
100 % IR	0.244 ± 0.021

Sample	Thickness [mm]
75 % IR / 25 % CR	0.214 ± 0.015
50 % IR / 50 % CR	0.202 ± 0.017
25 % IR / 75 % CR	0.197 ± 0.024
100 % NBR	0.091 ± 0.006
75 % NBR / 25 % CR	0.113 ± 0.002
50 % NBR / 50 % CR	0.119 ±0.005
25 % NBR / 75 % CR	0.179 ± 0.011
100 % CR	0.174 ± 0.020

The blends containing NR-latex are the thickest, whereat the thickness decreases with increasing amounts of CR-latex. Also the thickness of the IR/CR-latex blends is decreasing with increasing amounts of CR-latex. The pure NBR-latex has a thickness of only 0.091 mm and thus represents the thinnest sample. In contrast to the NR- and IR-blends, the thickness of the NBR/CR-latex blends increases with increasing amounts of CR-latex. The reason for the low thickness of the NBR/CR-latex blends may be that calcium chloride was used as a coagulant instead of calcium nitrate, which is generally used as a coagulant for NBR-latex [26].

Table 10: Thickness of the pre-vulcanized latex blends.

Sample	Thickness [mm]
100 % NR + PM30	0.307 ± 0.025
75 % NR / 25 % CR + PM30	0.279 ± 0.004
50 % NR / 50 % CR + PM30	0.248 ± 0.004
25 % NR / 75 % CR + PM30	0.220 ± 0.005
100 % IR + PM30	0.270 ± 0.022

Sample	Thickness [mm]
75 % IR / 25 % CR + PM30	0.233 ± 0.026
50 % IR / 50 % CR + PM30	0.206 ± 0.018
25 % IR / 75 % CR + PM30	0.198 ± 0.009
100 % NBR + ZnO	0.091 ± 0.004
75 % NBR / 25 % CR + ZnO	0.112 ± 0.005
50 % NBR / 50 % CR + ZnO	0.135 ± 0.004
25 % NBR / 75 % CR + ZnO	0.218 ± 0.004
100 % CR + PM30	0.193 ± 0.014
100 % CR + ZnO	0.191 ± 0.009

Table 10 shows the measured thicknesses for the pre-vulcanized blends. Compared to the samples without pre-vulcanization (Table 9), the thickness for all blends is almost similar, but the standard deviation is slightly smaller. On the basis of the thickness, no difference between CR-latex vulcanized with PM30 (100 % CR + PM30) and CR-latex vulcanized with ZnO (100 % CR + ZnO) can be observed.

Table 11: Thickness of the IR/CR-latex blends dried at 110 °C and of the IR/CR-latex blend, where PM30 together with ZnO were used for the pre-vulcanization.

Sample	Thickness [mm]
75 % IR / 25 % CR + PM30 [110 °C]	0.243 ± 0.005
50 % IR / 50 % CR + PM30 [110 °C]	0.225 ± 0.004
25 % IR / 75 % CR + PM30 [110 °C]	0.200 ± 0.005
50 % IR / 50 % CR + PM30 / ZnO	0.209 ± 0.013

Table 11 shows the results of the IR/CR-latex blends, which were dried at 110 °C, and of the IR/CR-latex blends containing PM30 and ZnO as vulcanization agents. The thickness of the IR/CR-latex blends dried at 110 °C for 30 minutes is comparable to that of the conventional pre-vulcanized IR/CR-latex blends. Though, the standard deviation is clearly smaller for all blending ratios.

The sample 50 % IR / 50 % CR + PM30 / ZnO, where the IR-latex was pre-vulcanized with PM30 and the CR-latex was pre-vulcanized with ZnO before mixing, has the same thickness as the sample 50 % IR / 50 % CR + PM30, where the two latexes were mixed together and pre-vulcanized using PM30.

No clear difference between samples with or without pre-vulcanization can be observed. The reason therefore is that beside the primary particle size, the thickness only depends on the coagulant and the respective dwell time. The pre-vulcanization influences only the cross-linking, which has no impact on the final thickness.

5.3 Miscibility of the different latex blends

To investigate, if the latexes are miscible or not, DSC measurements were carried out by the Semperit Technische Produkte GmbH. For immiscible systems, two distinct glass transition temperatures (T_g) are obtained, which correlate with that of the used polymers. Also partially miscible blends show two glass transition temperatures, but they are shifted form the value of one component towards the T_g of the other component. In case of completely miscible latex blends only one T_g is observed, which is between the T_gs of both blend components. The results for the samples without pre-vulcanization are shown in Table 12.

Table 12: Measured glass transition temperature of the different latex blends without pre-vulcanization.

Sample	**Glass transition temperature (T_g) [°C]**
100 % NR	-60
75 % NR / 25 % CR	-60 / -37
50 % NR / 50 % CR	-61 / -37
25 % NR / 75 % CR	-62 / -38

Sample	Glass transition temperature (T_g) [°C]
100 % IR	-61
75 % IR / 25 % CR	-61 / -38
50 % IR / 50 % CR	-62 / -38
25 % IR / 75 % CR	-62 / -38
100 % NBR	-22
75 % NBR / 25 % CR	-39 / -24
50 % NBR / 50 % CR	-39 / -20
25 % NBR / 75 % CR	-38 / -18
100 % CR	-39

All samples with a blend ratio 75:25, 50:50 and 75:25 show two distinct glass transition temperatures (T_g). For the NR/CR-latex blends the T_g at -60 °C belongs to the NR-latex and the T_g at -38 °C corresponds to the CR-latex. Since IR-latex has a similar structure as NR-latex, similar results were observed. The NBR/CR-latex blends show one T_g at -38 °C belonging to the CR-latex and one T_g at -22 °C corresponding to the NBR-latex. However, no shifting of the T_g can be observed for neither latex blend, which indicates that all blends represent immiscible systems.

For the IR/CR-latex blends without pre-vulcanization it is obvious that with increasing amounts of CR-latex the peak intensity of the T_g at -38 °C, corresponding to the CR-latex, increases, whereas the T_g at -60 °C, belonging to the IR-latex, decreases. The diagrams of the NR/CR-latex blends and the NBR/CR-latex blends show similar results. The diagrams for the latex blends without pre-vulcanization can be found in the appendix.

Table 13 shows the results for the latex blends with pre-vulcanization.

Table 13: Measured glass transition temperatures for the different pre-vulcanized latex blends.

Sample	Glass transition temperature (T_g) [°C]
100 % NR + PM30	-59
75 % NR / 25 % CR + PM30	-60 / -37(1)
50 % NR / 50 % CR + PM30	-60 / -37
25 % NR / 75 % CR + PM30	-61 / -37
100 % IR + PM30	-60
75 % IR / 25 % CR + PM30	-61 / -37
50 % IR / 50 % CR + PM30	-61 / -37
25 % IR / 75 % CR + PM30	-61 / -38
100 % NBR + ZnO	-22
75 % NBR / 25 % CR + ZnO	-39 / -22
50 % NBR / 50 % CR + ZnO	-39 / -21
25 % NBR / 75 % CR + ZnO	-39 / -21(1)
100 % CR + PM30	-38
100 % CR + ZnO	-39

(1) Only one T_g was evaluated in the diagram, though the second T_g is observable.

The results of the DSC measurements indicate that the pre-vulcanization does not influence the glass transition temperature. The measured glass transition temperatures of the pre-vulcanized latex blends are similar to that of the samples without pre-vulcanization. Again, no shifting of the T_g occurs, which indicates that the latexes are immiscible.

Figure 16 – Figure 20 show the DSC diagrams of the pre-vulcanized IR/CR-latex blends with the blending ratios 100:0, 75:25, 50:50, 25:75 and 0:100. Also for the pre-vulcanized samples the peak intensity at the T_g belonging to the CR-latex increases with increasing

amounts of CR-latex, whereas the peak at the other T_g is decreasing. The diagrams for the pre-vulcanized NR/CR- and the NBR/CR-latex blends can be found in the appendix.

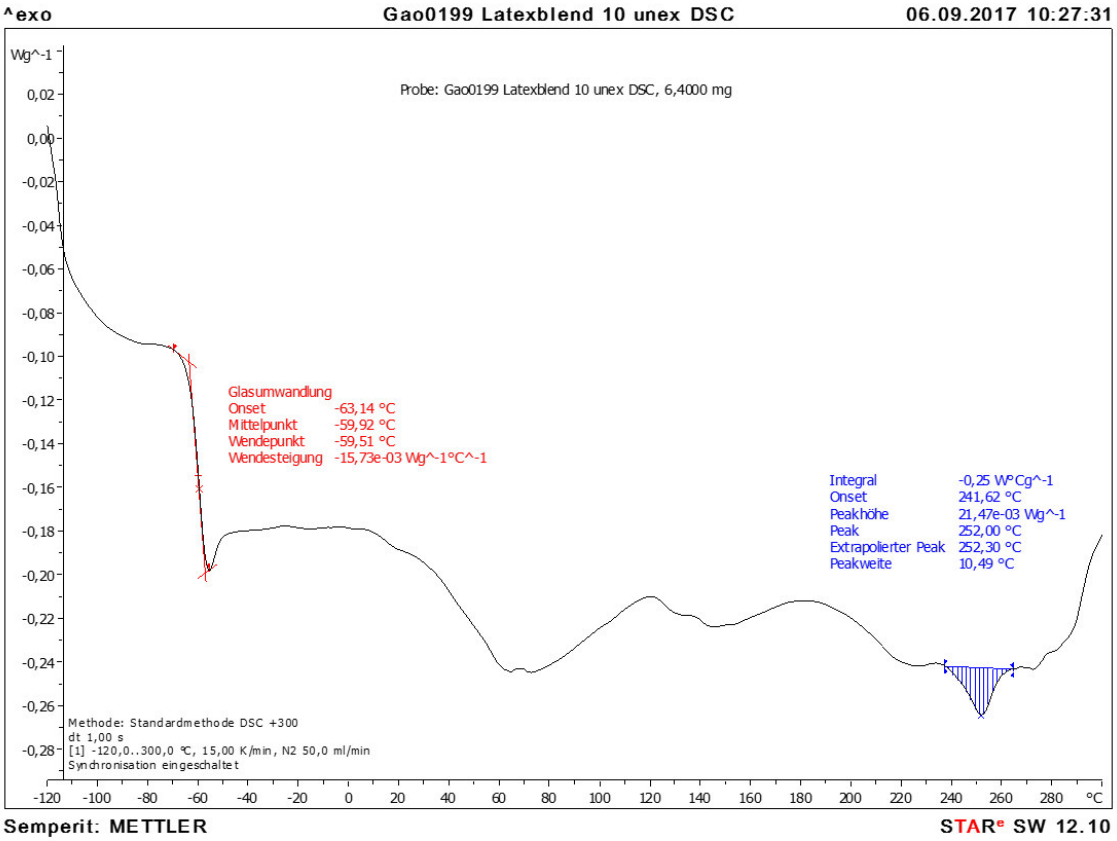

Figure 16: DSC diagram for the sample 100 % IR + PM30.

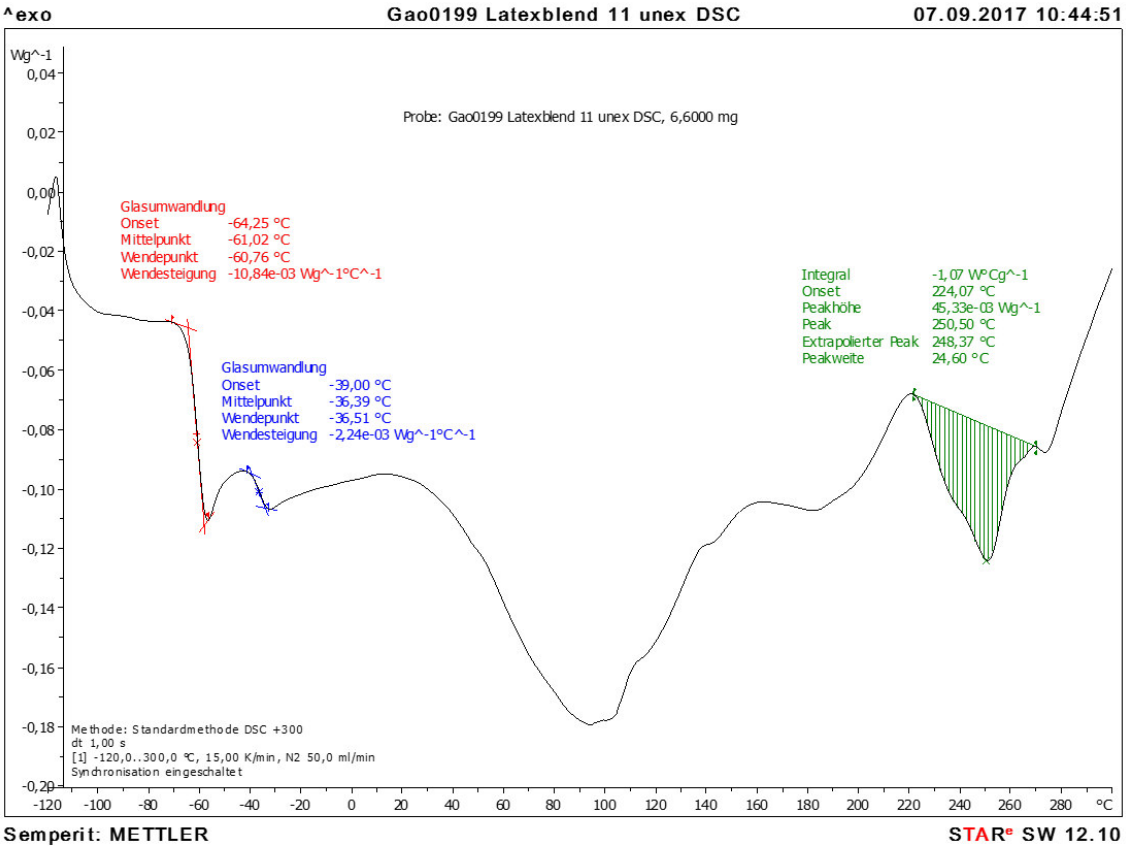

Figure 17: DSC diagram for the sample 75 % IR / 25 % CR + PM30.

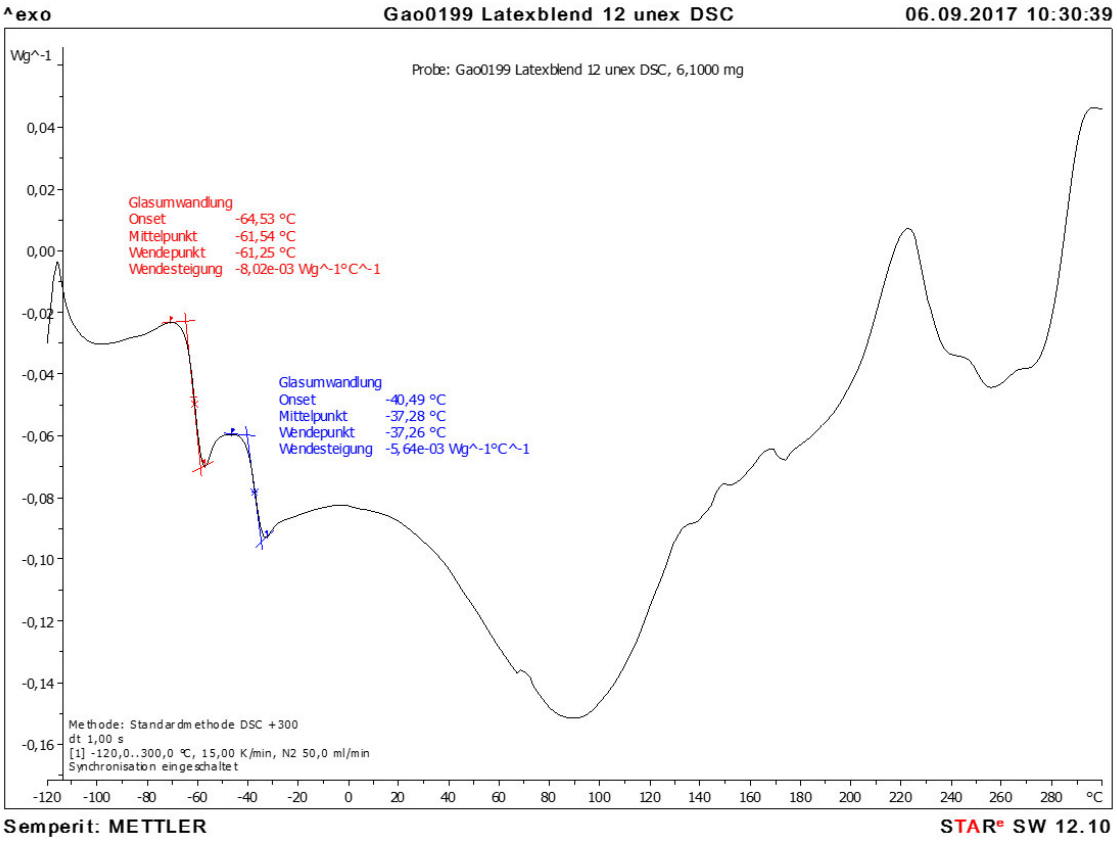

Figure 18: DSC diagram for the sample 50 % IR / 50 % CR + PM30.

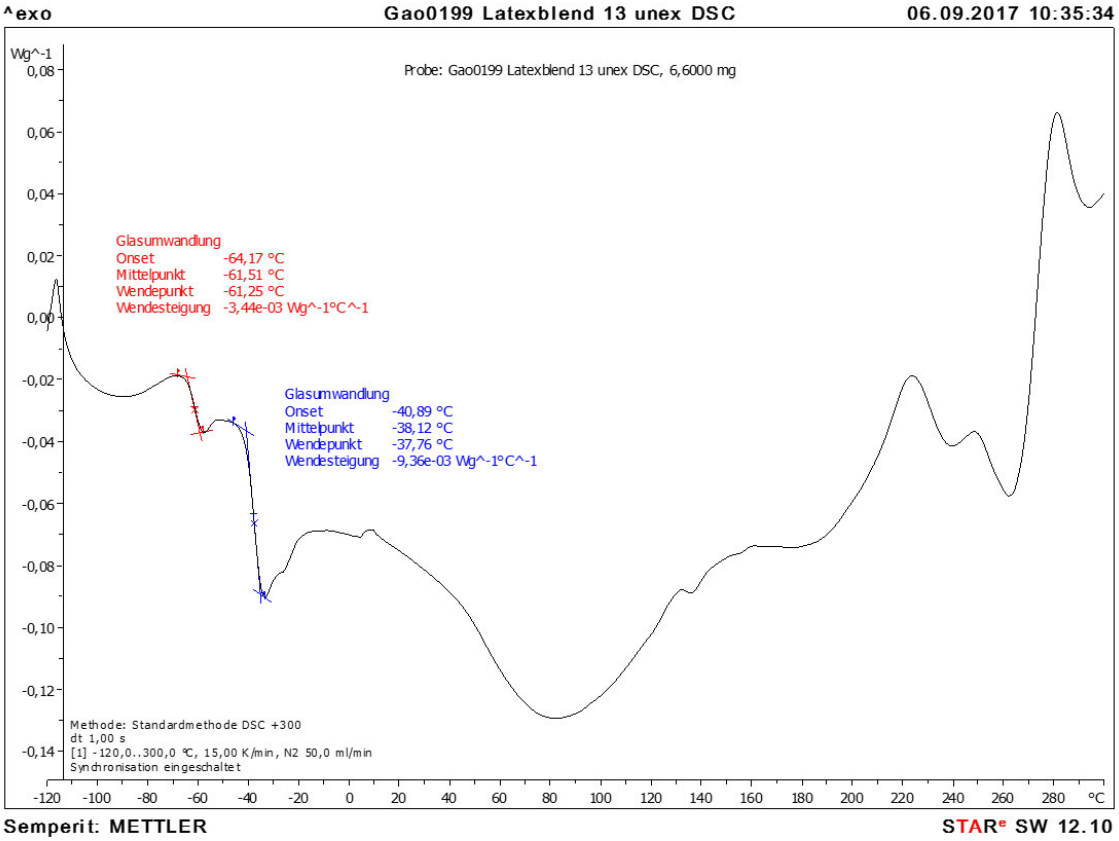

Figure 19: DSC diagram for the sample 25 % IR / 75 % CR + PM30.

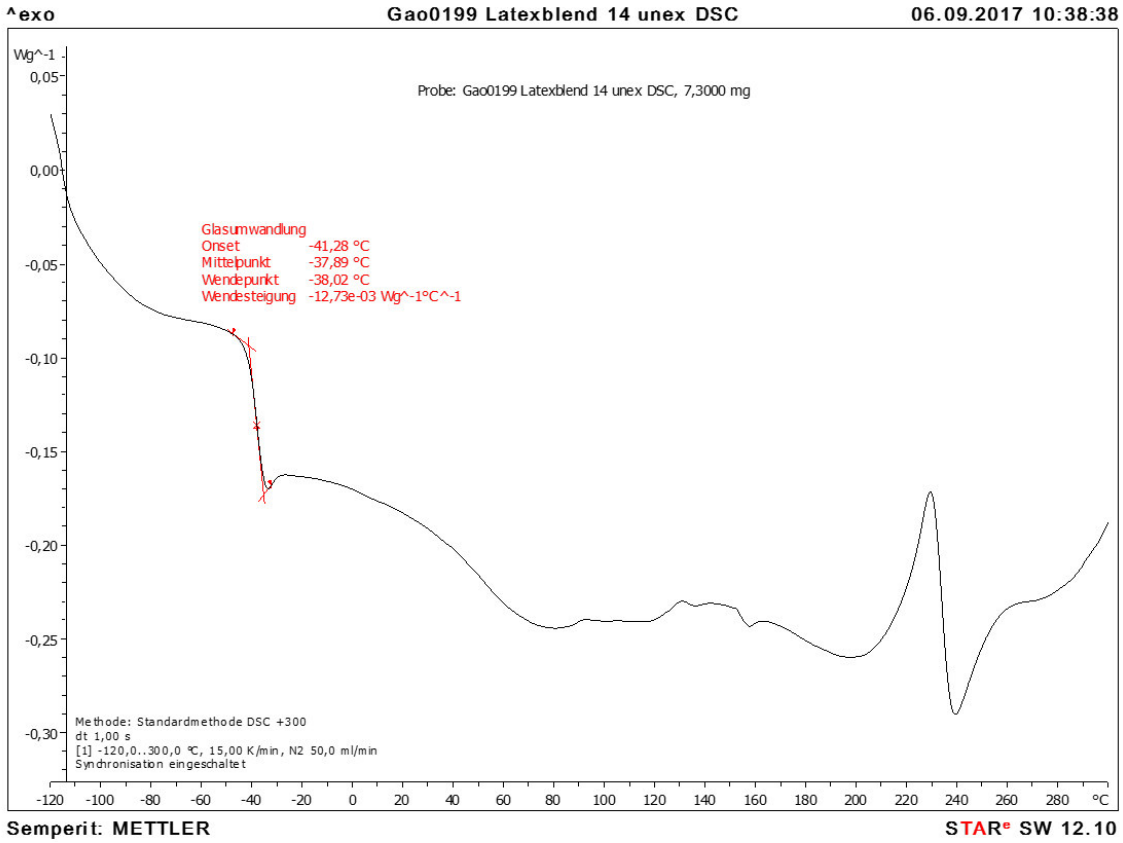

Figure 20: DSC diagram for the sample 100 % CR + PM30.

5.4 Morphology of the different latex blends

To investigate the morphology of the different latex blends, several experiments with the ESEM were carried out. During the measurements the samples got charged, resulting in an outshined picture produced by the secondary electrons (LFD detector). Hence, only the pictures of the back-scattered electrons (SSD detector) were interpreted. In this pictures, elements with a higher atomic number appear brighter than elements with a lower atomic number. With the ESEM Quanta 600 magnifications up to 3000 were possible. However, with the ESEM 200 no sharp pictures could be observed at magnifications more than 1200.

First, the surfaces without starch of different latex blends were investigated. The pictures for the NBR/CR-latex blends with and without pre-vulcanization as well as IR/CR-latex blends with different blending ratios are demonstrated in Figure 21 – Figure 33. All samples show similar results: no phase separation can be observed. Moreover, the distribution of the pre-vulcanization agents (PM30 or ZnO) seems very homogeneous. In some pictures bigger white spots can be observed, which are due to residual calcium, potassium, sulphur or zinc. They may be removed by washing the samples after drying. The dark spots on the sample 100 % CR + ZnO derive from residual starch (Figure 28). The white spot on the surface of 100 % CR + PM30 is due an oxygen inclusion (Figure 33).

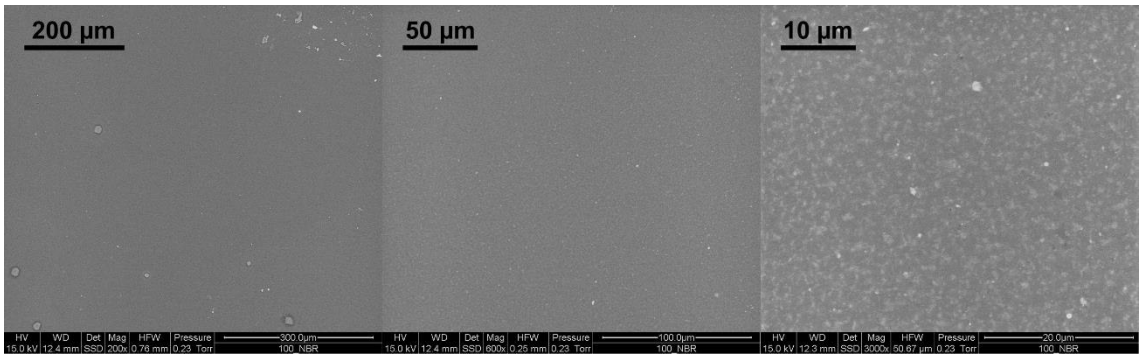

Figure 21: ESEM pictures of the surface of the sample 100 % NBR.

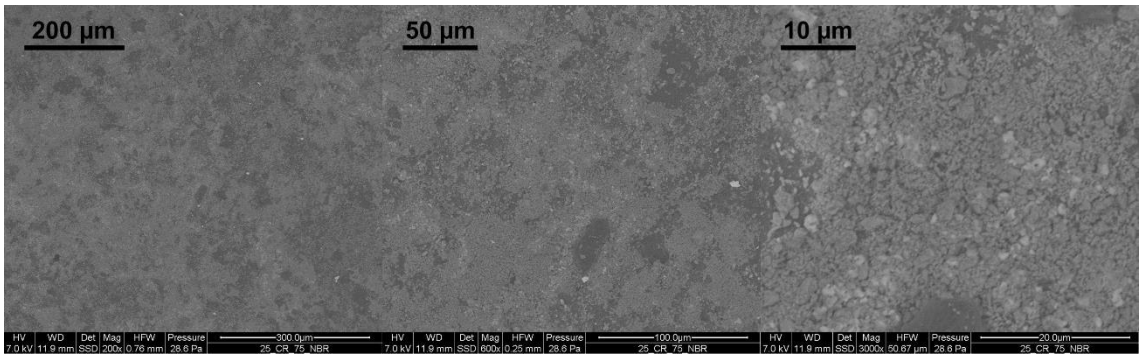

Figure 22: ESEM pictures of the surface of the sample 75 % NBR / 25 % CR.

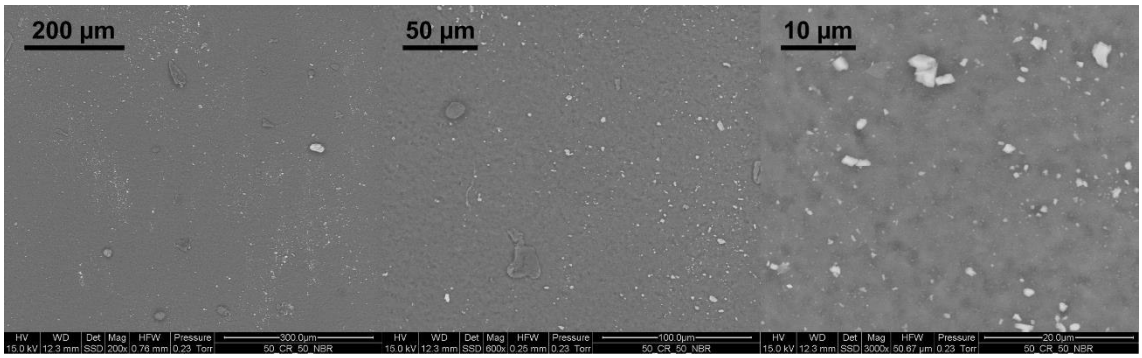

Figure 23: ESEM pictures of the surface of the sample 50 % NBR / 50 % CR.

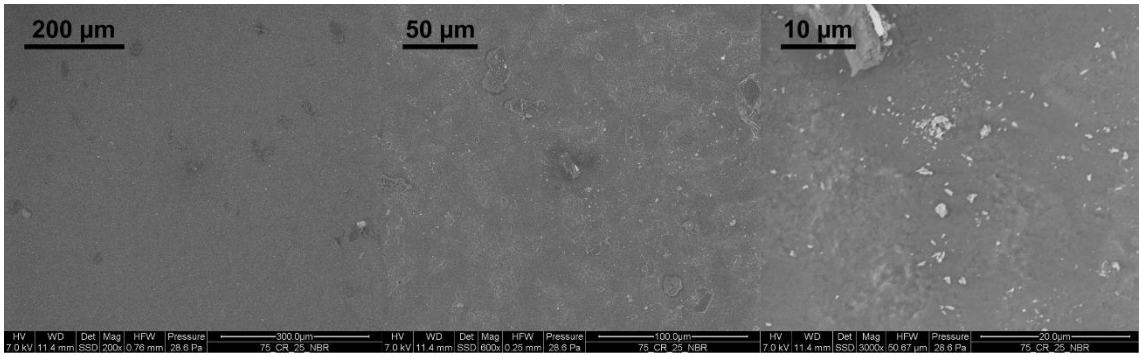

Figure 24: ESEM pictures of the surface of the sample 25 % NBR / 75 % CR.

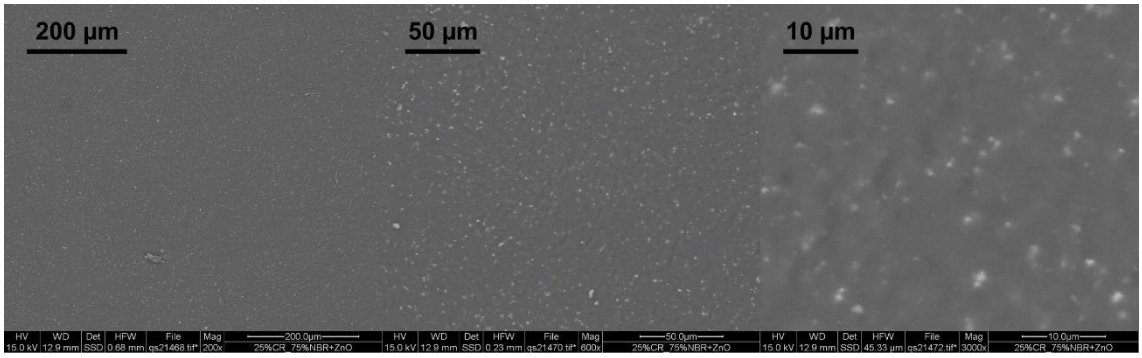

Figure 25: ESEM pictures of the surface of the sample 75 % NBR / 25 % CR + ZnO.

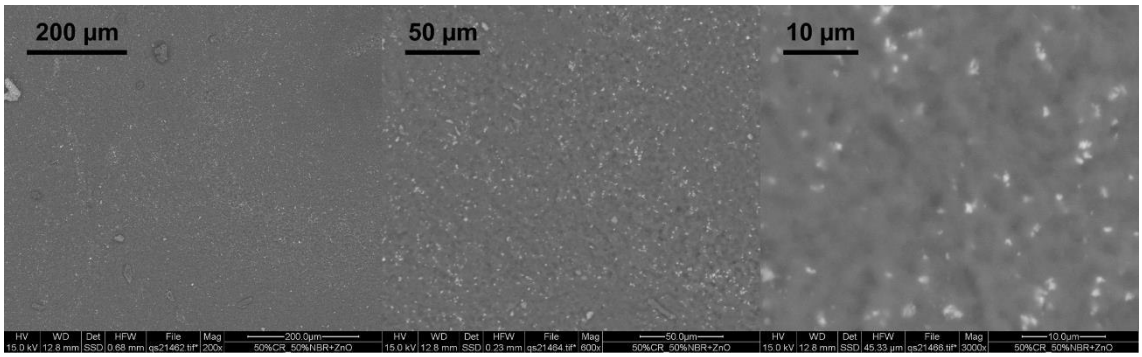

Figure 26: ESEM pictures of the surface of the sample 50 % NBR / 50 % CR + ZnO.

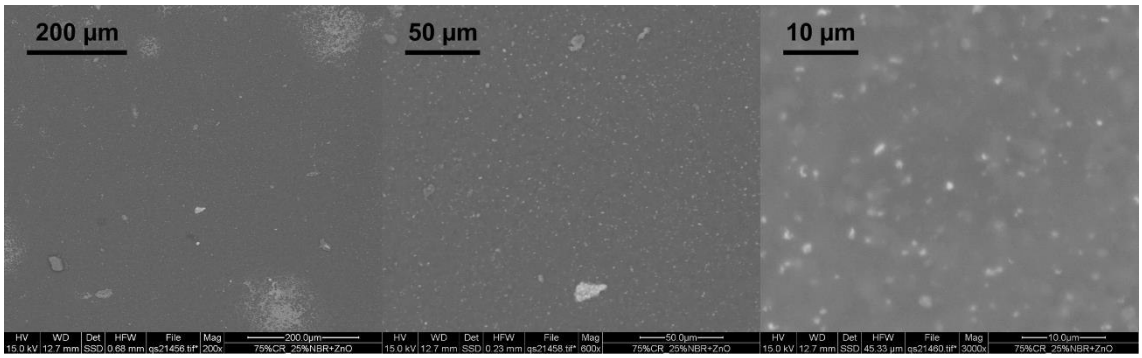

Figure 27: ESEM pictures of the surface of the sample 25 % NBR / 75 % CR + ZnO.

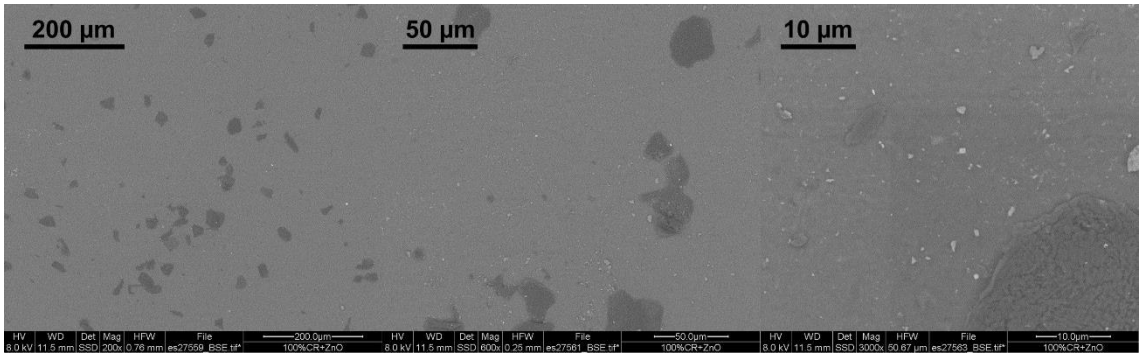

Figure 28: ESEM pictures of the surface of the sample 100 % CR + ZnO.

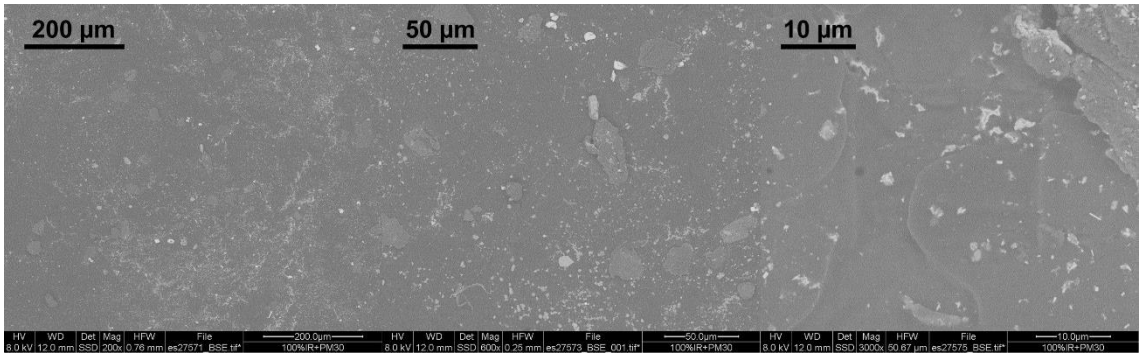

Figure 29: ESEM pictures of the surface of the sample 100 % IR + PM30.

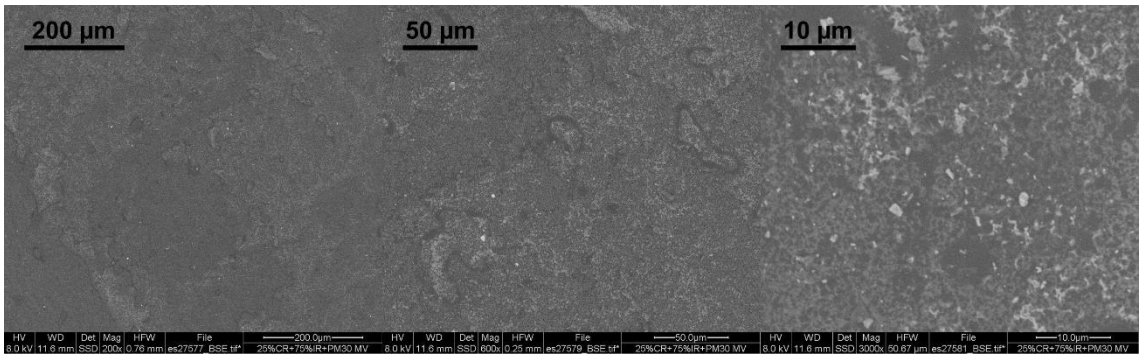

Figure 30: ESEM pictures of the surface of the sample 75 % IR / 25 % CR + PM30.

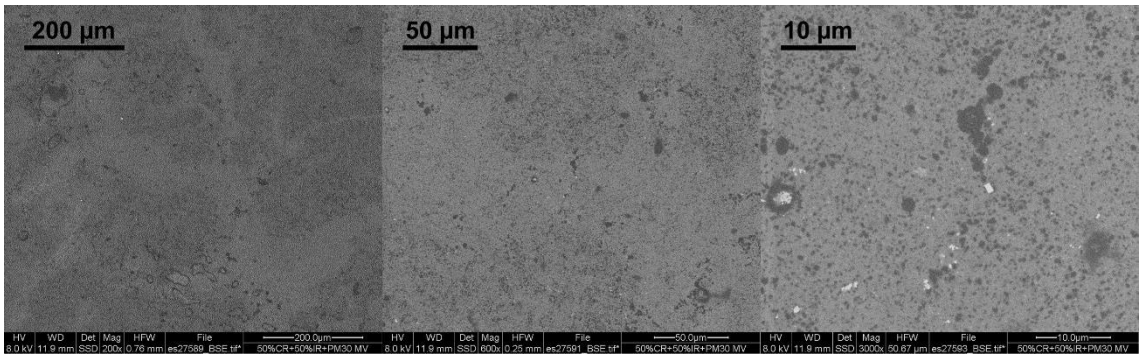

Figure 31: ESEM pictures of the surface of the sample 50 % IR / 50 % CR + PM30.

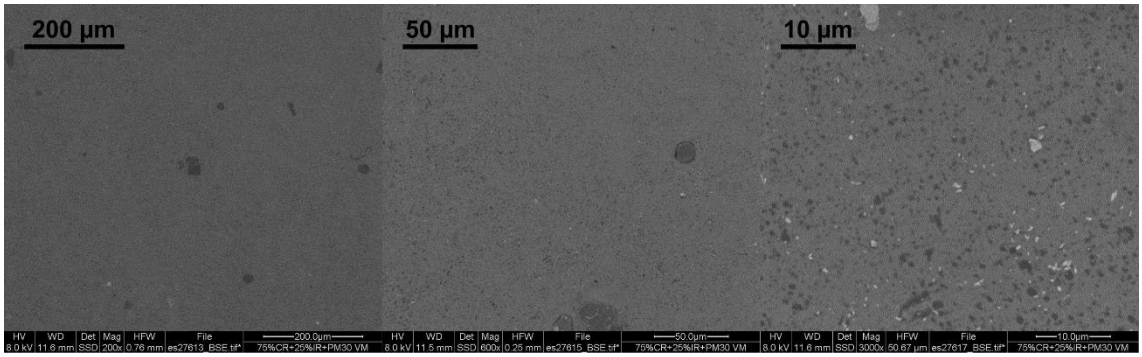

Figure 32: ESEM pictures of the surface of the sample 25 % IR / 75 % CR + PM30.

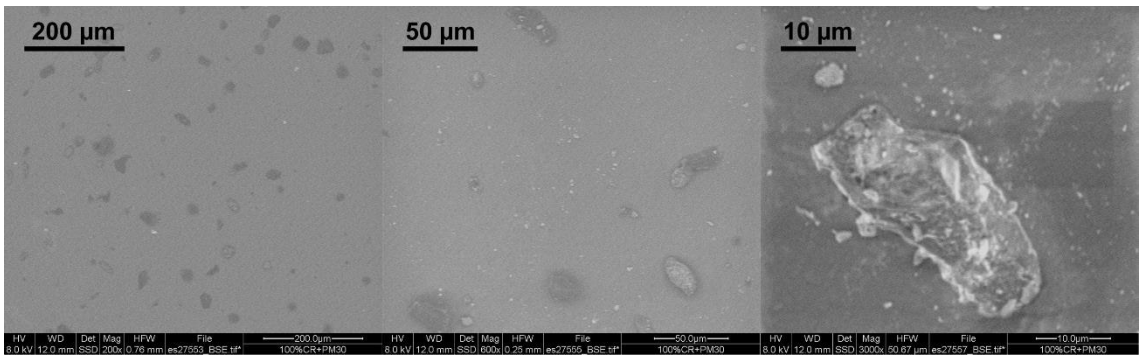

Figure 33: ESEM pictures of the surface of the sample 100 % CR + PM30.

Investigations of the fracture area of the thicker samples also show no phase separation (Figure 34 – Figure 38). Due to the different production, air bubbles and an inhomogeneous distribution of residual calcium, potassium, sulphur and zinc can be observed. In some pictures cubic particles can be seen. EDX measurements showed, that this cubes are zinc-chloride and potassium-chloride. However, the fracture area of the conventionally dipped latex blends (Figure 39 – Figure 43) show a very homogeneous distribution of vulcanization agents (PM30 and ZnO). No difference between the different blending ratios can be observed. The following figures show the results for the pre-vulcanized NBR/CR-latex blends in different blending ratios. The pictures of the other samples can be found in the appendix.

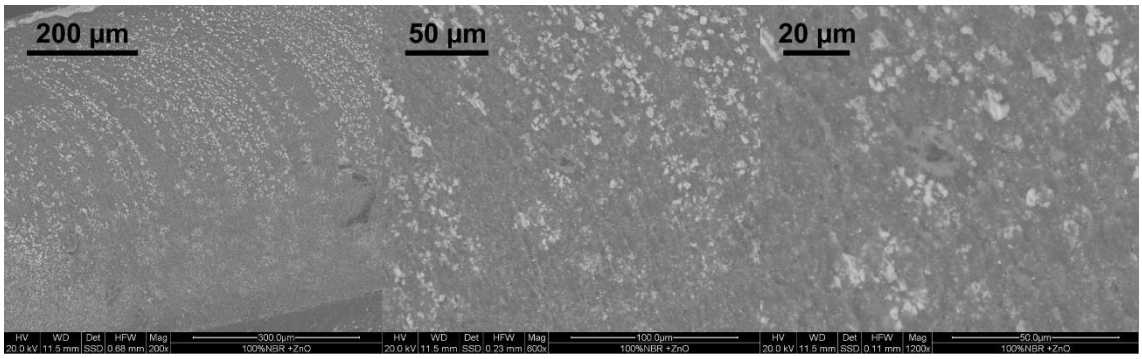

Figure 34: ESEM pictures of the fracture area of the thicker sample 100 % NBR + ZnO.

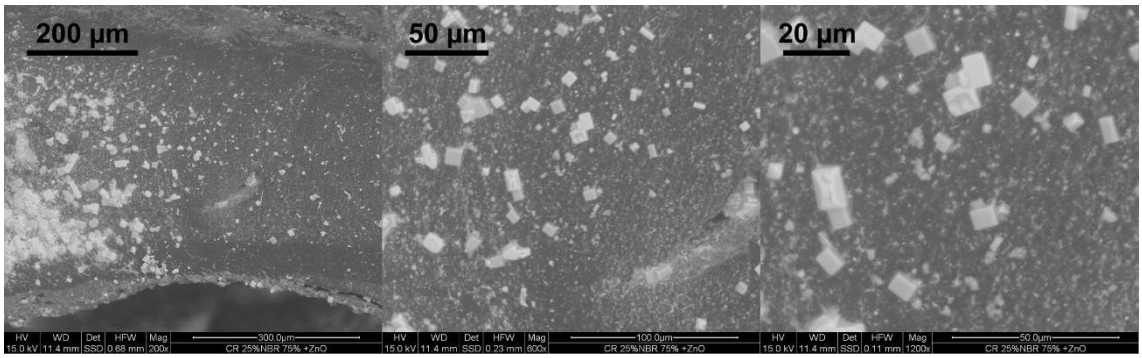

Figure 35: ESEM pictures of the fracture area of the thicker sample 75 % NBR / 25 % CR + ZnO.

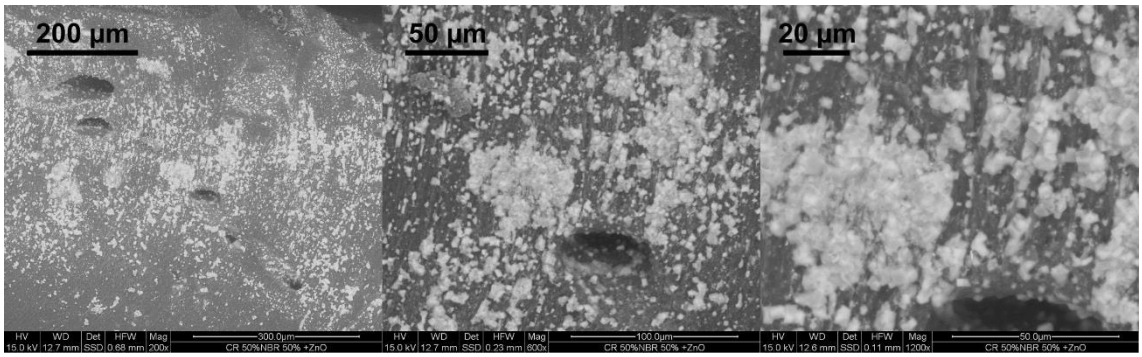

Figure 36: ESEM pictures of the fracture area of the thicker sample 50 % NBR / 50 % CR + ZnO.

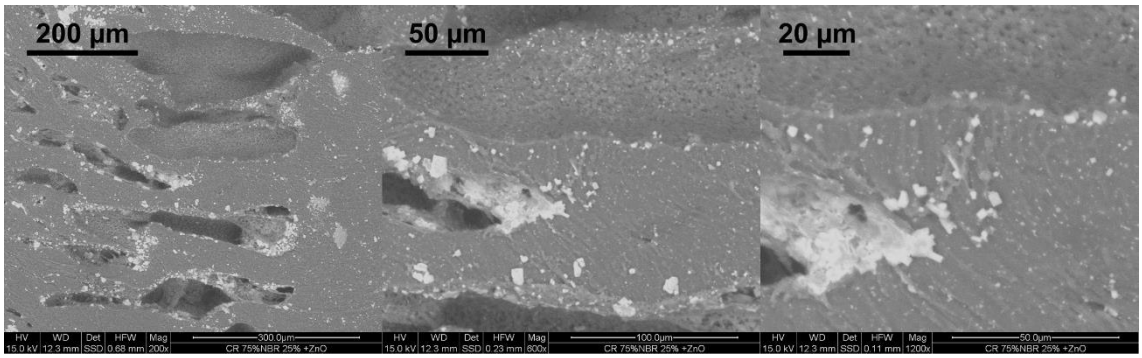

Figure 37: ESEM pictures of the fracture area of the thicker sample 25 % NBR / 75 % CR + ZnO.

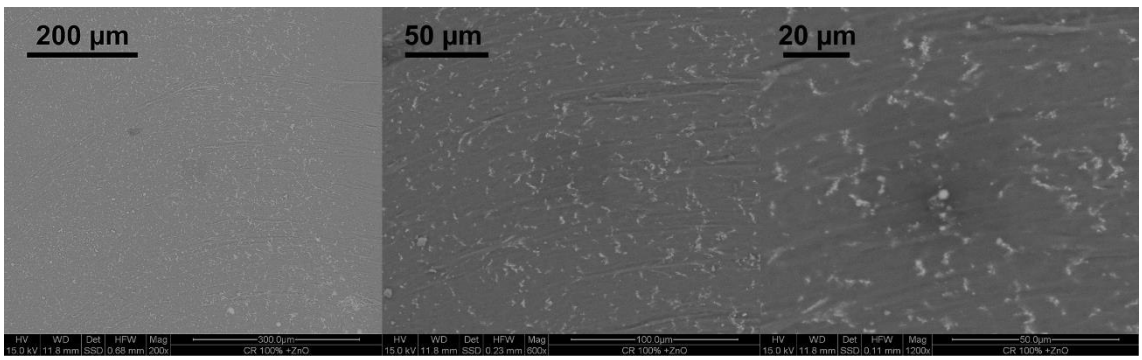

Figure 38: ESEM pictures of the fracture area of the thicker sample 100 % CR + ZnO.

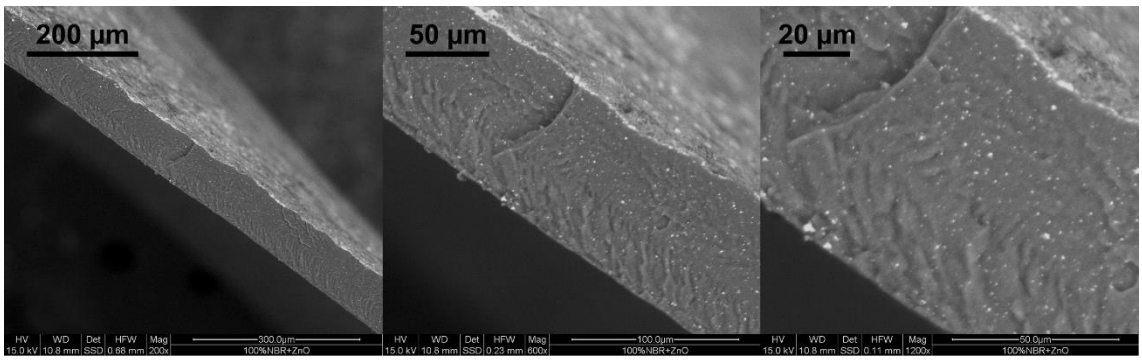

Figure 39: ESEM pictures of the fracture area of the sample 100 % NBR + ZnO.

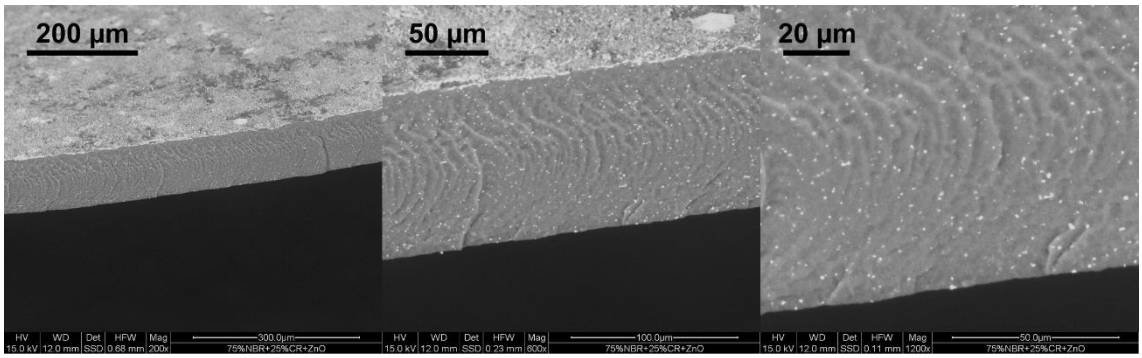

Figure 40: ESEM pictures of the fracture area of the sample 75 % NBR / 25 % CR + ZnO.

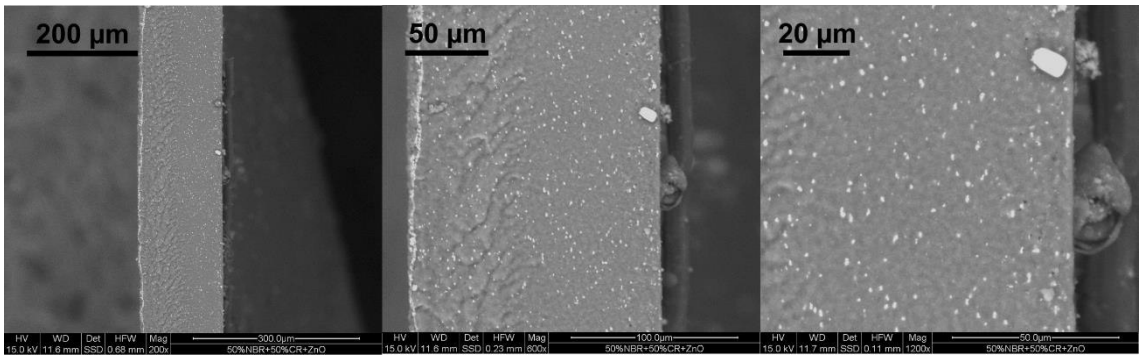

Figure 41: ESEM pictures of the fracture area of the sample 50 % NBR / 50 % CR + ZnO.

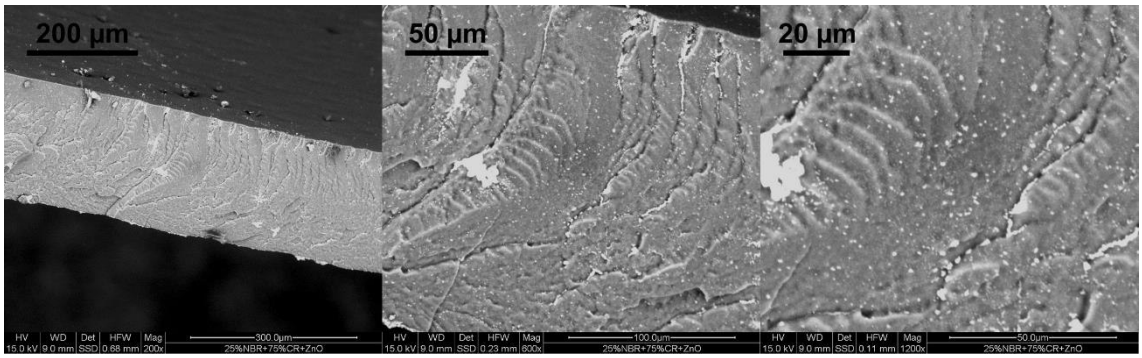

Figure 42: ESEM pictures of the fracture area of the sample 25 % NBR / 75 % CR + ZnO.

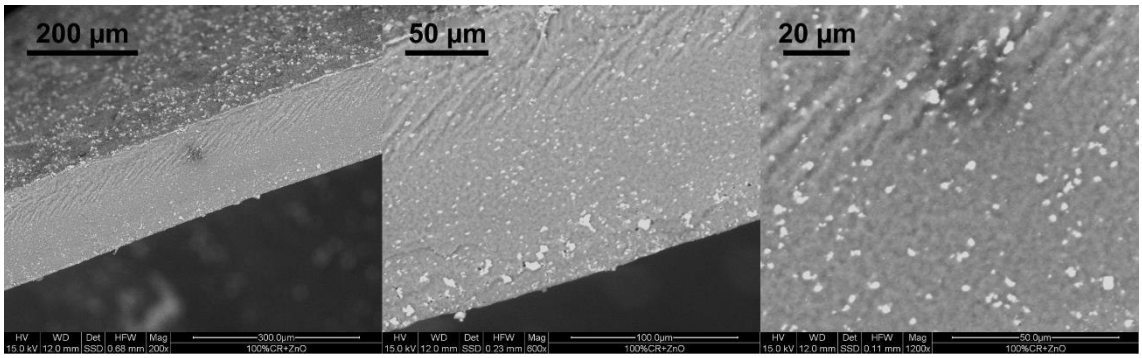

Figure 43: ESEM pictures of the fracture area of the sample 100 % CR + ZnO.

5.5 EDX-Mapping of the pre-vulcanized IR/CR-latex blends

To check the distribution of the Cl-atoms in the blends, EDX-mapping of the pre-vulcanized IR/CR-latex blends were done. Figure 44 – Figure 46 show the results of the samples with the blending ratio 75:25, 50:50 and 25:75 with an 800-fold magnification. The elements are indicated in different colours, where brighter spots represent a higher concentration of the element. A very homogeneous distribution can be observed for all elements in all samples. Darker spots in the carbon picture correlate with brighter spots in the calcium picture, indicating that the calcium is overlocking the carbon signal. Moreover, brighter spots of the chlorine match with brighter spots of the potassium, which means that KCl is formed.

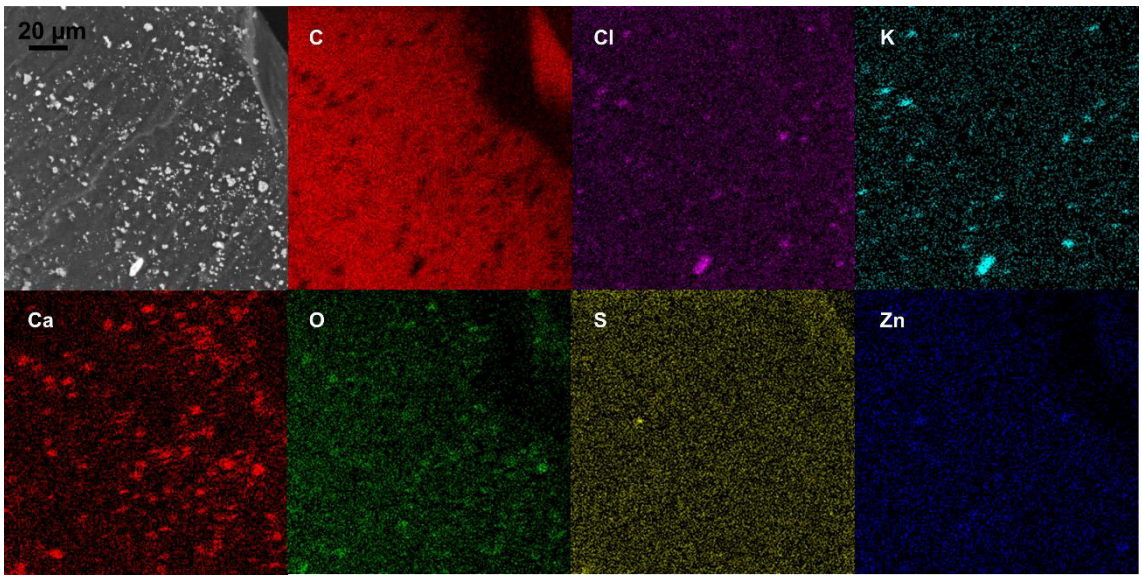

Figure 44: EDX-mapping of the fracture area of the sample 75 % IR / 25 % CR + PM30 [800x].

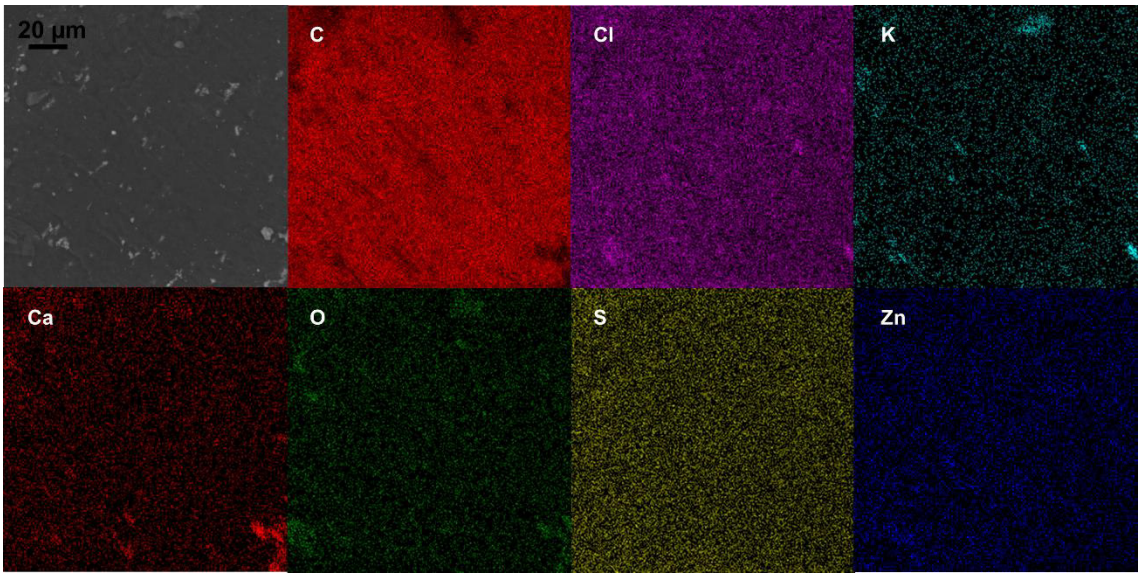

Figure 45: EDX-mapping of the fracture area of the sample 50 % IR / 50 % CR + PM30 [800x].

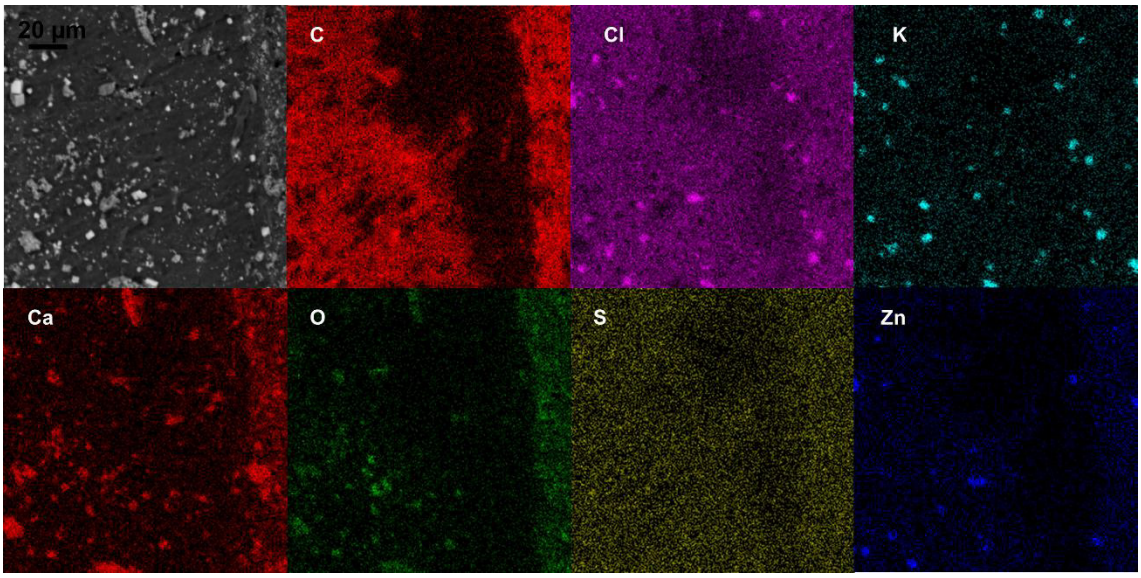

Figure 46: EDX-mapping of the fracture area of the sample 25 % IR / 75 % CR + PM30 [800x].

Additionally, EDX-mapping of the fracture area of the IR/CR-latex blend with the ratio 50:50 with a 1600-fold magnification were performed (Figure 47). Despite the higher magnification, similar results are obtained.

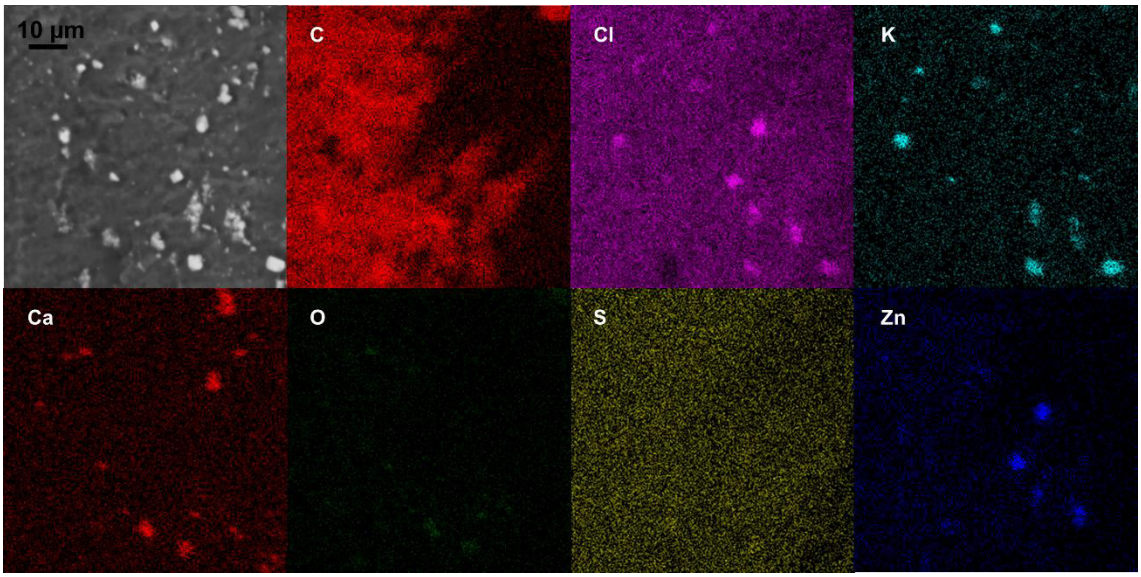

Figure 47: EDX-mapping of the fracture area of the sample 25 % IR / 75 % CR + PM30 [1600x].

However, EDX-mapping is a good option to get a general idea about the distribution of the elements in the sample. Maybe the 1600-fold magnification is still too small to observe significant differences of the distribution of the particular elements.

5.6 Mechanical properties of the different latex blends

To investigate the mechanical properties tensile tests were performed. The results constitute an average of at least 5 measurements. Unless otherwise specified, the results obtained from the measurements with the shouldered bars having a clamping length of 50 mm are shown.

5.6.1 Stress-strain behaviour of the latex blends without pre-vulcanization

Table 14 shows the tensile strength, ultimate elongation and the stress at 100 % elongation for the different latex blends without pre-vulcanization.

Table 14: Measured stress at 100 % elongation, tensile strength and ultimate elongation for the latex blends without pre-vulcanization.

Sample	**Stress at 100 % elongation [N/mm²]**	**Tensile strength [N/mm²]**	**Ultimate elongation [%]**
100 % NR	0.52 ± 0.02	2.57 ± 0.25	570 ± 19

Sample	Stress at 100 % elongation [N/mm²]	Tensile strength [N/mm²]	Ultimate elongation [%]
75 % NR / 25 % CR	0.66 ± 0.02	8.19 ± 0.99	775 ± 31
50 % NR / 50 % CR	0.70 ± 0.03	8.35 ± 0.56	853 ± 20
25 % NR / 75 % CR	0.85 ± 0.05	9.07 ± 0.65	925 ± 19
100 % IR	0.48 ± 0.05	0.54 ± 0.04	644 ± 93
75 % IR / 25 % CR	0.27 ± 0.04	0.50 ± 0.05	797 ± 48
50 % IR / 50 % CR	0.42 ± 0.07	1.45 ± 0.11	861 ± 49
25 % IR / 75 % CR	0.84 ± 0.03	4.76 ± 0.29	1127 ± 33
100 % NBR	3.44 ± 0.17	41.07 ± 4.39	556 ± 7
75 % NBR / 25 % CR	3.22 ± 0.11	27.76 ± 2.90	521 ± 22
50 % NBR / 50 % CR	2.43 ± 0.09	19.81 ± 1.07	560 ± 16
25 % NBR / 75 % CR	1.55 ± 0.04	15.00 ± 0.65	719 ± 15
100 % CR	0.99 ± 0.02	12.82 ± 0.59	1029 ± 17

The NR/CR-latex blends without pre-vulcanization show a relatively poor tensile strength, whereas for the blending ratio 100:0 the lowest value is observed. According to measurements with the shouldered bars having a clamping length of 75 mm, the tensile strength of pure NR-latex should be at least beyond 10 N/mm² with an ultimate elongation of more than 870 %. Apparently something went wrong with the preparation of this sample. Compared to the IR/CR- and NBR/CR-latex blends, NR/CR-latex blends exhibit the highest ultimate elongations.

The IR/CR-latex blends have the worst tensile strength compared to the other systems. The tensile strength for the blending ratio 75:25 is slightly smaller than for the pure IR-latex. Though, the tensile strength increases almost tenfold with increasing amounts of CR-latex, whereas the ultimate elongation increases around 30 % exceeding even the pure CR-latex.

The reason for the poor tensile strength of the NR/CR- and IR/CR-latex blends without pre-vulcanization is the low amount of cross-linking. By the addition of sulphur, the cross-linking can occur via bridges between the chains, leading to a higher tensile strength of NR/CR- and IR/CR-latex blends.

In contrast, NBR/CR-latex blends show a decreasing tensile strength with increasing amounts of CR-latex. Pure NBR-latex exhibits the highest tensile strength with 41 N/mm². Also for this system the ultimate elongation increases with increasing amounts of CR-latex.

The trend of the stress at 100 % elongation is similar to that of the tensile strength for all blend systems.

5.6.2 Stress-strain behaviour of the pre-vulcanized latex blends

Table 15 shows the results of the tensile tests for the pre-vulcanized latex blends.

Table 15: Measured stress at 100 % elongation, tensile strength and ultimate elongation for the pre-vulcanized latex blends.

Sample	Stress at 100 % elongation [N/mm²]	Tensile strength [N/mm²]	Ultimate elongation [%]
100 % NR + PM30	1.23 ± 0.04	33.46 ± 1.15	821 ± 17
75 % NR / 25 % CR + PM30	1.07 ± 0.02	28.64 ± 0.95	919 ± 26
50 % NR / 50 % CR + PM30	0.98 ± 0.02	18.83 ± 1.18	885 ± 30
25 % NR / 75 % CR + PM30	0.90 ± 0.04	14.36 ± 0.69	865 ± 26
100 % IR + PM30	0.64 ± 0.02	15.09 ± 1.66	942 ± 70
75 % IR / 25 % CR + PM30	0.60 ± 0.04	15.83 ± 2.83	981 ± 71
50 % IR / 50 % CR + PM30	0.58 ± 0.02	14.30 ± 0.55	1060 ± 40
25 % IR / 75 % CR + PM30	0.57 ± 0.04	11.93 ± 0.36	1192 ± 57
100 % NBR + ZnO	3.44 ± 0.14	35.23 ± 1.25	593 ± 18
75 % NBR / 25 % CR + ZnO	2.73 ± 0.06	21.05 ± 2.48	558 ± 37

Sample	Stress at 100 % elongation [N/mm²]	Tensile strength [N/mm²]	Ultimate elongation [%]
50 % NBR / 50 % CR + ZnO	2.09 ± 0.07	15.77 ± 1.62	604 ± 31
25 % NBR / 75 % CR + ZnO	1.24 ± 0.03	12.19 ± 1.03	815 ± 34
100 % CR + PM30	0.73 ± 0.05	13.89 ± 0.97	1249 ± 48
100% CR + ZnO	0.70 ± 0.04	14.00 ± 0.79	1255 ± 43

In contrast to the samples without pre-vulcanization, the NR/CR-latex blends have very good mechanical properties (Figure 48). The tensile strength of the pure NR-latex is about 33 N/mm². However, it decreases more than a half with increasing amounts of CR-latex. On the other hand, the ultimate elongation is higher for the blends with the ratio 75:25 and 50:50 than the pure NR-latex, even though it declines with increasing amounts of CR-latex.

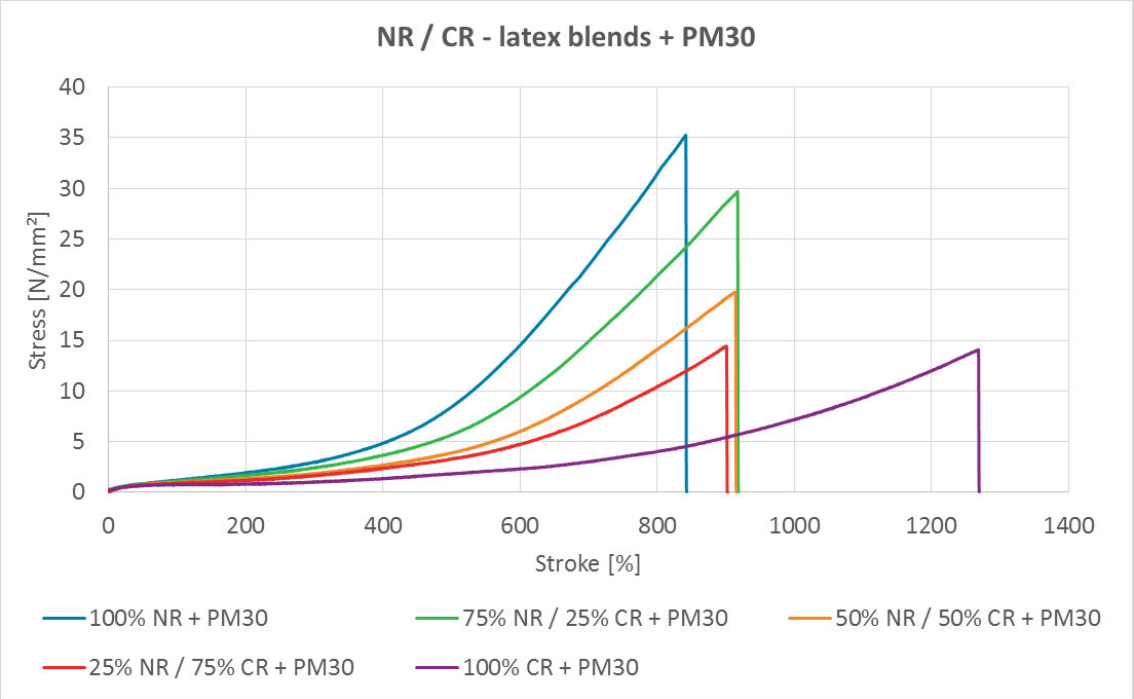

Figure 48: Stress-strain diagrams of the pre-vulcanized NR/CR-latex blends.

Also the pre-vulcanized IR/CR-latex blends show much better mechanical properties than the systems without pre-vulcanization. Unlike the other systems, there is only a very

slight decrease of the tensile strength from 15 N/mm² to 12 N/mm², whereas the ultimate elongation is increasing from 981 % to 1192 %.

The stress-strain diagrams of the pre-vulcanized IR/CR-latex blends (Figure 49) look similar to that of the NR/CR-latex blends (Figure 48). Both systems show a slight increase of the stress at the beginning, which remains under 2 N/mm² until a strain of at least 200 %, for IR/CR-latex blends even 400 %, is reached. At the end of the stress-strain curve a steep slope is observed, which decreases with increasing amounts of CR-latex.

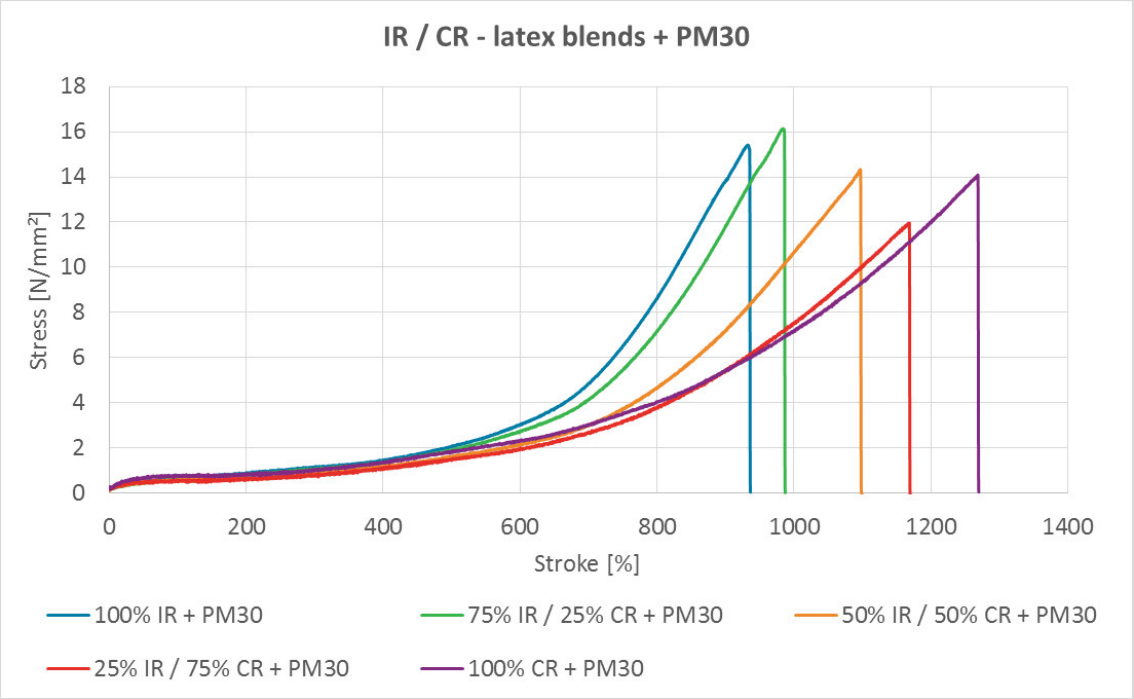

Figure 49: Stress-strain diagrams of the pre-vulcanized IR/CR-latex blends.

Also the NBR/CR-latex blends exhibit a very good tensile strength, which is comparable with the other systems. However, the tensile strength of the pre-vulcanized samples is lower than that without pre-vulcanization, which may be due to the incorrect vulcanization agent. Generally, the cross-linking is taking place at the double bond via sulphide bridges. Though, ZnO was used as a vulcanization agent in consideration to the CR-latex, which apparently has a negative influence on the branching of NBR-latex. With increasing amounts of CR-latex, the tensile strength of the pre-vulcanized NBR/CR-latex blends decreases more than a half, whereas the ultimate elongation is clearly improved.

The stress-strain diagrams of the NBR/CR-latex blends (Figure 50) look different than those of the NR/CR-latex blends and the IR/CR-latex blends. The samples with a low

amount of CR-latex show almost no constant stress area, there is always an obvious raising of the curve.

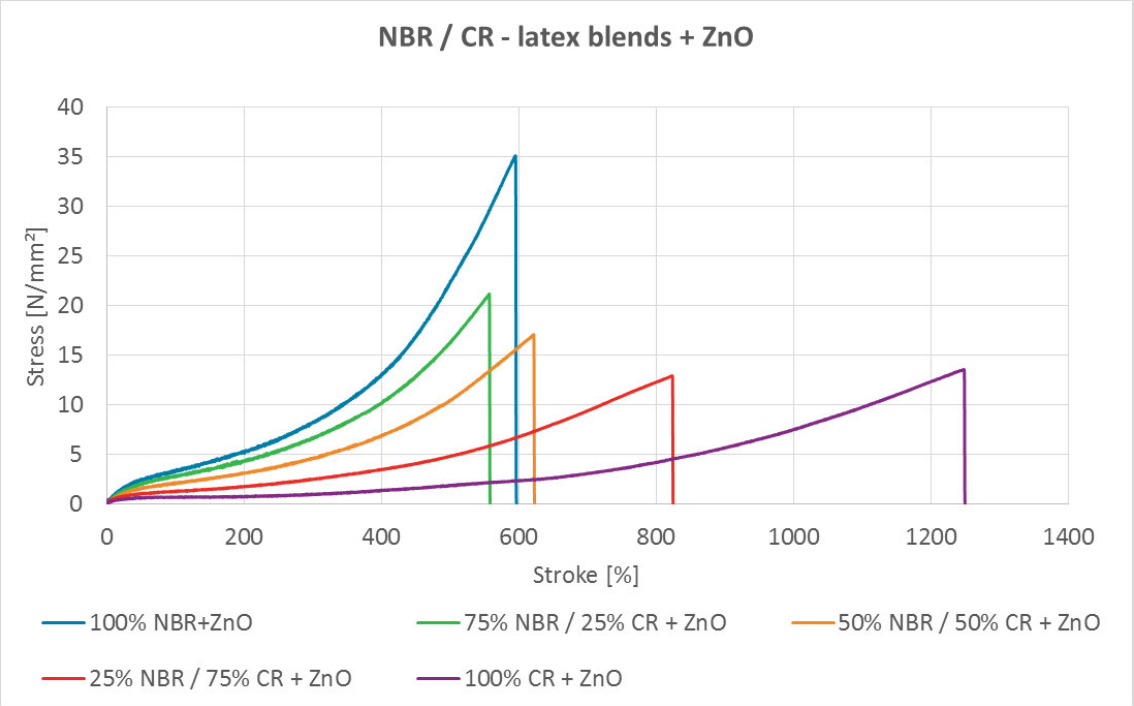

Figure 50: Stress-strain diagram of the pre-vulcanized NBR/CR-latex blends.

Considering the pure CR-latex with and without pre-vulcanization, the mechanical properties are very similar regardless of the type of vulcanization agent or whether pre-vulcanization occurs or not. This indicates that the pre-vulcanization is incomplete, which may be due to the not optimized vulcanization conditions.

5.6.3 Comparison of the results obtained from the two different shouldered bars (50 mm and 75 mm)

Table 16 shows the tensile strength obtained from tensile tests with the shouldered bars having a clamping length of 50 mm and 75 mm for the IR/CR-latex blends with and without pre-vulcanization in different blend ratios. The sign > indicates that the top of the tensile tester was reached before tearing occurred.

For the samples without pre-vulcanization, a slightly higher tensile strength can be observed with the 50 mm shouldered bars. For the pre-vulcanized samples the difference is within the margin of deviation.

Table 16: Tensile strength of the IR/CR-latex blends with and without pre-vulcanization measured with the 50 mm and 75 mm shouldered bars.

Sample	75 mm: Tensile strength [N/mm²]	50 mm: Tensile strength [N/mm²]
100 % IR	0.18 ± 0.04	0.54 ± 0.04
75 % IR / 25 % CR	0.34 ± 0.01	0.50 ± 0.05
50 % IR / 50 % CR	1.04 ± 0.18	1.45 ± 0.11
25 % IR / 75 % CR	> 3.79 ± 0.10	4.76 ± 0.29
100 % CR	> 7.89 ± 0.72	12.82 ± 0.59
100 % IR + PM30	> 16.36 ± 1.66	15.09 ± 1.66
75 % IR / 25 % CR + PM30	> 5.42 ± 0.75	15.83 ± 2.83
50 % IR / 50 % CR + PM30	> 3.41 ± 0.11	14.30 ± 0.55
25 % IR / 75 % CR + PM30	> 6.76 ± 0.33	11.93 ± 0.36
100% CR + PM30	> 8.39 ± 0.17	13.89 ± 0.97

Table 17 shows the resulting stress at 100 % elongation for the IR/CR-latex blends with and without pre-vulcanization measured with the shouldered bars having a clamping length of 50 mm and 75 mm. With certain exceptions the stress at 100 % elongation is quite similar regardless of the clamping length of the shouldered bars. For the samples without pre-vulcanization having a blending ratio of 25:75 and 0:100 as well as the pre-vulcanized sample with the blending ration 50:50 a difference of more than 0.25 N/mm² is observed, which may be due to measuring inaccuracy.

Table 17: Tensile strength of the IR/CR-latex blends with and without pre-vulcanization measured with the 50 mm and 75 mm shouldered bars.

Sample	75 mm: Stress at 100 % elongation [N/mm²]	50 mm: Stress at 100 % elongation [N/mm²]
100 % IR	0.33 ± 0.06	0.48 ± 0.05
75 % IR / 25 % CR	0.28 ± 0.01	0.27 ± 0.04
50 % IR / 50 % CR	0.36 ± 0.01	0.42 ± 0.07
25 % IR / 75 % CR	0.57 ± 0.04	0.84 ± 0.03
100 % CR	0.76 ± 0.10	0.99 ± 0.02
100 % IR + PM30	0.69 ± 0.03	0.64 ± 0.02
75 % IR / 25 % CR + PM30	0.54 ± 0.05	0.60 ± 0.04
50 % IR / 50 % CR + PM30	0.28 ± 0.06	0.58 ± 0.02
25 % IR / 75 % CR + PM30	0.59 ± 0.03	0.57 ± 0.04
100% CR + PM30	0.77 ± 0.02	0.73 ± 0.05

Table 18 demonstrates the ultimate elongation of the IR/CR-latex blends in different blending ratios. Also the ultimate elongation of the samples measured with the 75 mm shouldered bars are in the same range as that measured with the 50 mm shouldered bars.

Table 18: Ultimate elongation of the IR/CR-latex blends with and without pre-vulcanization measured with the 50 mm and 75 mm shouldered bars.

Sample	75 mm: Ultimate elongation [%]	50 mm: Ultimate elongation [%]
100 % IR	494 ± 73	644 ± 93
75 % IR / 25 % CR	623 ± 38	797 ± 48
50 % IR / 50 % CR	687 ± 97	861 ± 49
25 % IR / 75 % CR	> 1035 ± 28	1127 ± 33

Sample	75 mm: Ultimate elongation [%]	50 mm: Ultimate elongation [%]
100 % CR	> 1025 ± 51	1029 ± 17
100 % IR + PM30	> 882 ± 30	942 ± 70
75 % IR / 25 % CR + PM30	> 1002 ± 24	981 ± 71
50 % IR / 50 % CR + PM30	> 874 ± 38	1060 ± 40
25 % IR / 75 % CR + PM30	> 1067 ± 32	1192 ± 57
100% CR + PM30	> 1078 ± 3	1249 ± 48

The results obtained by the shouldered bars having a clamping length of 50 mm cannot be compared with 100 % certainty with the bars having a clamping length of 75 mm, but they deliver a good evidence since the values are in the same range.

5.6.4 Influence of the drying temperature

To investigate the influence of the drying temperature, IR/CR-latex blends with different blending ratios were prepared, which were dried at 110°C for 30 minutes in the presence of a vulcanization agent (PM30).

The results obtained by the shouldered bars having a clamping length of 75 mm are shown in Table 19. The mechanical properties are very similar to the conventional pre-vulcanized and dried samples. For further investigations, the sample with the blending ratio 25:75 was tested with the 50 mm shouldered bar (Table 20).

Table 19: Measured stress at 100 % elongation, yield strength and ultimate elongation of the IR/CR-latex blends dried at 110 °C using the 75 mm shouldered bar.

Sample	Stress at 100 % elongation [N/mm²]	Tensile strength [N/mm²]	Ultimate elongation [%]
75 % IR / 25 % CR + PM30 [110°C]	0.43 ± 0.03	> 6.71 ± 0.43	> 920 ± 30
50 % IR / 50 % CR + PM30 [110°C]	0.39 ± 0.03	> 3.94 ± 0.26	> 997 ± 38
25 % IR / 75 % CR + PM30 [110°C]	0.55 ± 0.03	> 7.70 ± 0.04	> 1079 ± 2

Table 20 shows that he stress at 100 % elongation as well as the ultimate elongation is almost the same as for the conventional produced and pre-vulcanized IR/CR-latex blend (25:75). Only the tensile strength is slightly lower for the sample dried at 110 °C for 30 minutes. Hence, it makes no clear difference if the samples a pre-vulcanized and dried at 100 °C for 15 minutes or if they are only dried at 110 °C for 30 minutes.

Table 20: Measured stress at 100 % elongation, yield strength and ultimate elongation of the IR/CR-latex blends dried at 110 °C using the 50 mm shouldered bar.

Sample	Stress at 100 % elongation [N/mm²]	Tensile strength [N/mm²]	Ultimate elongation [%]
25 % IR / 75 % CR + PM30 [110°C]	0.58 ± 0.03	8.12 ± 0.70	1164 ± 77

5.6.5 Stress-strain behaviour of pre-vulcanized IR/CR-latex blends using PM30 and ZnO as vulcanizing agent

Table 21 demonstrates the results of the tensile test for the pre-vulcanized IR/CR-latex blend with the blending ratio 50:50 using PM30 together with ZnO as vulcanizing agent. Compared to the conventional pre-vulcanized IR/CR-latex blend, the tensile strength is very low. This may be due to an incomplete or wrong pre-vulcanization. Furthermore, the two latexes were pre-vulcanized separately, so no cross-linking between the latexes can occur during the pre-vulcanization. The stress at 100 % elongation as well as the ultimate elongation are almost the same as for the conventional pre-vulcanized sample.

Table 21: Measured stress at 100 % elongation, yield strength and ultimate elongation of the IR/CR-latex blend using PM30 together with ZnO as vulcanizing agent.

Sample	**Stress at 100 % elongation [N/mm²]**	**Tensile strength [N/mm²]**	**Ultimate elongation [%]**
50 % IR / 50 % CR + PM30 / ZnO	0.51 ± 0.04	5.65 ± 0.79	1068 ± 30

6 SUMMARY AND OUTLOOK

The aim of the thesis was to investigate a latex blend, which can be used as a material for synthetic examination gloves. It should possess better or the same mechanical properties with additional wear comfort as the gloves made out of natural rubber latex. Three different blend systems were investigated: NR/CR-, IR/CR- and NBR/CR-latex blends. The NR-latex containing sample was generated for the purpose of comparison. Thin-film latex blends were produced by the coagulant dipping method. To investigate the influence of the blend ratio on the mechanical properties, blends with the ratios 100:0, 75:25, 50:50, 25:75 and 0:100 (w:w, based on the dry rubber content) were made.

The thickness of the produced thin-film latex blends was determined with a micrometre screw. The results indicate that the final thickness of the NR/CR- and IR/CR-latex blends decreases with increasing amounts of CR-latex. On the other hand, the thickness of the NBR/CR-latex blends increases with increasing amounts of CR-latex. Since the thickness of the thin-films only depends on the primary particle size, the used coagulant and the respective dwell time, no difference between samples with or without pre-vulcanization could be observed.

To investigate if the latexes are miscible or not, DSC measurements were carried out by the Semperit Technische Produkte GmbH. For all blends with the ratios 75:25, 50:50 and 25:75 two distinct glass transition temperatures were observed. No shifting of the glass transition point could be observed, which indicates that the produced latex blends represent immiscible systems.

To investigate the morphology of the samples, experiments with an environmental scanning electron microscope coupled with an energy dispersive X-ray spectrometer (ESEM-EDX) were carried out. Different sample preparations were performed, whereat the surface as well as the fracture area were observed. All pre-vulcanized samples have a very homogeneous distribution of the vulcanization agents and no phase separation could be observed. Additional EDX-mapping confirm an even distribution of the elements. However, further attempts should be done to achieve higher magnifications. Maybe the investigation of ultra-thin sections prepared by cryogenic cutting can give more information about the morphology of the latex blends.

The mechanical properties were determined by tensile tests. For the NR/CR- and IR/CR-latex blends the mechanical properties were clearly improved by pre-vulcanization. The tensile strength of NBR/CR-latex blends without pre-vulcanization is better than with pre-vulcanization, indicating that the wrong vulcanization agent might be used. On the other hand the ultimate elongation of the NBR/CR-latex blends is improved by the pre-vulcanization.

As it is shown in Figure 51, the tensile strength of all pre-vulcanized latex blends decreases with increasing amounts of CR-latex. NR/CR-latex blends show the highest tensile strength, followed by NBR/CR-latex blends and IR/CR-latex blends.

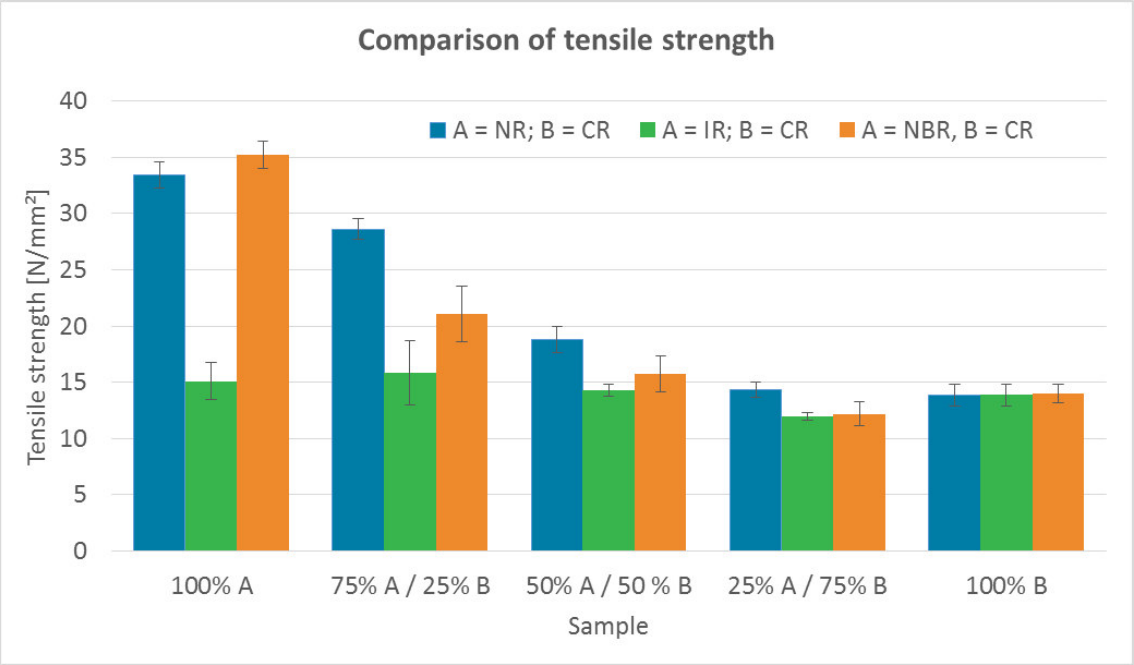

Figure 51: Comparison of the tensile strength of the different pre-vulcanized latex blends.

In contrast, the ultimate elongation of all latex blends is clearly improved with increasing amounts of CR-latex, which is shown in Figure 52. The highest ultimate elongation is observed for the IR/CR-latex blends, whereas NBR/CR-latex blends exhibit the lowest ultimate elongation.

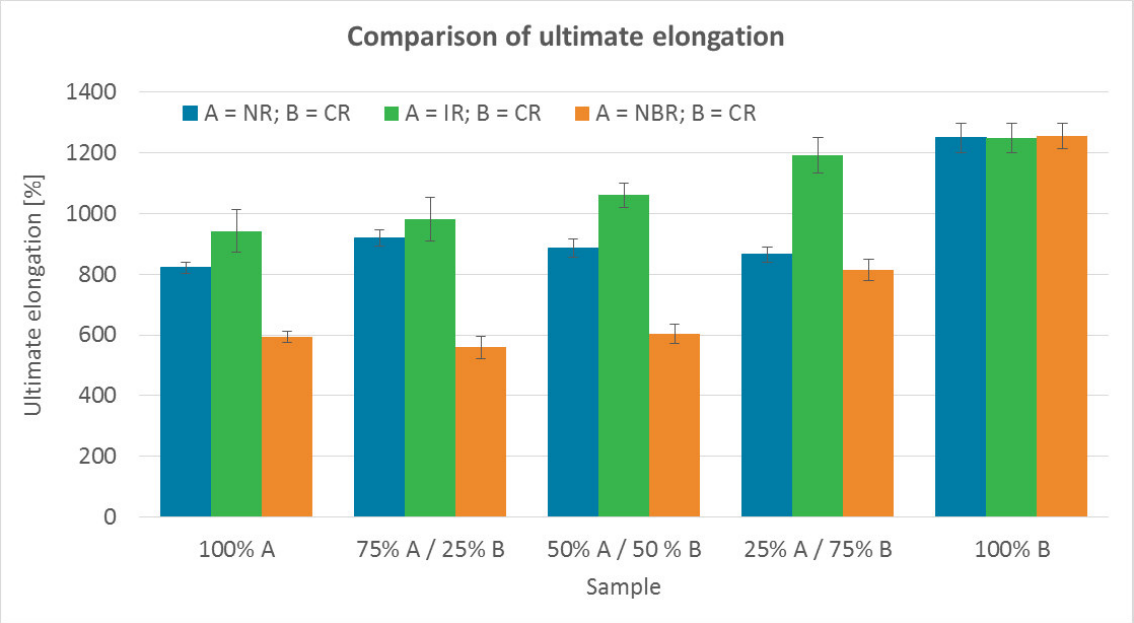

Figure 52: Comparison of the ultimate elongation of the different pre-vulcanized latex blends.

The stress-strain diagrams for all pre-vulcanized samples show an increase of the area where the stress is constant below 2 N/mm². This indicates that the wear comfort is improved, especially concerning the NBR/CR-latex blends.

This work should constitute a preliminary study. Further investigations have to be done to improve the tensile strength. More focus has to be put on the preparation conditions of the CR-latex. Additional experiments with compounding additives especially concerning the NBR-latex are necessary.

7 REFERENCES

[1] H.-H. Greve, M. Happ, C. Oppenheimer-Stix, R. LaFlair, W. Hofmann, R. Koopmann, and J. Neu, "Rubber," *Ullman's Encyclopedia of Industrial Chemistry, Volume A23: Refactory Ceramics to Silicon Carbide*. VCH, pp. 221–472, 1993.

[2] F. Röthemeyer and F. Sommer, *Kautschuktechnologie*. Hanser, 2006.

[3] "Statista," *Malaysian Rubber Board*, 2017. [Online]. Available: https://www.statista.com/statistics/275399/world-consumption-of-natural-and-synthetic-caoutchouc/. [Accessed: 18-Oct-2017].

[4] R. J. Del Vecchio, *Fundamentals of Rubber Technology*. ACS, 2003.

[5] J. Bussink and H. T. Van De Grampel, "Polymer Blends," *Ullman's Encyclopedia of Industrial Chemistry, Volume A21: Plastic, Properties and Testing to Polyvinyl Compounds*. VCH, pp. 273–304, 1992.

[6] C. D. Han, *Multiphase Flow in Polymer Processing*. Academic Press, 1981.

[7] R. M. Ottenbrite, L. A. Utracki, and S. Inoue, *Current Topics in Polymer Science*. Hanser, 1987.

[8] J. Feng, M. A. Winnik, R. R. Shivers, and B. Clubb, "Polymer Blend Latex Films: Morphology and Transparency," *Macromolecules*, vol. 28, no. 23, pp. 7671–7682, 1995.

[9] J. L. Keddie, P. Meredith, R. A. L. Jones, and A. M. Donald, "Kinetics of film formation in acrylic latices studied with multiple-angle-of-indicence ellipsometry and envirnomental SEM," *Macromolecules*, vol. 28, pp. 2673–2682, 1995.

[10] A. A. Patel, J. R. Feng, M. A. Winnik, G. J. Vancso, and C. B. D. Mcbain, "Characterization of latex blend films by atomic force microscopy," *Polymer (Guildf).*, vol. 37, no. 25, pp. 5577–5582, 1996.

[11] S. Prasertsri, F. Lagarde, N. Rattanasom, C. Sirisinha, and P. Daniel, "Raman spectroscopy and thermal analysis of gum and silica-filled NR/SBR blends

prepared from latex system," *Polym. Test.*, vol. 32, no. 5, pp. 852–861, 2013.

[12] R. Stephen, K. Joseph, Z. Oommen, and S. Thomas, "Molecular transport of aromatic solvents through microcomposites of natural rubber (NR), carboxylated styrene butadiene rubber (XSBR) and their blends," *Compos. Sci. Technol.*, vol. 67, no. 6, pp. 1187–1194, 2007.

[13] N. Moonprasith, K. Suchiva, and O. Tongcher, "Blending in Latex Form of Natural Rubber and Nitrile Latices : A Preliminary Study of Morphology and Mechanical Properties," Material Tech. Seminar, Thailand, 2006.

[14] S. Zhong and Z. Chen, "Properties of latex blends and its modified cement mortars," *Cem. Concr. Res.*, vol. 32, no. 10, pp. 1515–1524, 2002.

[15] Y. Ohama, "Polymer-based admixtures," *Cem. Concr. Compos.*, vol. 20 (2-3), no. 2–3, pp. 189–212, 1998.

[16] E. Yip and P. Cacioli, "The manufacture of gloves from natural rubber latex," *J. Allergy Clin. Immunol.*, vol. 110, no. 2, pp. S3–S14, 2002.

[17] D. Mangaraj, "Elastomer Blends," *Rubber Chem. Technol.*, vol. 75, no. 3, pp. 365–427, 2002.

[18] G. Menges, H. Edmund, W. Michaeli, and E. Schmachtenberg, *Menges Werkstoffkunde Kunststoffe*. Hanser, 2011.

[19] A. Franck, *Kunststoff - Kompendium*. Vogel, 2000.

[20] L. M. Robeson, *Polymer Blends: A Comprehensive Review*. Hanser, 2007.

[21] O. Schwarz, F.-W. Ebeling, F. Richter, H. Huberth, H. Schirber, and N. Schlör, *Kunststoffkunde*. Vogel, 2016.

[22] W. Dierkes, "Raw Materials and Compounds in Rubber Industry," University of Twente, 2007.

[23] H. M. Weitz and E. Loser, "Isoprene," *Ullman's Encyclopedia of Industrial Chemistry, Volume A14: Immobilized Biocatalysts to Isoprene*. VCH, pp. 627–644, 1989.

[24] P. Henderson, "Preparation of synthetic polyisoprene latex and its use in coagulant dipping," *Latex 2001*, pp. 77–89, 2001.

[25] W. Hofmann, *Rubber Technology Handbook*. Hanser, 1989.

[26] "Technical Note : NR-Latex & Latex Products," Nocil Limited, 2010.

[27] T. Akabane, "Production method & market trend of rubber gloves," *Nippon Gomu Kyokaishi*, vol. 9, pp. 369–373, 2015.

8 LIST OF FIGURES

Figure 1: Consumption of natural and synthetic rubber worldwide [3]..... 1

Figure 2: Possible free energy of mixing ΔG_{mix} curves for binary mixtures (based on [17]). 4

Figure 3: Phase diagram for polymer blends showing the upper critical solution temperature (UCST) and the lower critical solution temperature (LCST) (based on [20]). 5

Figure 4: Latex particle. 6

Figure 5: Chemical structure of poly(*cis*-1,4-isoprene). 8

Figure 6: Chemical structure of poly(*trans*-1,4-isoprene), poly(1,2-isoprene) and poly(3,4-isoprene). 8

Figure 7: Tensile strength of the pure and un-vulcanized NR and IR; strain speed: 10 cm/min; temperature: 25°C (based on [22]). 10

Figure 8: Chemical structure of poly(acrylonitrile-*co*-1,3-butadiene). 10

Figure 9: Schematic production of NBR (based on [1]). a) Stirred tank 1; b) Stirred tank *n*; c) Shortstopping vessel; d) Degassing 11

Figure 10: Chemical structure of poly(*trans*-1,4-chloroprene)..... 12

Figure 11: Schematic production of polychloroprene (based on [1]). a) Polymerization reactor; b) Stripper; c) Purification; d) Neutralization; e) Peptization; f) Rotating cooling drum; g) Coagulation by freezing; h) Latex concentration; i) Chopping machine; j) Dursting machine; k) Roping machine; l) Dryer; m) Washing 13

Figure 12: Incorporation of chloroprene monomers into the polymer chain. 13

Figure 13: Coagulant dipping mechanism (based on [24]). 17

Figure 14: Coagulant dipping method. 22

Figure 15: Geometry of the shouldered bars. 25

Figure 16: DSC diagram for the sample 100 % IR + PM30. 34

Figure 17: DSC diagram for the sample 75 % IR / 25 % CR + PM30. 35

Figure 18: DSC diagram for the sample 50 % IR / 50 % CR + PM30. 35

Figure 19: DSC diagram for the sample 25 % IR / 75 % CR + PM30. 36

Figure 20: DSC diagram for the sample 100 % CR + PM30..... 36

Figure 21: ESEM pictures of the surface of the sample 100 % NBR. 37

Figure 22: ESEM pictures of the surface of the sample 75 % NBR / 25 % CR. 38

Figure 23: ESEM pictures of the surface of the sample 50 % NBR / 50 % CR. 38

Figure 24: ESEM pictures of the surface of the sample 25 % NBR / 75 % CR. 38

Figure 25: ESEM pictures of the surface of the sample 75 % NBR / 25 % CR + ZnO. 38

Figure 26: ESEM pictures of the surface of the sample 50 % NBR / 50 % CR + ZnO. 39

Figure 27: ESEM pictures of the surface of the sample 25 % NBR / 75 % CR + ZnO. 39

Figure 28: ESEM pictures of the surface of the sample 100 % CR + ZnO. 39

Figure 29: ESEM pictures of the surface of the sample 100 % IR + PM30. 39

Figure 30: ESEM pictures of the surface of the sample 75 % IR / 25 % CR + PM30. . 40

Figure 31: ESEM pictures of the surface of the sample 50 % IR / 50 % CR + PM30. . 40

Figure 32: ESEM pictures of the surface of the sample 25 % IR / 75 % CR + PM30. . 40

Figure 33: ESEM pictures of the surface of the sample 100 % CR + PM30..... 40

Figure 34: ESEM pictures of the fracture area of the thicker sample 100 % NBR + ZnO. 41

Figure 35: ESEM pictures of the fracture area of the thicker sample 75 % NBR / 25 % CR + ZnO..... 41

Figure 36: ESEM pictures of the fracture area of the thicker sample 50 % NBR / 50 % CR + ZnO..... 42

Figure 37: ESEM pictures of the fracture area of the thicker sample 25 % NBR / 75 % CR + ZnO..... 42

Figure 38: ESEM pictures of the fracture area of the thicker sample 100 % CR + ZnO. 42

Figure 39: ESEM pictures of the fracture area of the sample 100 % NBR + ZnO..... 42

Figure 40: ESEM pictures of the fracture area of the sample 75 % NBR / 25 % CR + ZnO. 43

Figure 41: ESEM pictures of the fracture area of the sample 50 % NBR / 50 % CR + ZnO. 43

Figure 42: ESEM pictures of the fracture area of the sample 25 % NBR / 75 % CR + ZnO. 43

Figure 43: ESEM pictures of the fracture area of the sample 100 % CR + ZnO. 43

Figure 44: EDX-mapping of the fracture area of the sample 75 % IR / 25 % CR + PM30 [800x]. 44

Figure 45: EDX-mapping of the fracture area of the sample 50 % IR / 50 % CR + PM30 [800x]. 45

Figure 46: EDX-mapping of the fracture area of the sample 25 % IR / 75 % CR + PM30 [800x]. 45

Figure 47: EDX-mapping of the fracture area of the sample 25 % IR / 75 % CR + PM30 [1600x]. 46

Figure 48: Stress-strain diagrams of the pre-vulcanized NR/CR-latex blends. 49

Figure 49: Stress-strain diagrams of the pre-vulcanized IR/CR-latex blends. 50

Figure 50: Stress-strain diagram of the pre-vulcanized NBR/CR-latex blends. 51

Figure 51: Comparison of the tensile strength of the different pre-vulcanized latex blends. 58

Figure 52: Comparison of the ultimate elongation of the different pre-vulcanized latex blends. 59

Figure 53: DSC diagram for the sample 100 % NR. 71

Figure 54: DSC diagram for the sample 75 % NR / 25 % CR. 72

Figure 55: DSC diagram for the sample 50 % NR / 50 % CR. 72

Figure 56: DSC diagram for the sample 25 % NR / 75 % CR. 73

Figure 57: DSC diagram for the sample 100 % IR-latex. 74

Figure 58: DSC diagram for the sample 75 % IR / 25 % CR. 75

Figure 59: DSC diagram for the sample 50 % IR / 50 % CR. 75

Figure 60: DSC diagram for the sample 25 % IR / 75 % CR. 76

Figure 61: DSC diagram for the sample 100 % CR. 76

Figure 62: DSC diagram for the sample 100 % NBR. 77

Figure 63: DSC diagram for the sample 75 % NBR / 25 % CR. 78

Figure 64: DSC diagram for the sample 50 % NBR / 50 % CR. 78

Figure 65: DSC diagram for the sample 25 % NBR / 75 % CR. 79

Figure 66: DSC diagram for the sample 100 % NR + PM30. 80

Figure 67: DSC diagram for the sample 75 % NR / 25 % CR + PM30. 81

Figure 68: DSC diagram for the sample 50 % NR / 50 % CR + PM30. 81

Figure 69: DSC diagram for the sample 25 % NR / 75 % CR + PM30. 82

Figure 70: DSC diagram for the sample 100 % NBR + ZnO. 83

Figure 71: DSC diagram for the sample 75 % NBR / 25 % CR + ZnO. 84

Figure 72: DSC diagram for the sample 50 % NBR / 50 % CR + ZnO. 84

Figure 73: DSC diagram for the sample 25 % NBR / 75 % CR + ZnO. 85

Figure 74: DSC diagram for the sample 100 % CR + ZnO. 85

Figure 75: ESEM pictures of the surface of the sample 100 % NR + PM30. 86

Figure 76: ESEM pictures of the fracture area of the thicker sample 100 % NR. 86

Figure 77: ESEM pictures of the fracture area of the thicker sample 75 % NR / 25 % CR. 86

Figure 78: ESEM pictures of the fracture area of the thicker sample 50 % NR / 50 % CR. 87

Figure 79: ESEM pictures of the fracture area of the thicker sample 25 % NR / 75 % CR. 87

Figure 80: ESEM pictures of the fracture area of the thicker sample 100 % NR + PM30. 87

Figure 81: ESEM pictures of the fracture area of the thicker sample 75 % NR / 25 % CR + PM30. 87

Figure 82: ESEM pictures of the fracture area of the thicker sample 50 % NR / 50 % CR + PM30. 88

Figure 83: ESEM pictures of the fracture area of the thicker sample 25 % NR / 75 % CR + PM30. 88

Figure 84: ESEM pictures of the fracture area of the thicker sample 100 % IR. 88

Figure 85: ESEM pictures of the fracture area of the thicker sample 75 % IR / 25 % CR. 89

Figure 86: ESEM pictures of the fracture area of the thicker sample 50 % IR / 50 % CR. 89

Figure 87: ESEM pictures of the fracture area of the thicker sample 25 % IR / 75 % CR. 89

Figure 88: ESEM pictures of the fracture area of the thicker sample 100 % CR. 89

Figure 89: ESEM pictures of the fracture area of the thicker sample 100 % IR + PM30. 90

Figure 90: ESEM pictures of the fracture area of the thicker sample 75 % IR / 25 % CR + PM30. 90

Figure 91: ESEM pictures of the fracture area of the thicker sample 50 % IR / 50 % CR + PM30. 90

Figure 92: ESEM pictures of the fracture area of the thicker sample 25 % IR / 75 % CR + PM30. 90

Figure 93: ESEM pictures of the fracture area of the thicker sample 100 % CR + PM30. 91

Figure 94: ESEM pictures of the fracture area of the sample 75 % IR / 25 % CR + PM30 [110°C]..... 91

Figure 95: ESEM pictures of the fracture area of the sample 50 % IR / 50 % CR + PM30 [110°C]..... 91

Figure 96: ESEM pictures of the fracture area of the sample 25 % IR / 75 % CR + PM30 [110°C]..... 91

Figure 97: ESEM pictures of the fracture area of the thicker sample 100 % NBR. 92

Figure 98: ESEM pictures of the fracture area of the thicker sample 50 % NBR / 50 % CR. 92

9 LIST OF TABLES

Table 1: List of used chemicals. 21

Table 2: List of used devices. 21

Table 3: Blend ratios for NR/CR-latex blends. 22

Table 4: Blend ratios for IR/CR-latex blends. 23

Table 5: Blend ratios for NBR/CR-latex blends. 24

Table 6: Parameters for the tensile tests. 25

Table 7: Parameters for the ESEM-EDX experiments. 26

Table 8: Parameters for the DSC measurements. 27

Table 9: Thickness of the latex blends without pre-vulcanization. 28

Table 10: Thickness of the pre-vulcanized latex blends. 29

Table 11: Thickness of the IR/CR-latex blends dried at 110 °C and of the IR/CR-latex blend, where PM30 together with ZnO were used for the pre-vulcanization. 30

Table 12: Measured glass transition temperature of the different latex blends without pre-vulcanization. 31

Table 13: Measured glass transition temperatures for the different pre-vulcanized latex blends. 33

Table 14: Measured stress at 100 % elongation, tensile strength and ultimate elongation for the latex blends without pre-vulcanization. 46

Table 15: Measured stress at 100 % elongation, tensile strength and ultimate elongation for the pre-vulcanized latex blends. 48

Table 16: Tensile strength of the IR/CR-latex blends with and without pre-vulcanization measured with the 50 mm and 75 mm shouldered bars. 52

Table 17: Tensile strength of the IR/CR-latex blends with and without pre-vulcanization measured with the 50 mm and 75 mm shouldered bars. 53

Table 18: Ultimate elongation of the IR/CR-latex blends with and without pre-vulcanization measured with the 50 mm and 75 mm shouldered bars. 53

Table 19: Measured stress at 100 % elongation, yield strength and ultimate elongation of the IR/CR-latex blends dried at 110 °C using the 75 mm shouldered bar. 55

Table 20: Measured stress at 100 % elongation, yield strength and ultimate elongation of the IR/CR-latex blends dried at 110 °C using the 50 mm shouldered bar. 55

Table 21: Measured stress at 100 % elongation, yield strength and ultimate elongation of the IR/CR-latex blend using PM30 together with ZnO as vulcanizing agent. 56

10 APPENDIX

10.1 DSC diagrams

10.1.1 DSC diagrams of the NR/CR-latex blends without pre-vulcanization

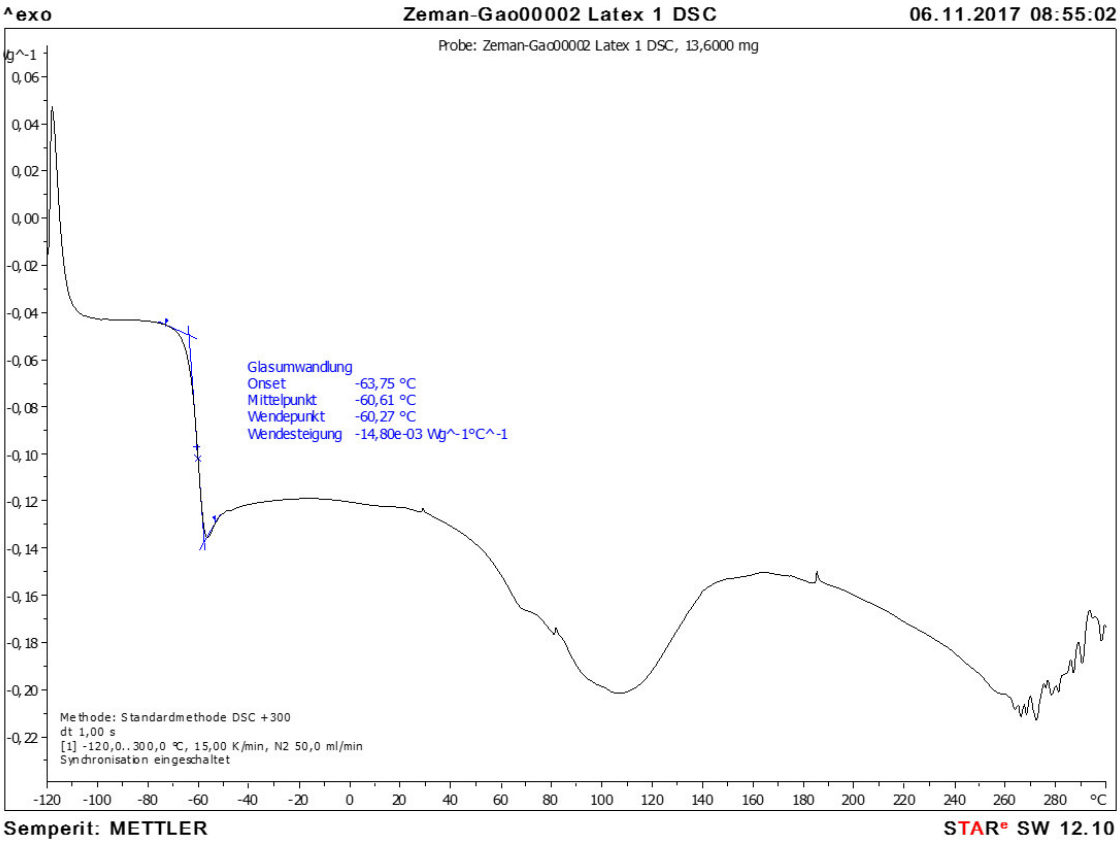

Figure 53: DSC diagram for the sample 100 % NR.

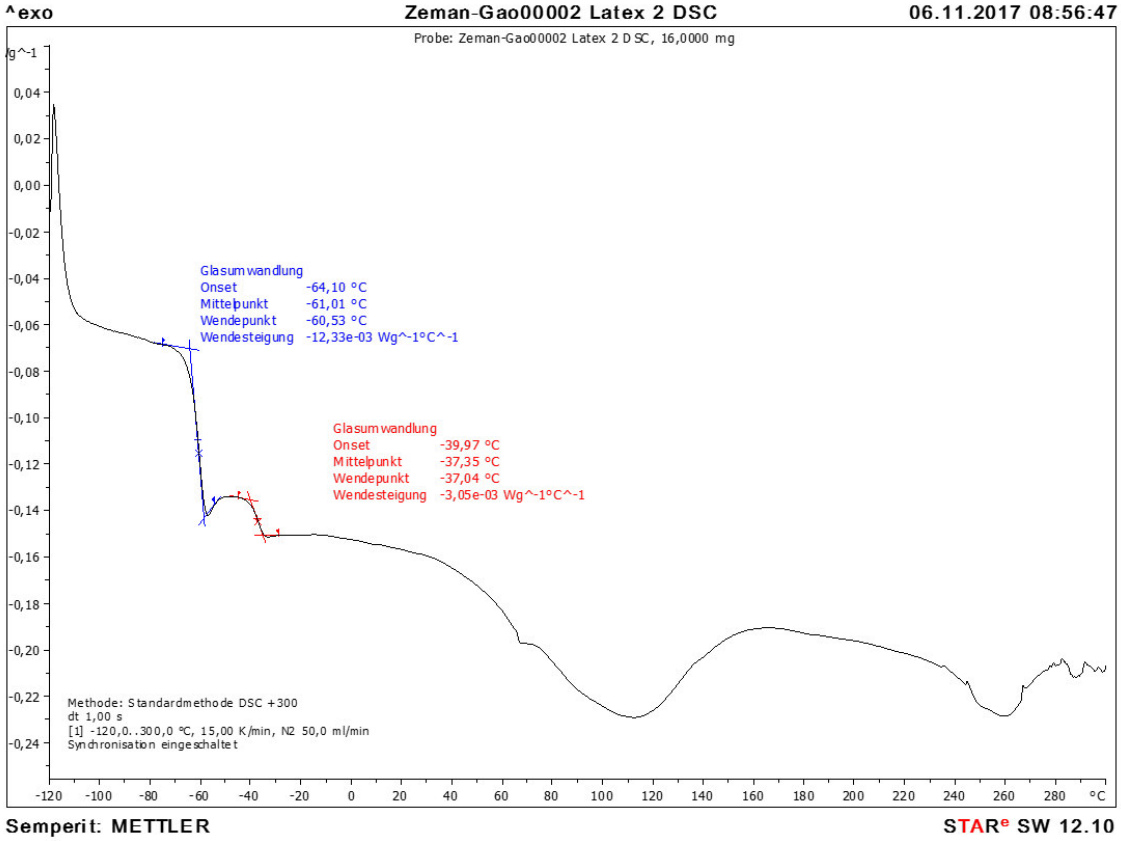

Figure 54: DSC diagram for the sample 75 % NR / 25 % CR.

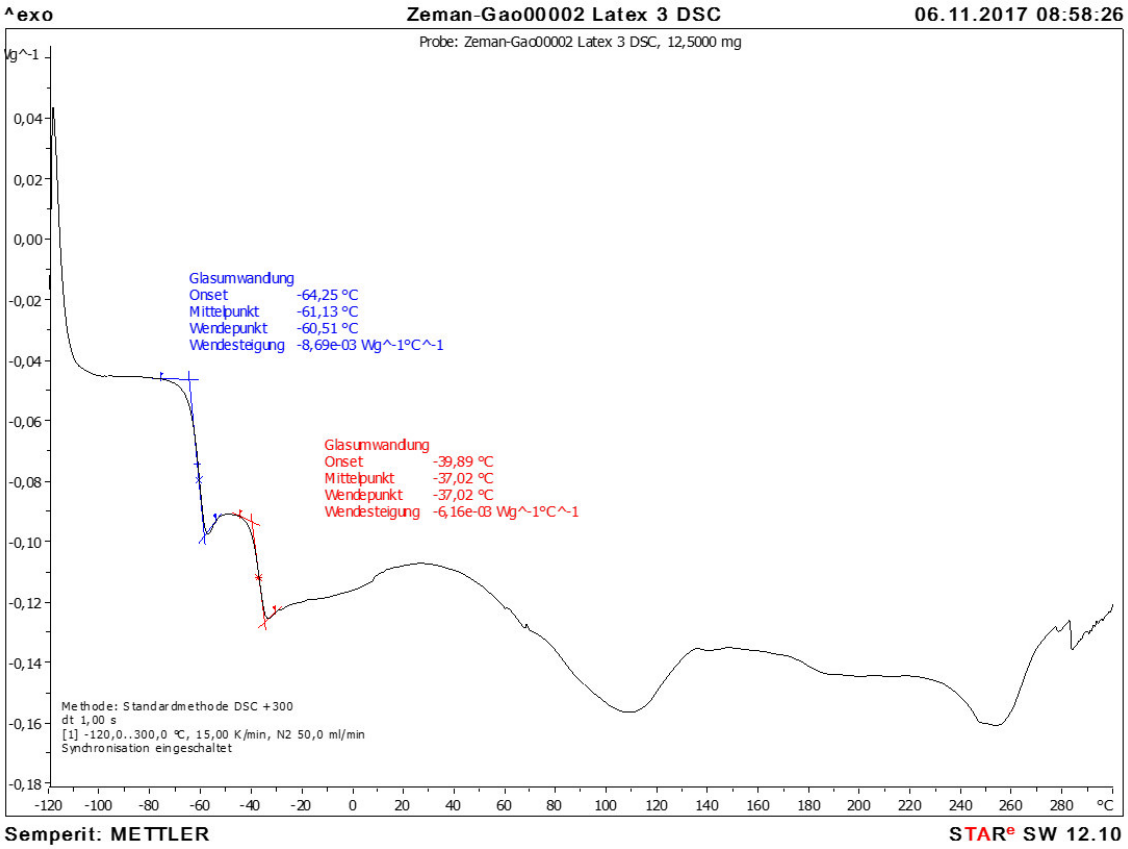

Figure 55: DSC diagram for the sample 50 % NR / 50 % CR.

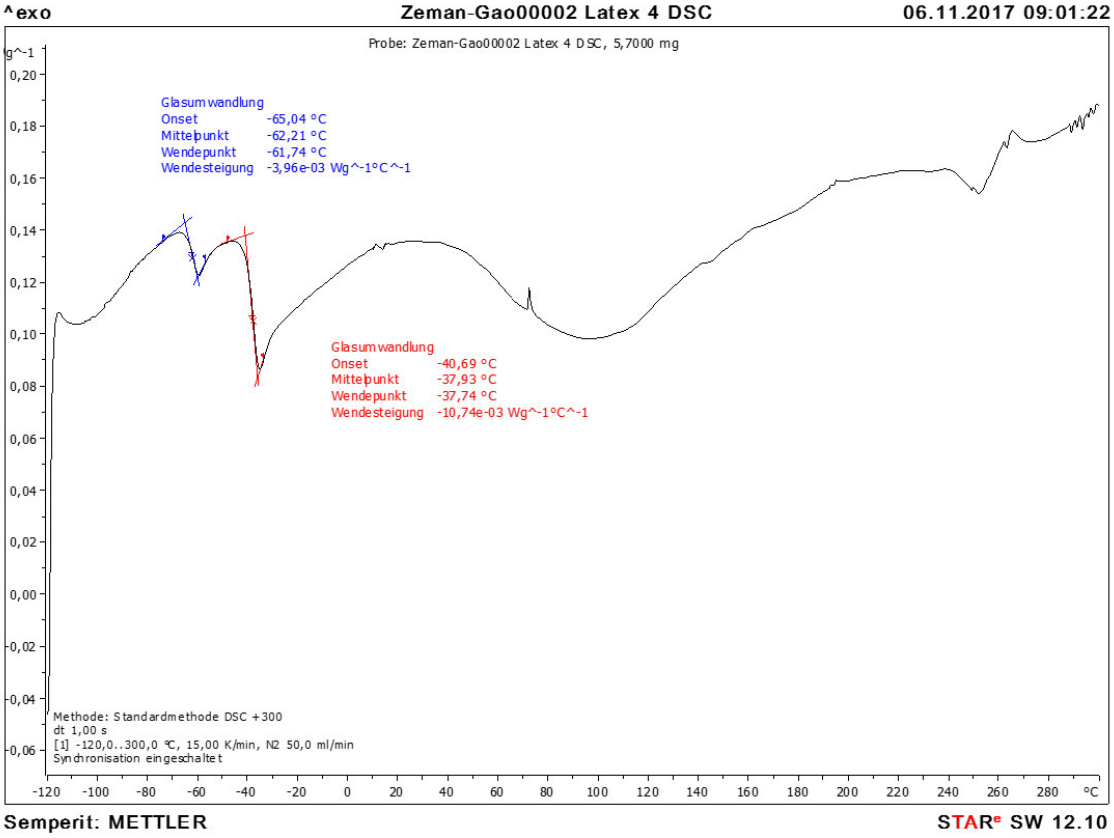

Figure 56: DSC diagram for the sample 25 % NR / 75 % CR.

10.1.2 DSC diagrams of the IR/CR-latex blends without pre-vulcanization

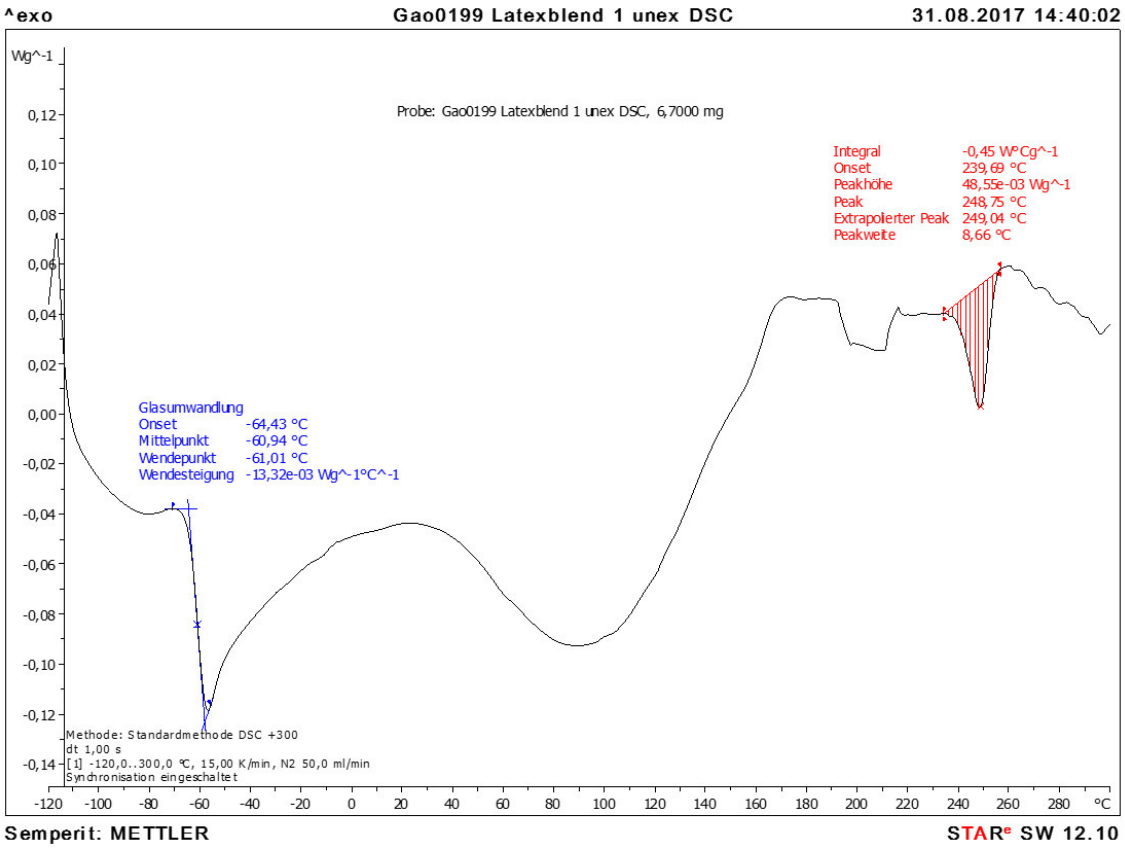

Figure 57: DSC diagram for the sample 100 % IR-latex.

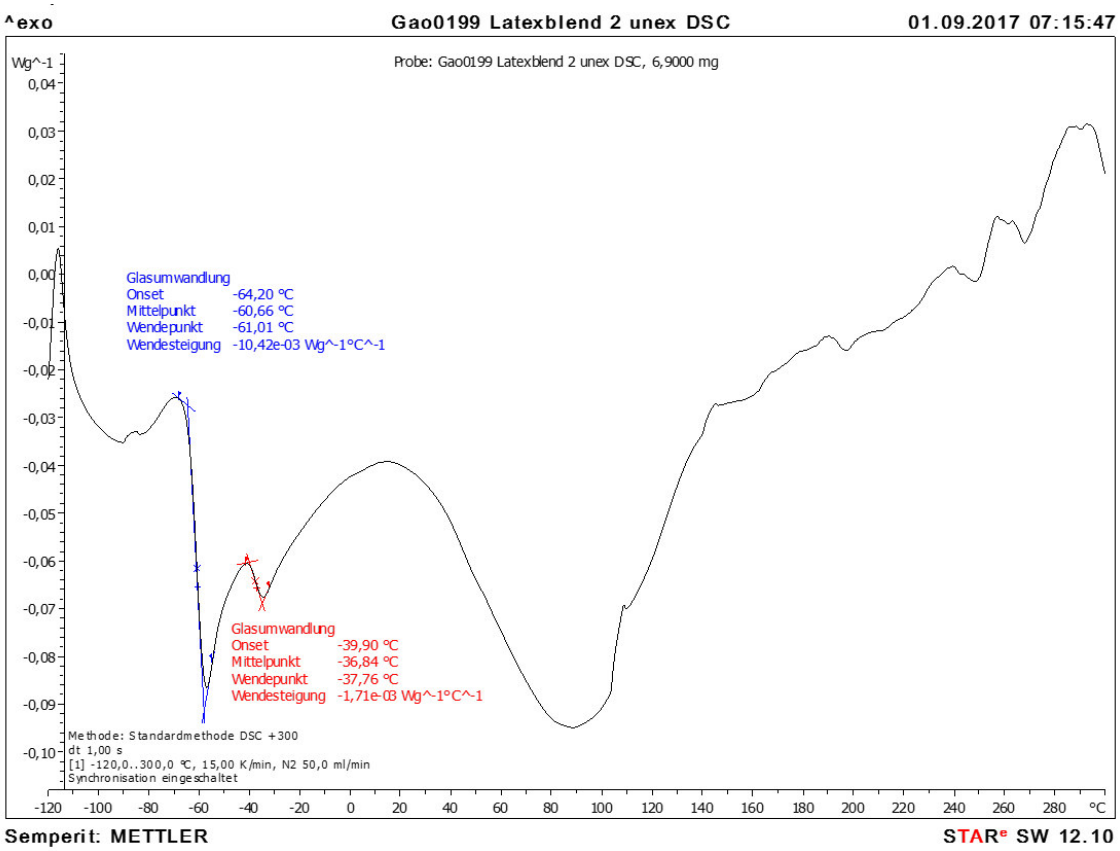

Figure 58: DSC diagram for the sample 75 % IR / 25 % CR.

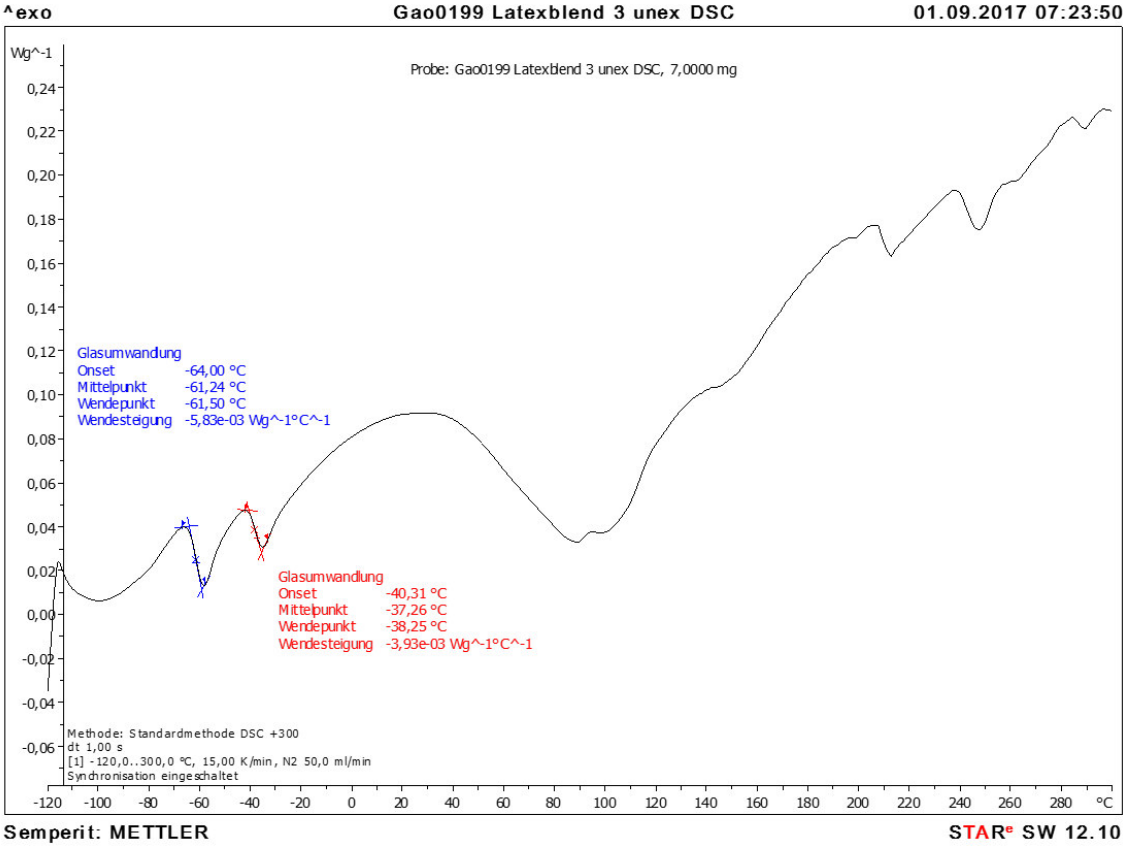

Figure 59: DSC diagram for the sample 50 % IR / 50 % CR.

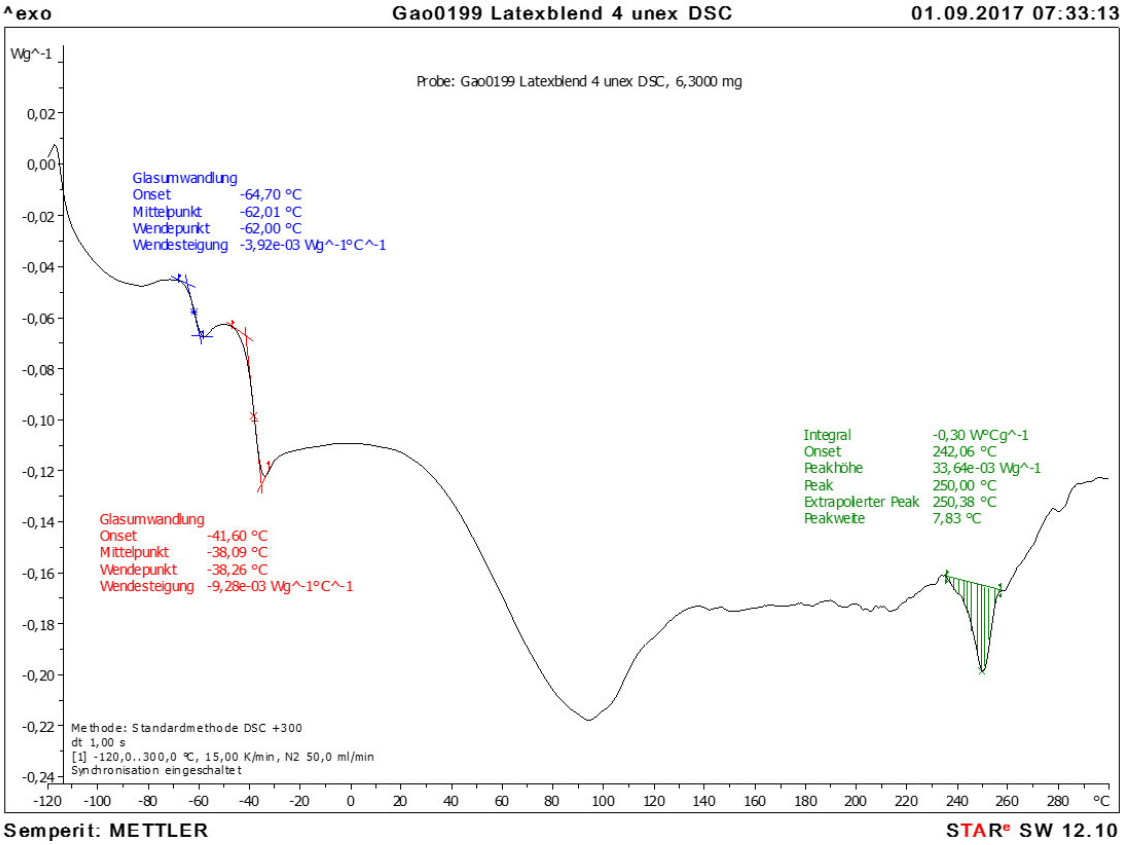

Figure 60: DSC diagram for the sample 25 % IR / 75 % CR.

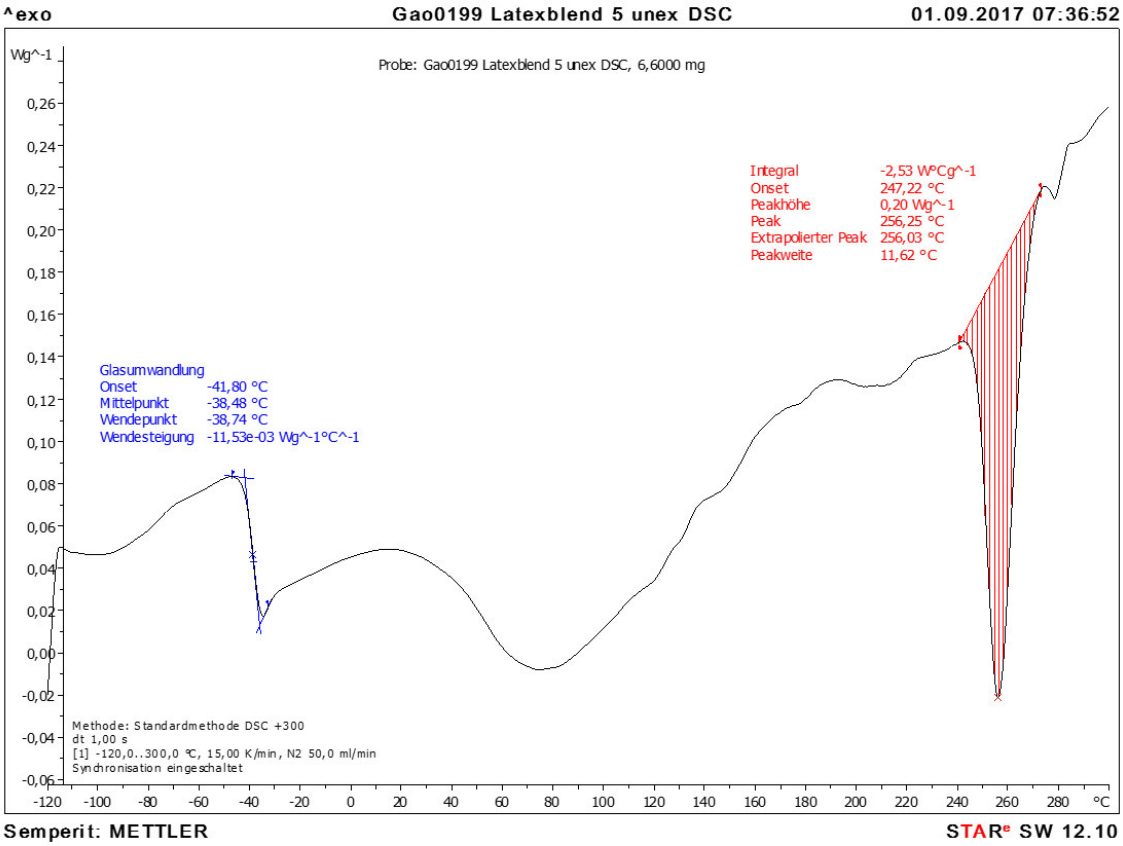

Figure 61: DSC diagram for the sample 100 % CR.

10.1.3 DSC diagrams of the NBR/CR-latex blends without pre-vulcanization

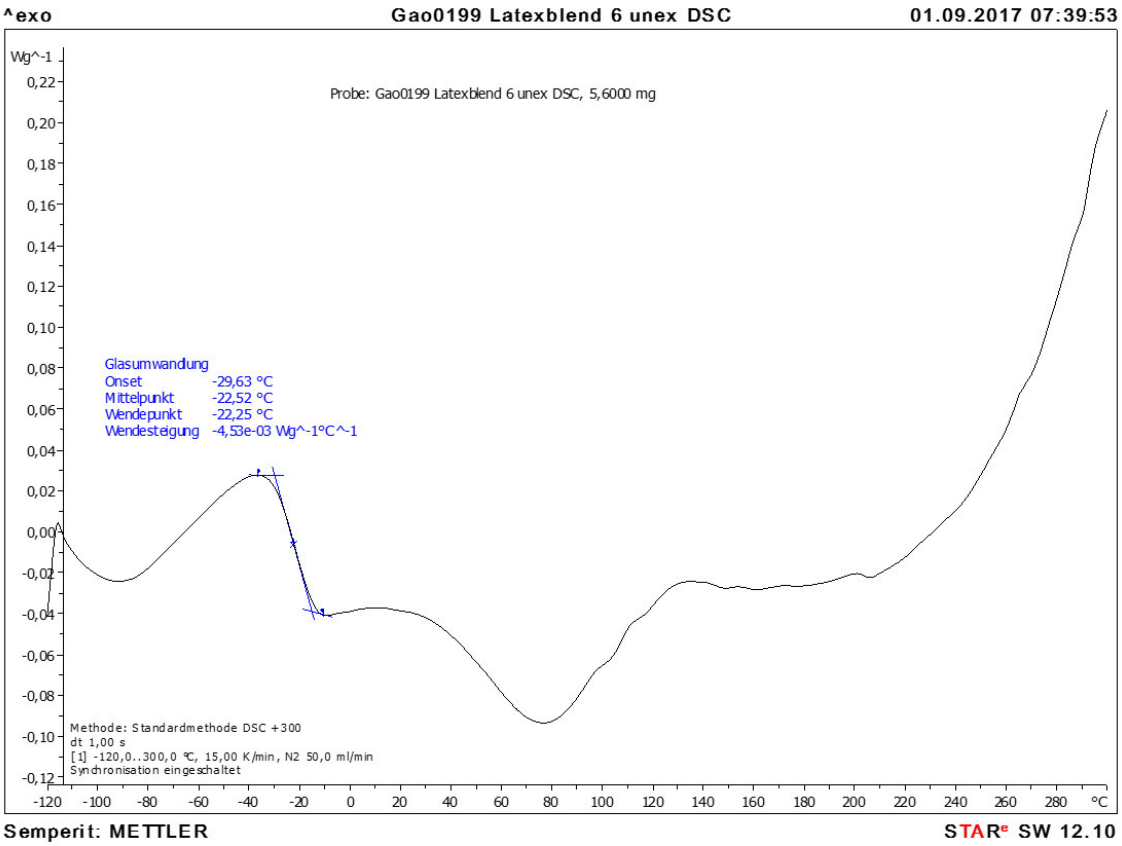

Figure 62: DSC diagram for the sample 100 % NBR.

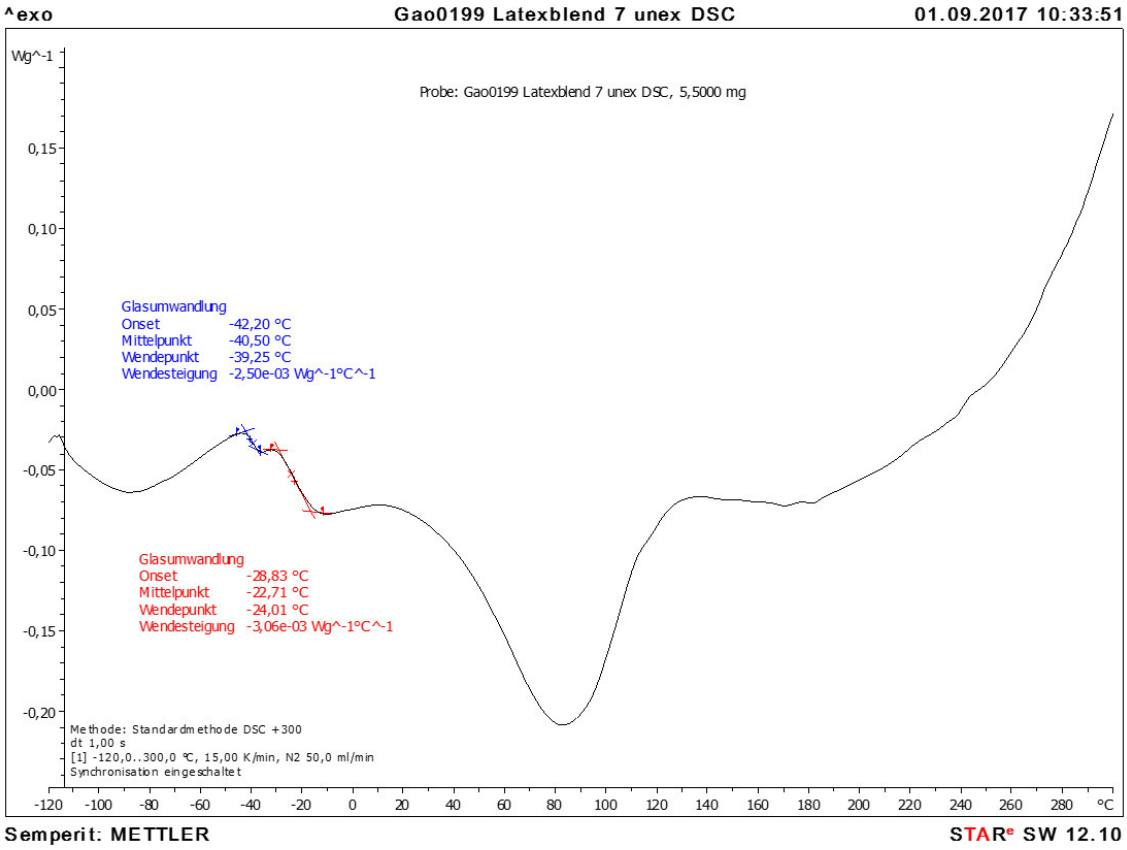

Figure 63: DSC diagram for the sample 75 % NBR / 25 % CR.

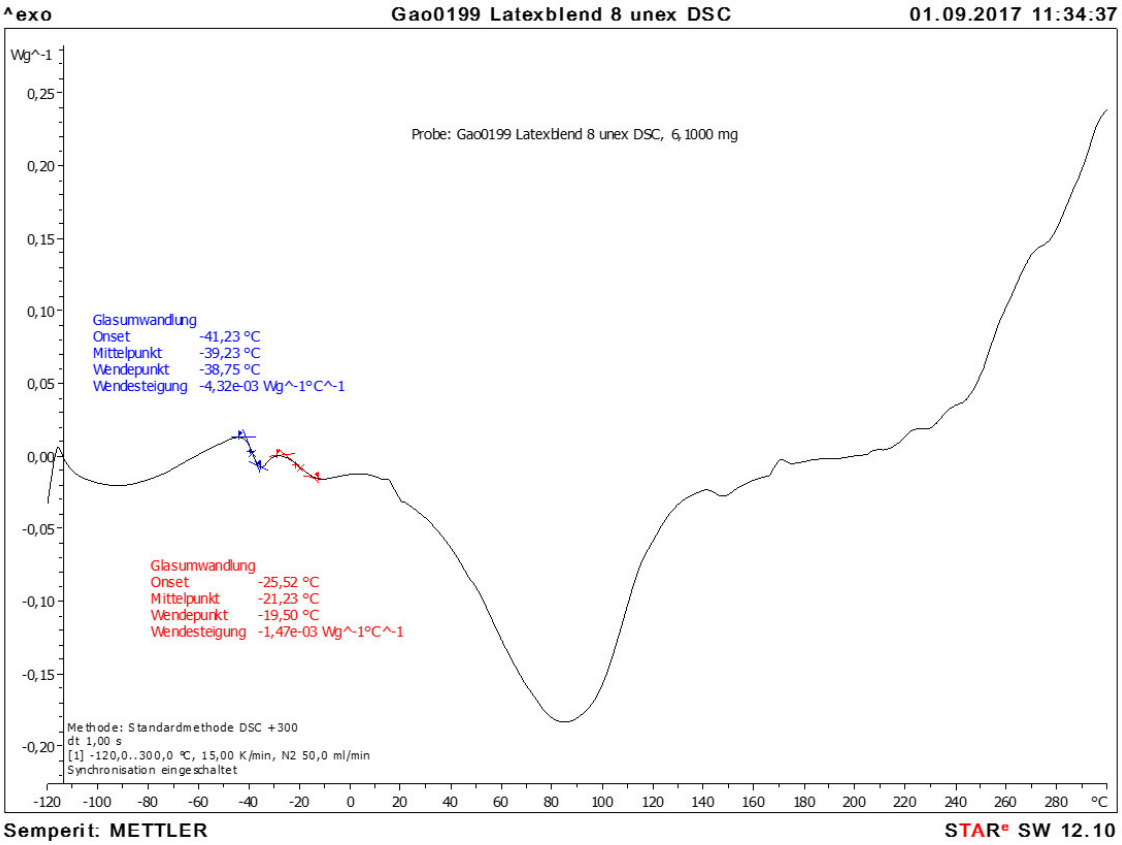

Figure 64: DSC diagram for the sample 50 % NBR / 50 % CR.

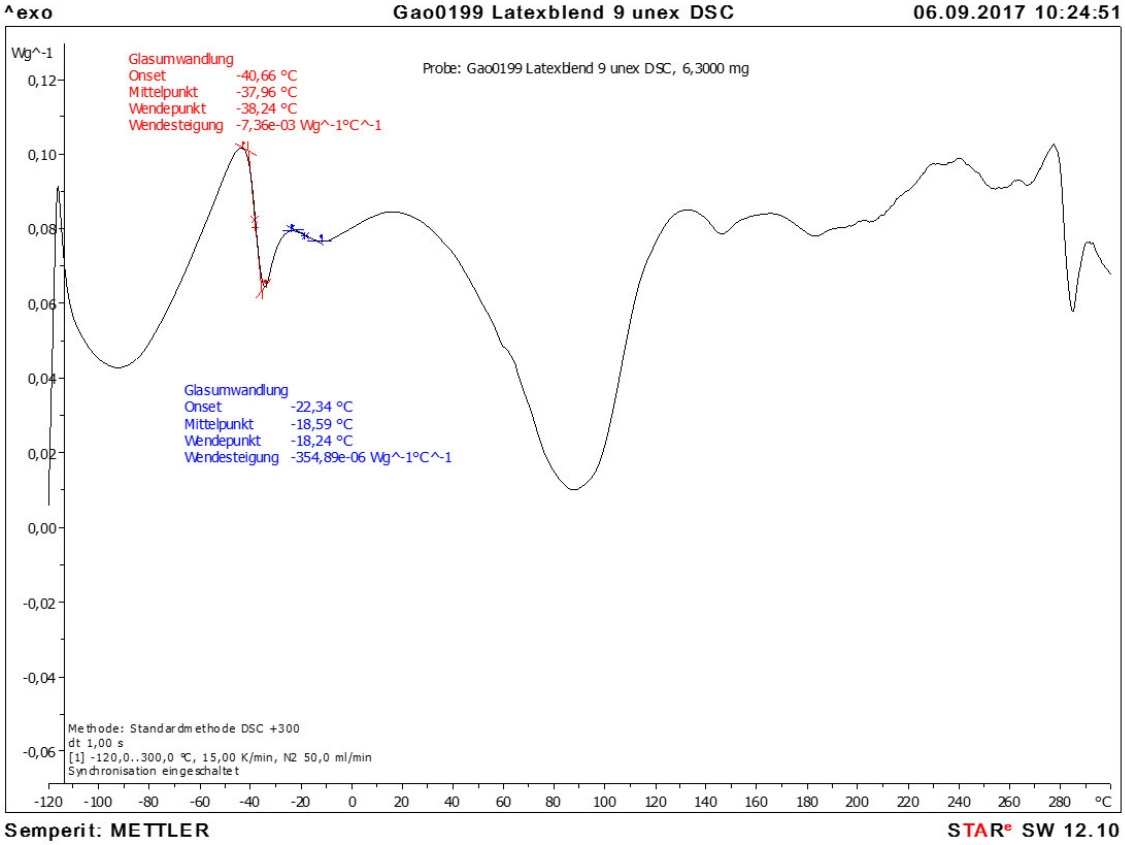

Figure 65: DSC diagram for the sample 25 % NBR / 75 % CR.

10.1.4 DSC diagrams of the pre-vulcanized NR/CR-latex blends

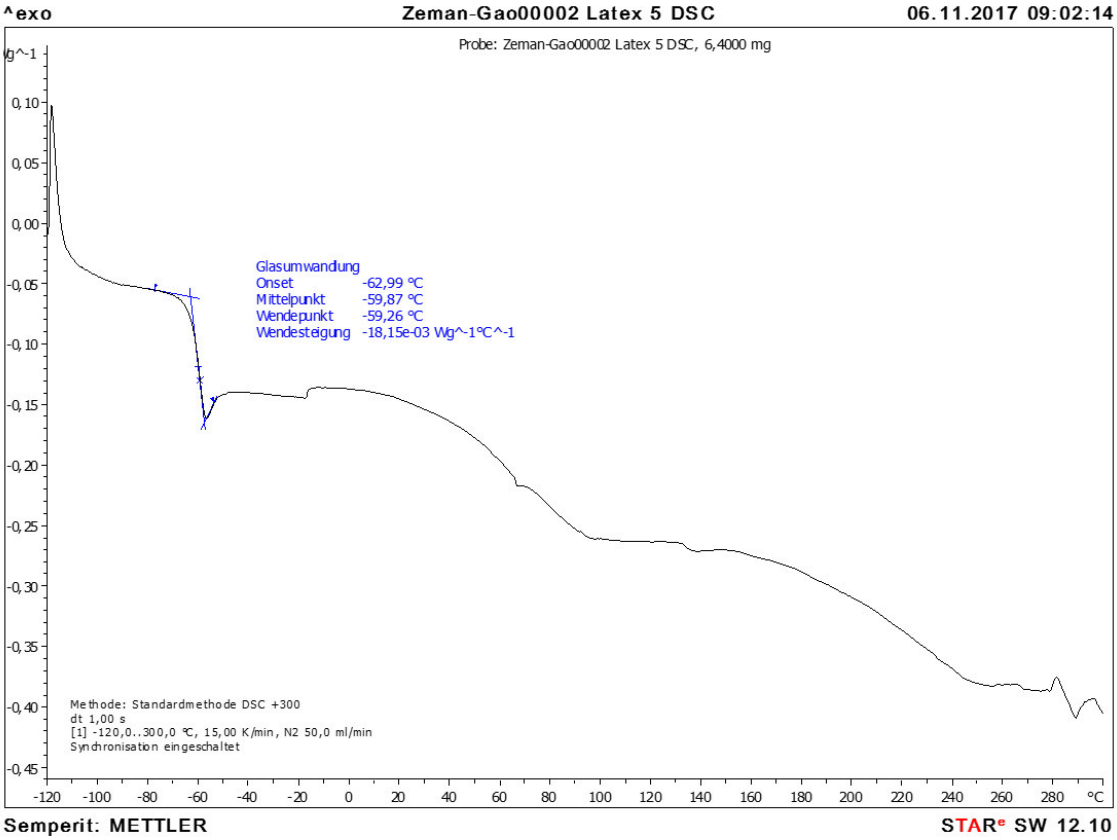

Figure 66: DSC diagram for the sample 100 % NR + PM30.

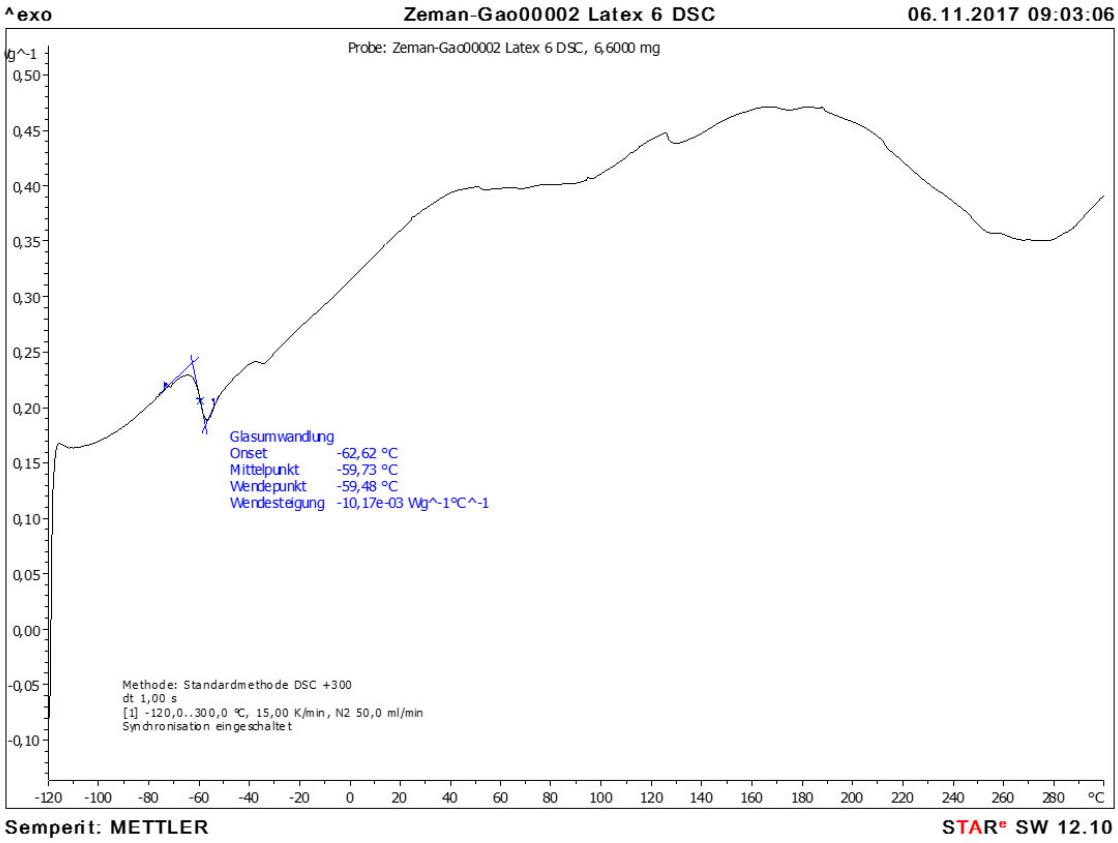

Figure 67: DSC diagram for the sample 75 % NR / 25 % CR + PM30.

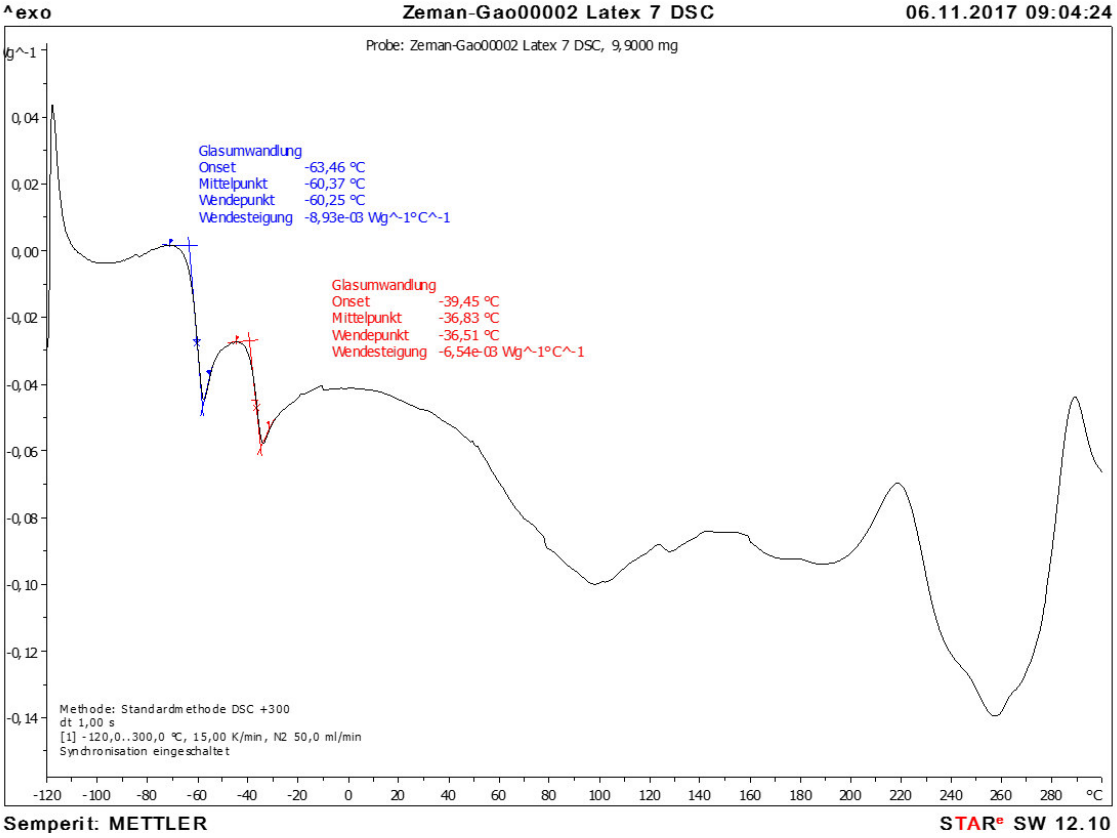

Figure 68: DSC diagram for the sample 50 % NR / 50 % CR + PM30.

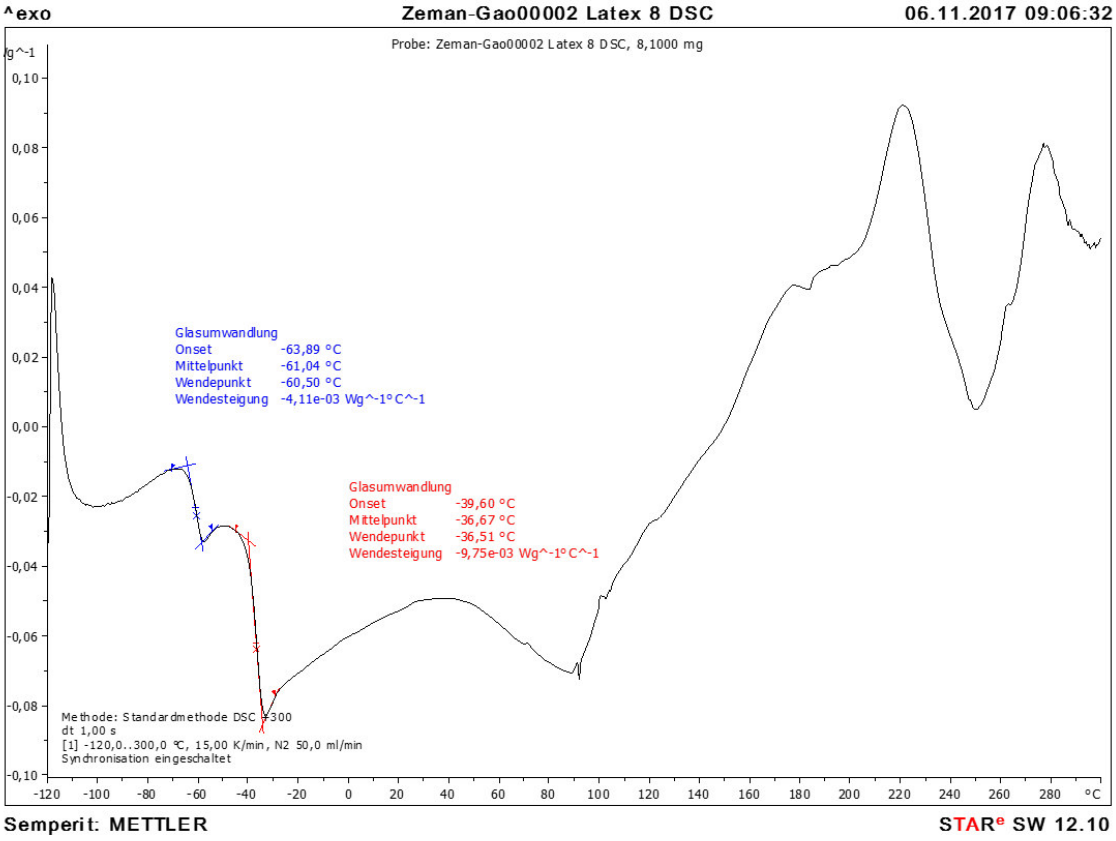

Figure 69: DSC diagram for the sample 25 % NR / 75 % CR + PM30.

10.1.5 DSC diagrams of the pre-vulcanized NBR/CR-latex blends

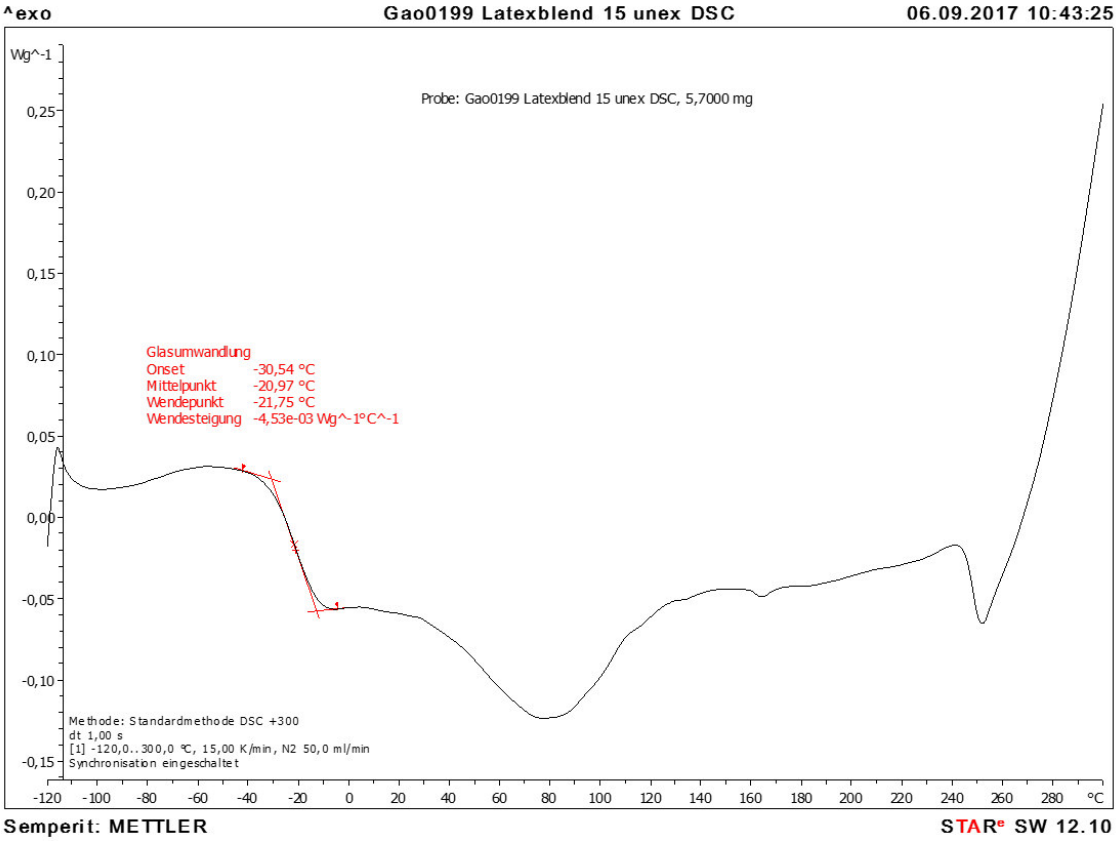

Figure 70: DSC diagram for the sample 100 % NBR + ZnO.

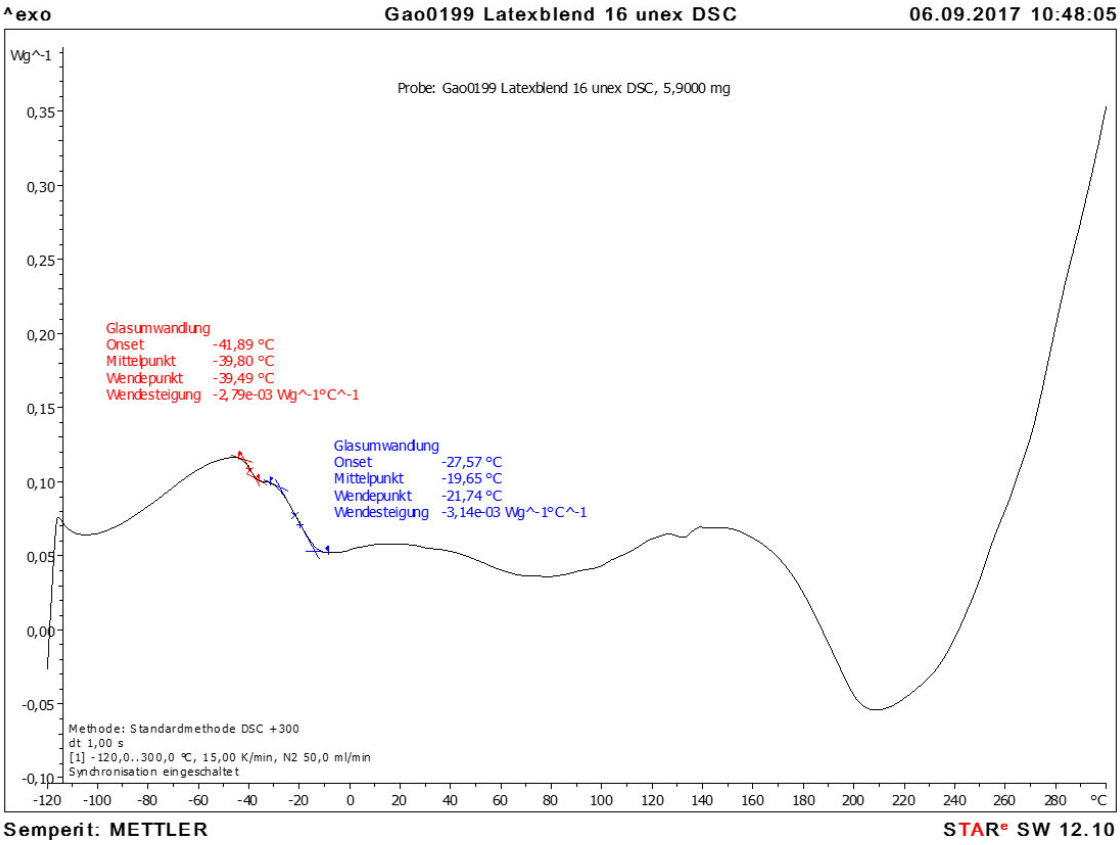

Figure 71: DSC diagram for the sample 75 % NBR / 25 % CR + ZnO.

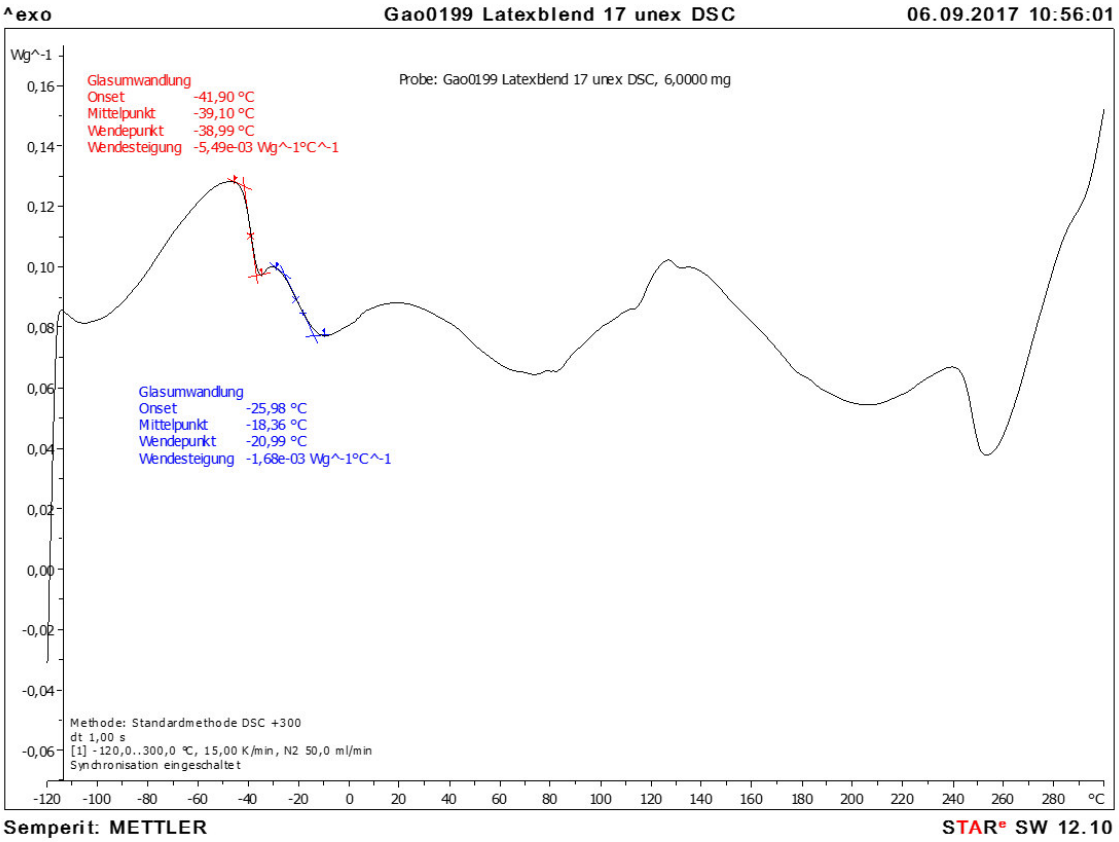

Figure 72: DSC diagram for the sample 50 % NBR / 50 % CR + ZnO.

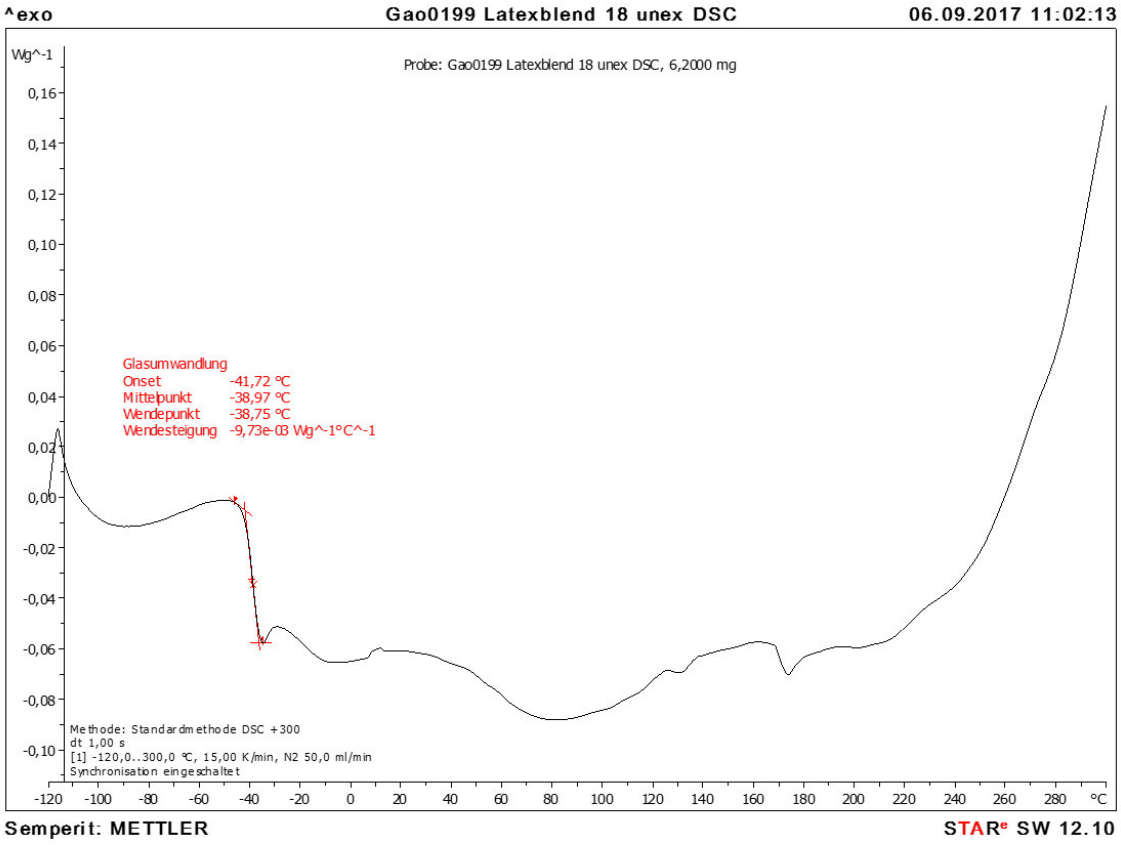

Figure 73: DSC diagram for the sample 25 % NBR / 75 % CR + ZnO.

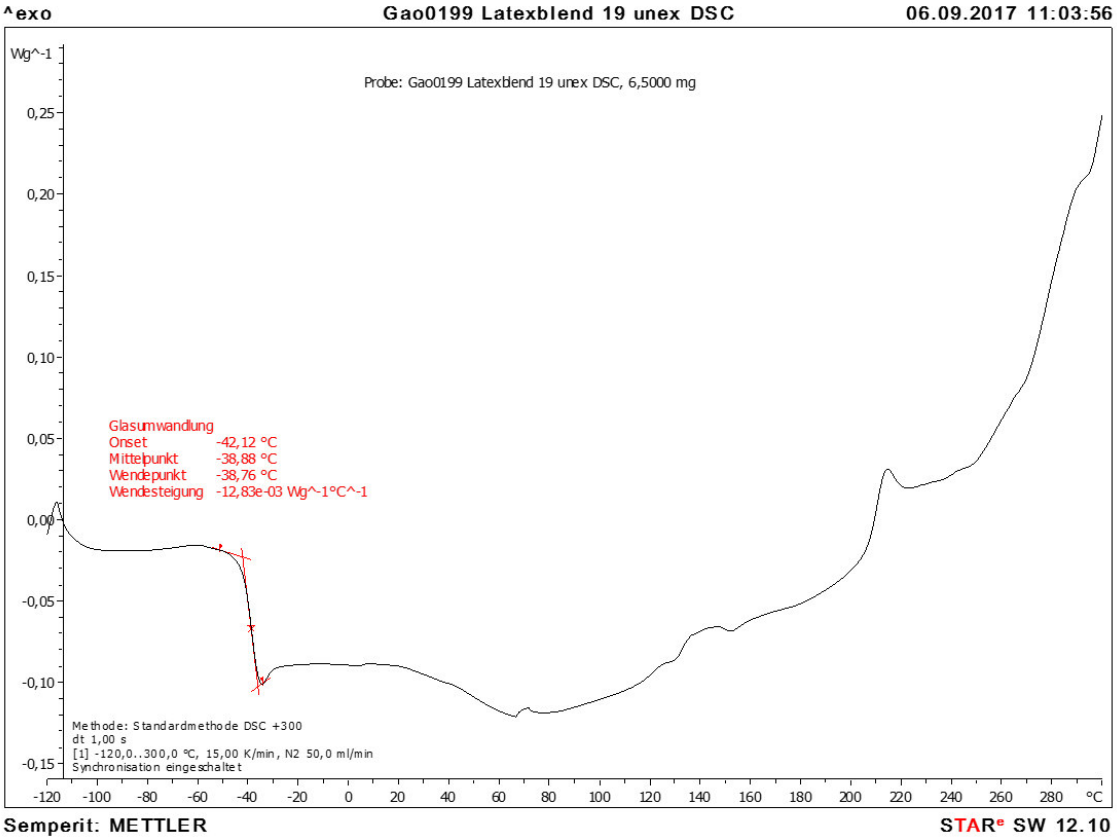

Figure 74: DSC diagram for the sample 100 % CR + ZnO.

10.2 ESEM results

10.2.1 ESEM pictures of the NR/CR-latex blends with and without pre-vulcanization

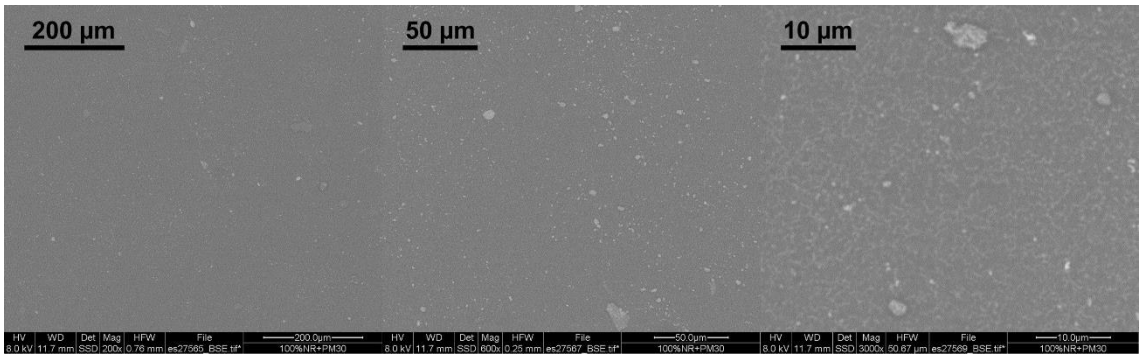

Figure 75: ESEM pictures of the surface of the sample 100 % NR + PM30.

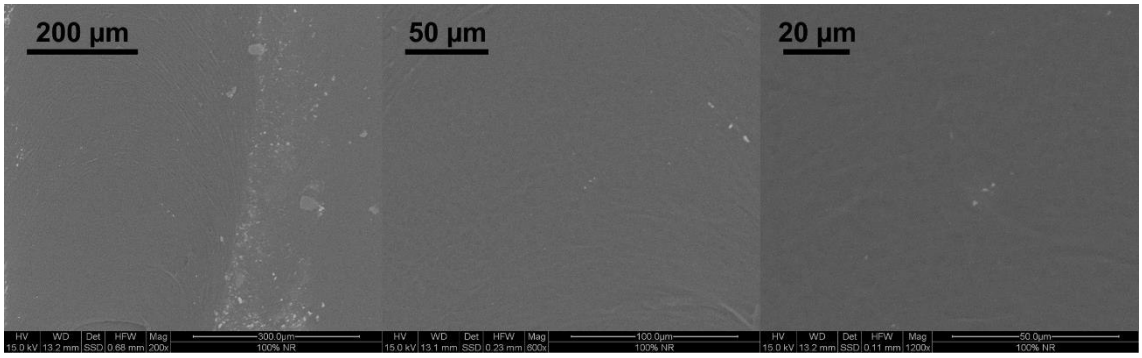

Figure 76: ESEM pictures of the fracture area of the thicker sample 100 % NR.

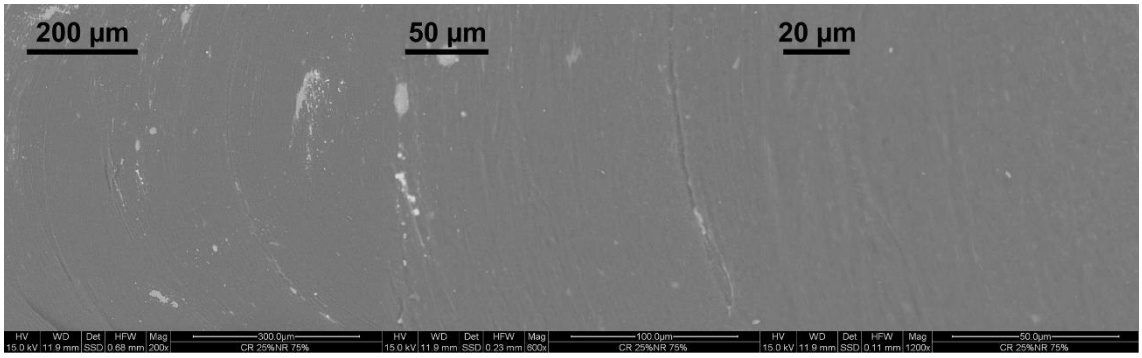

Figure 77: ESEM pictures of the fracture area of the thicker sample 75 % NR / 25 % CR.

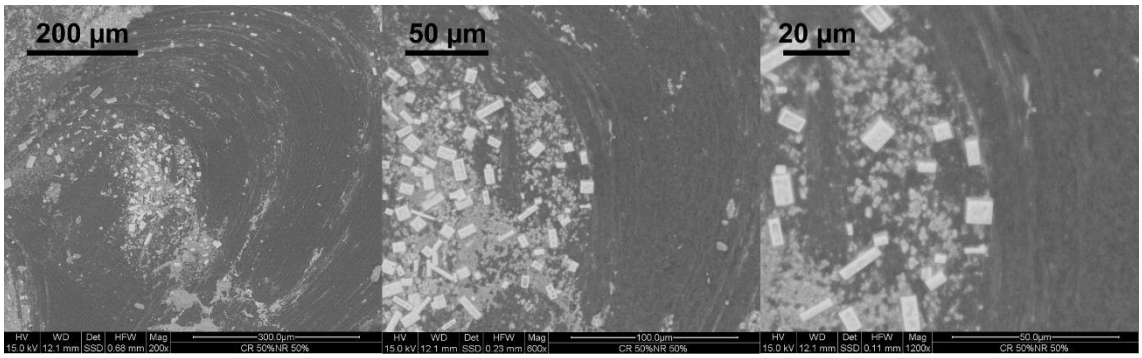

Figure 78: ESEM pictures of the fracture area of the thicker sample 50 % NR / 50 % CR.

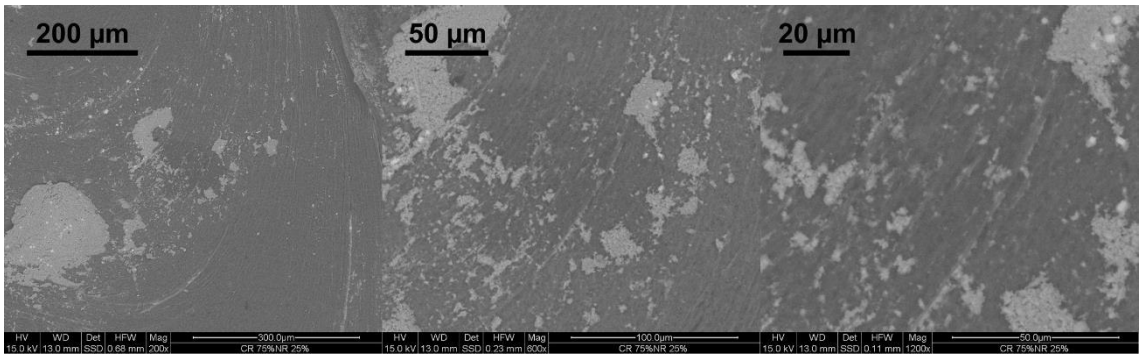

Figure 79: ESEM pictures of the fracture area of the thicker sample 25 % NR / 75 % CR.

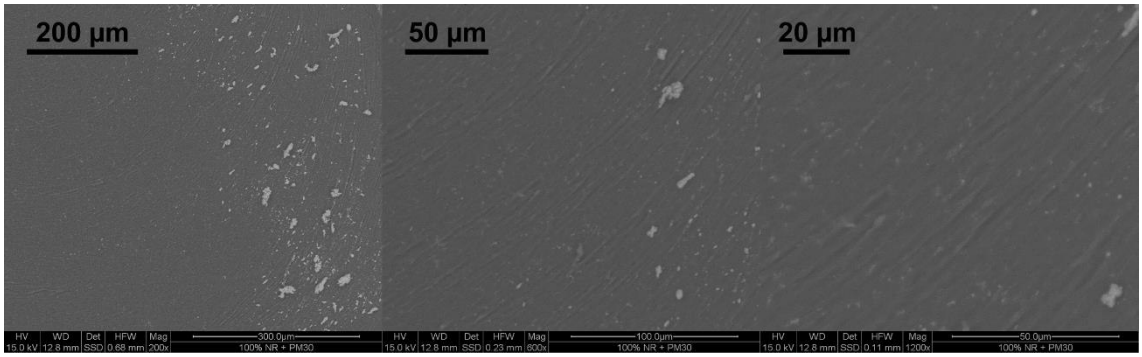

Figure 80: ESEM pictures of the fracture area of the thicker sample 100 % NR + PM30.

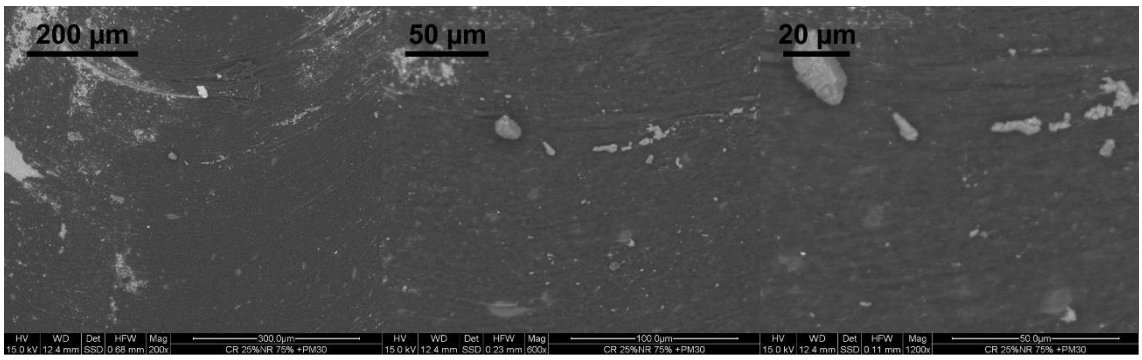

Figure 81: ESEM pictures of the fracture area of the thicker sample 75 % NR / 25 % CR + PM30.

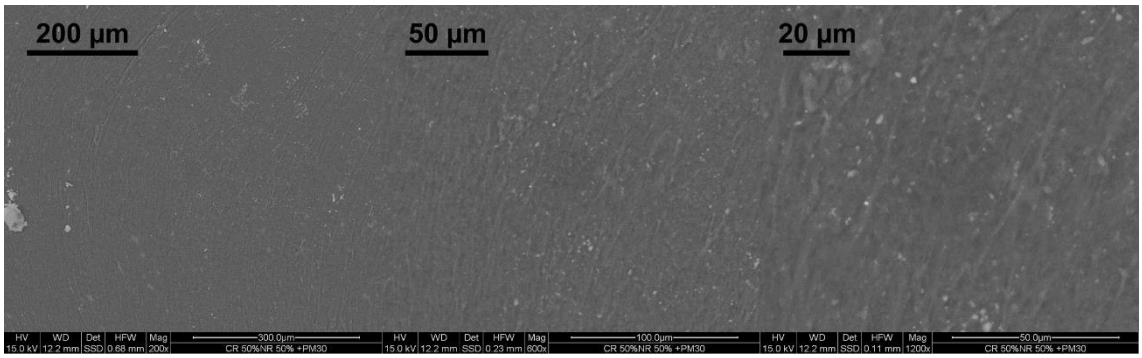

Figure 82: ESEM pictures of the fracture area of the thicker sample 50 % NR / 50 % CR + PM30.

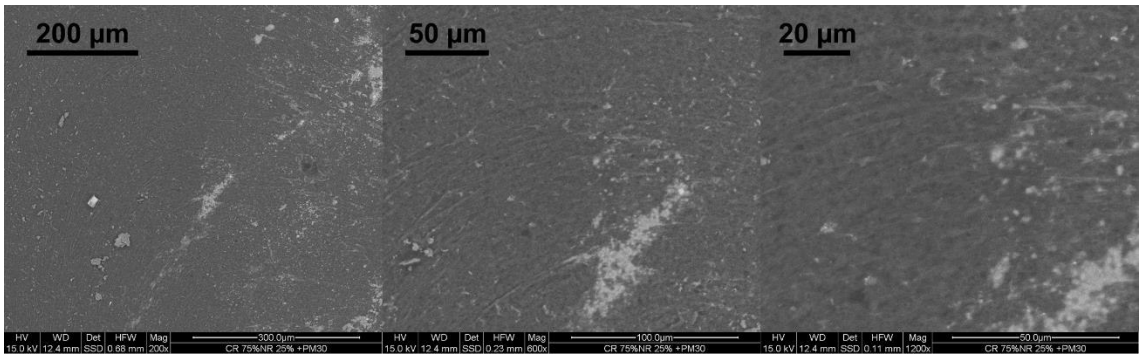

Figure 83: ESEM pictures of the fracture area of the thicker sample 25 % NR / 75 % CR + PM30.

10.2.2 ESEM pictures of the IR/CR-latex blends with and without pre-vulcanization

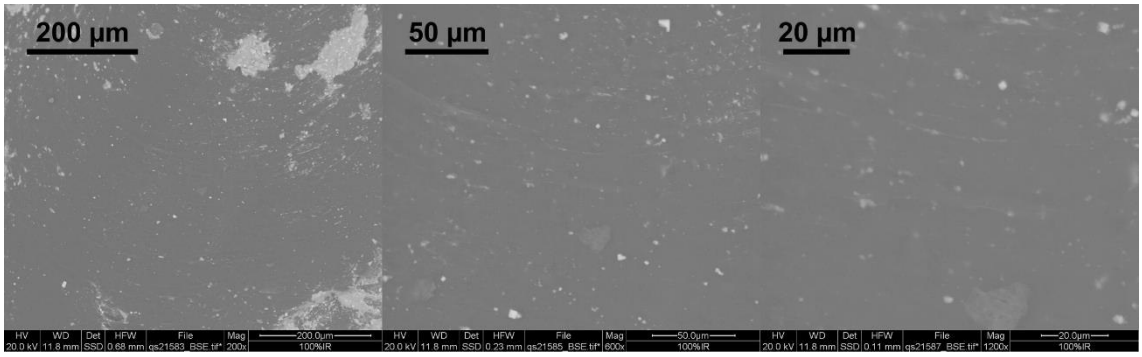

Figure 84: ESEM pictures of the fracture area of the thicker sample 100 % IR.

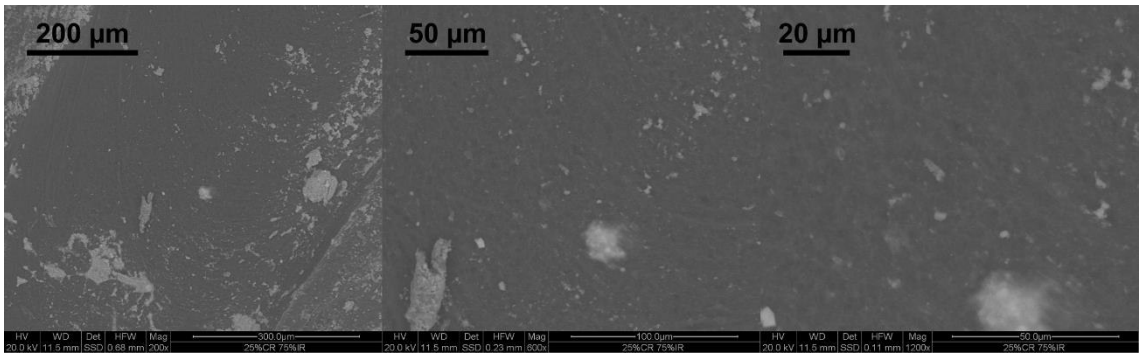

Figure 85: ESEM pictures of the fracture area of the thicker sample 75 % IR / 25 % CR.

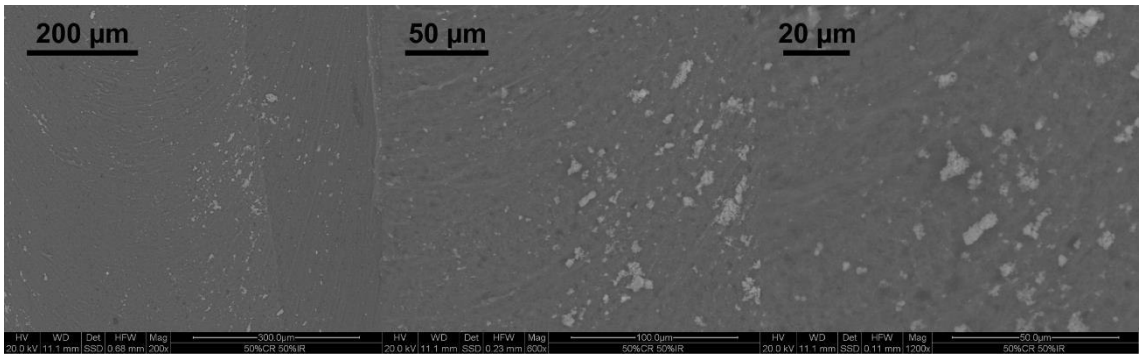

Figure 86: ESEM pictures of the fracture area of the thicker sample 50 % IR / 50 % CR.

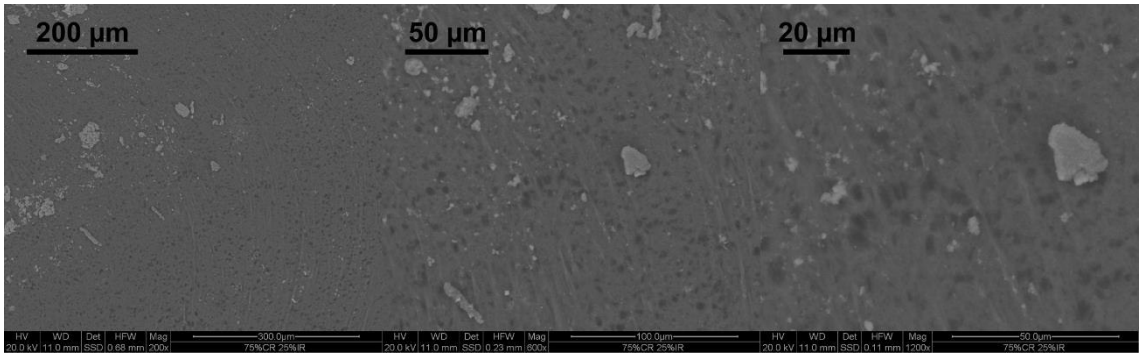

Figure 87: ESEM pictures of the fracture area of the thicker sample 25 % IR / 75 % CR.

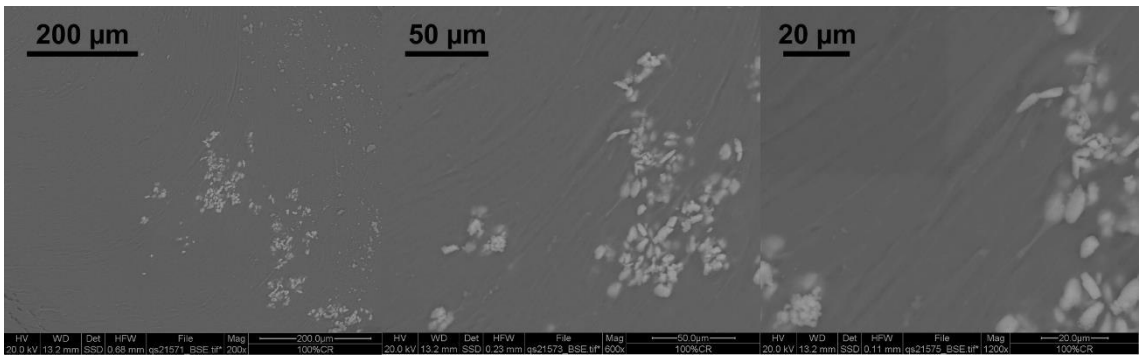

Figure 88: ESEM pictures of the fracture area of the thicker sample 100 % CR.

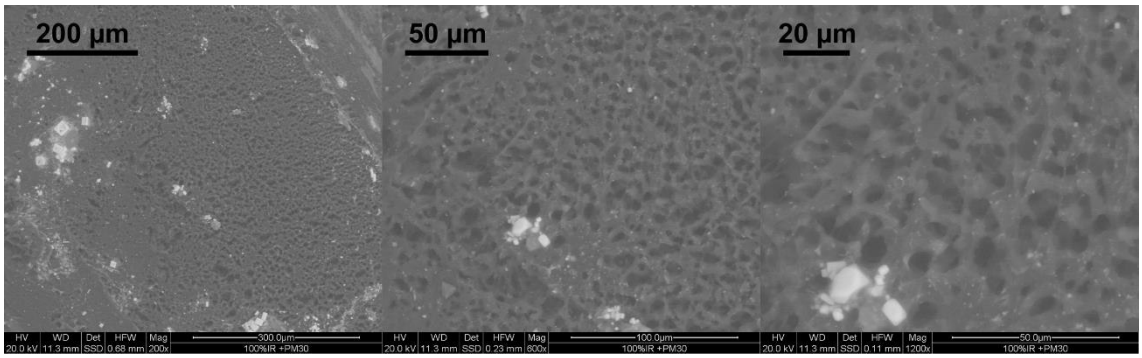

Figure 89: ESEM pictures of the fracture area of the thicker sample 100 % IR + PM30.

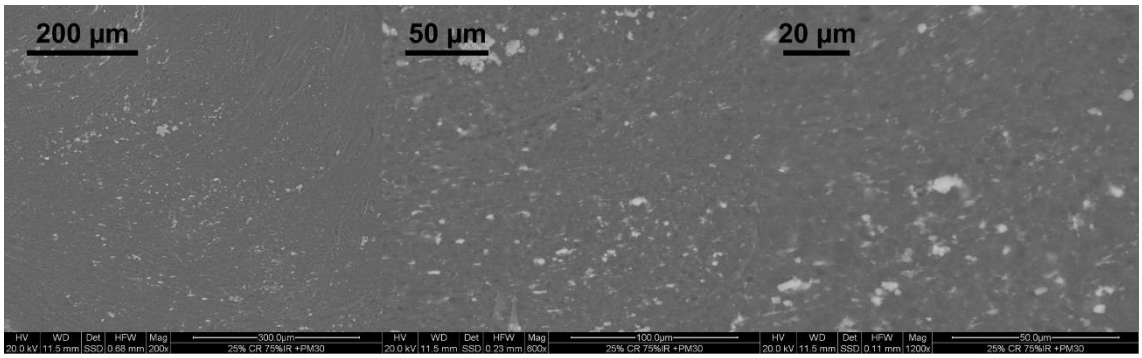

Figure 90: ESEM pictures of the fracture area of the thicker sample 75 % IR / 25 % CR + PM30.

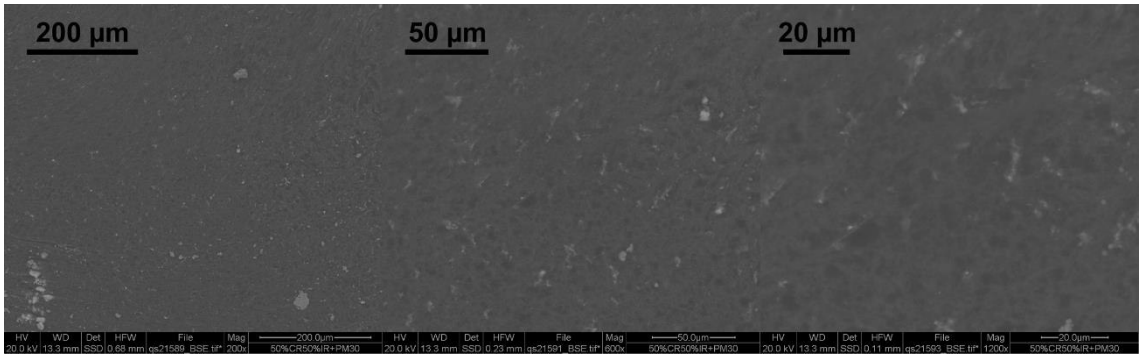

Figure 91: ESEM pictures of the fracture area of the thicker sample 50 % IR / 50 % CR + PM30.

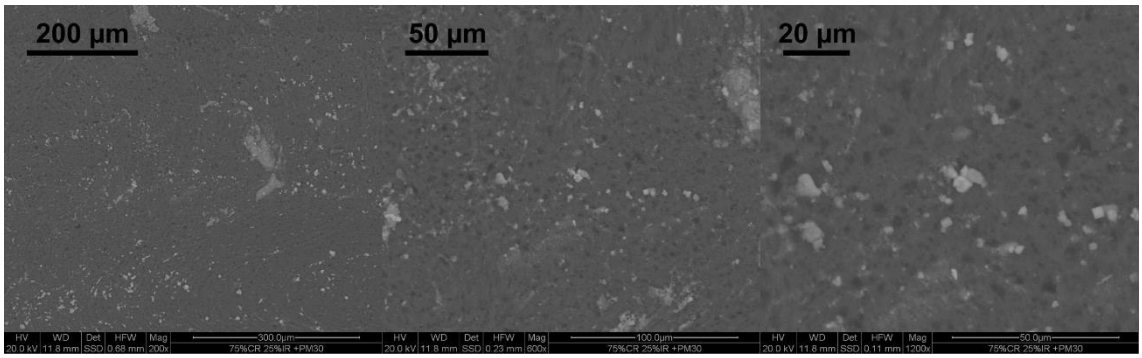

Figure 92: ESEM pictures of the fracture area of the thicker sample 25 % IR / 75 % CR + PM30.

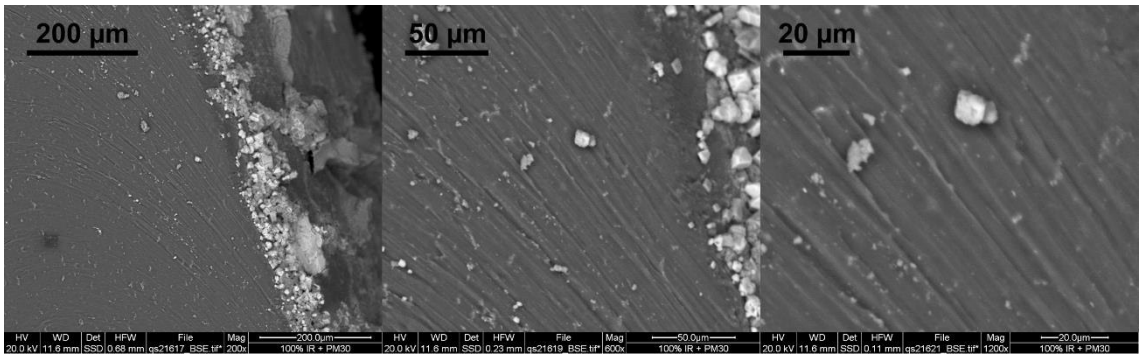

Figure 93: ESEM pictures of the fracture area of the thicker sample 100 % CR + PM30.

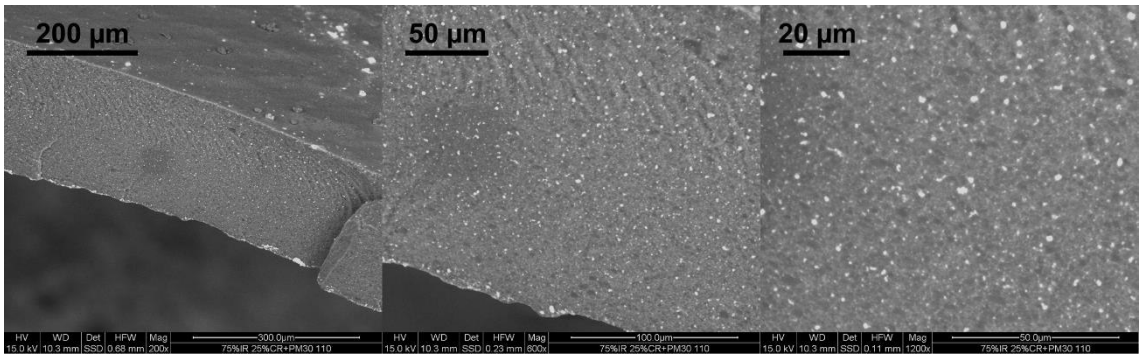

Figure 94: ESEM pictures of the fracture area of the sample 75 % IR / 25 % CR + PM30 [110°C].

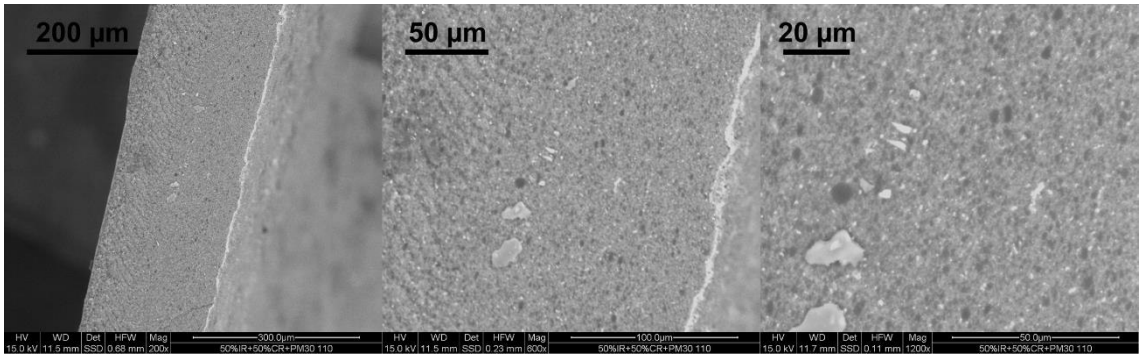

Figure 95: ESEM pictures of the fracture area of the sample 50 % IR / 50 % CR + PM30 [110°C].

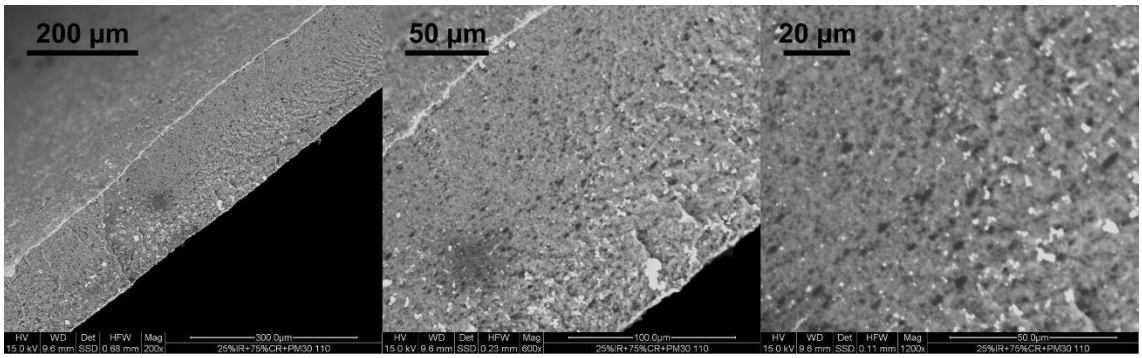

Figure 96: ESEM pictures of the fracture area of the sample 25 % IR / 75 % CR + PM30 [110°C].

10.2.3 ESEM pictures of the NBR/CR-latex blends

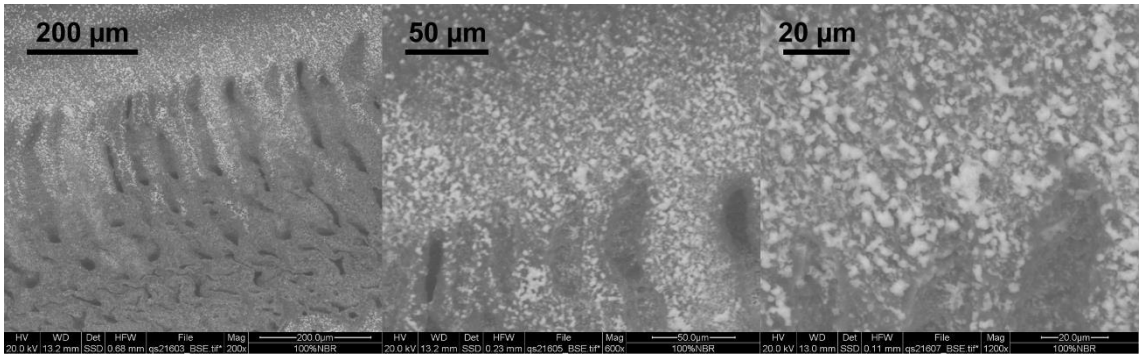

Figure 97: ESEM pictures of the fracture area of the thicker sample 100 % NBR.

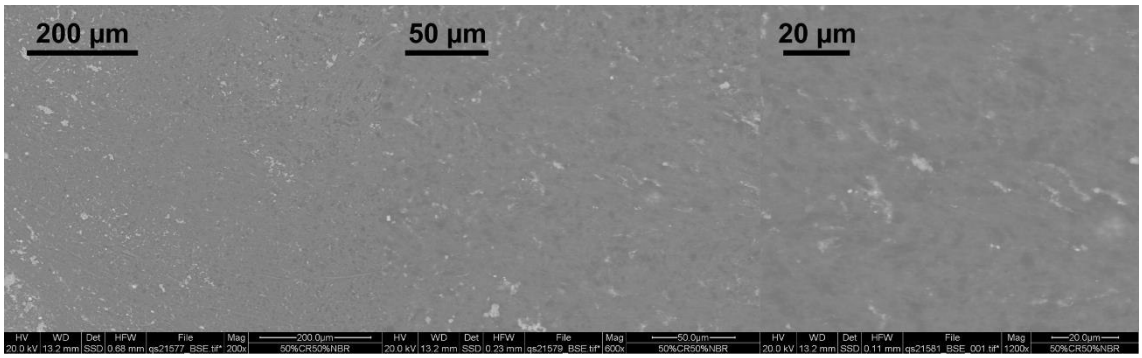

Figure 98: ESEM pictures of the fracture area of the thicker sample 50 % NBR / 50 % CR.